Characterization of direct Myc target genes in *Drosophila melanogaster*

and

Investigating the interaction of Chinmo and Myc

Charakterisierung direkter Myc Zielgene in *Drosophila melanogaster*

und

Interaktionsanalyse der Proteine Chinmo und Myc

Doctoral thesis

for a doctoral degree

at the Graduate School of Life Sciences,

Julius-Maximilians-Universität Würzburg, Section Biomedicine

submitted by

Eva Kristine Herter

from Stuttgart

Würzburg, 2015

Members of the Thesis Committee:

Chairperson: Prof. Dr Jörg Schultz

Primary Supervisor: Prof. Dr. Peter Gallant

Supervisor (Second): Prof. Dr. Thomas Raabe

Supervisor (Third): Prof. Dr. Charlotte Förster

Submitted on:

Date of Public Defence:

Date of Receipt of Certificates:

Substantial parts of this thesis were published in the following article:

Herter EK, Stauch M, Gallant M, Wolf E, Raabe T, Gallant P: snoRNAs are a novel class of biologically relevant Myc targets. *BMC Biology* 2015, 13: 1-17.

Table of Contents

Table of Contents.....

List of figures.....

List of tables.....

Summary 1

Zusammenfassung 2

1 Introduction **3**

1.1 Transcription factor Myc 3
1.1.1 Functional domains of Myc 3
1.1.2 Transcriptional regulation by Myc 4
1.1.3 Myc-Max network 5
1.1.4 Growth control in *Drosophila* 6
1.2 Ribosome biogenesis 9
1.2.1 Function of snoRNPs 9
1.2.2 The role of snoRNAs in cancer 11
1.2.3 Control of protein production by Myc 12
1.3 Myc-interactors: The BTB-Zf protein Chinmo 14
1.3.1 The role of Chinmo in brain development 15
1.3.2 Chinmo regulates growth 15
1.4 Objectives of the thesis 18

2 Materials **19**

2.1 Strains and cell lines 19
2.1.1 Bacterial strains 19
2.1.2 *Drosophila melanogaster* cell lines 19
2.2 Cultivation media and supplements 19
2.2.1 Media and antibiotics for bacterial cell culture 19
2.2.2 Media for cell culture 20
2.2.3 Further supplements 20
2.3 Nucleic acids 20
2.3.1 Oligonucleotides 20
2.3.2 Plasmids 25
2.4 Antibodies 26
2.4.1 Primary antibodies 26
2.4.2 Secondary antibodies 27
2.5 Chemicals 27
2.6 Enzymes, standards and kits 27
2.6.1 Enzymes 27
2.6.2 Standards 27

2.6.3 Kits 28
2.7 Buffer and solutions 28
2.8 Consumables and equipment 33
2.8.1 Equipment 33
2.9 Fly lines 35

3 Methods 37

3.1 Molecular biology methods 37
3.1.1 Transfection of bacteria with plasmid DNA and plasmid amplification 37
3.1.2 Isolation of plasmid DNA from bacteria 37
3.1.3 Ethanol precipitation of nucleic acids 37
3.1.4 Nucleic acid quantitation 38
3.1.5 Separation of proteins from aqueous nucleic acid solutions 38
3.1.6 Sequence specific hydrolysis of DNA (restriction digest) 38
3.1.7 Separation of DNA and RNA fragments via gel electrophoresis 38
3.1.8 DNA extraction and purification from agarose gels 39
3.1.9 Ligation of DNA fragments 39
3.1.10 Isolation of total RNA from larvae or tissue culture 39
3.1.11 cDNA synthesis 40
3.1.12 Polymerase chain reaction (PCR) 41
3.1.13 Chromatin immunoprecipitation (ChIP) 42
3.1.14 ChIP seq 43
3.1.15 Bioinformatical analysis 43
3.1.16 dsRNA synthesis 44
3.1.17 Northern blot 44
3.2 Cell biology methods 45
3.2.1 Passaging of cells 45
3.2.2 Freezing and thawing cells 45
3.2.3 Transfection of plasmid DNA 45
3.2.4 Transfection of dsRNA 47
3.2.5 Induction of inducible fly cells 47
3.2.6 Luciferase reporter gene assay 47
3.3 Protein biochemistry methods 47
3.3.1 Generation of protein lysates for Western blot 47
3.3.2 SDS polyacrylamide gel electrophoresis (SDS-PAGE) 48
3.3.3 Staining Protein gels with Coomassie Blue 48
3.3.4 Western blot 48
3.3.5 Stripping antibodies from nitrocellulose membranes 49
3.3.6 Immunoprecipitation 49
3.3.7 Bacterial expression and purification of GST fusion proteins 50
3.3.8 Protein determination by the Bradford method 50
3.4 Fly specific methods 50
3.4.1 Fly culturing 50
3.4.2 Heat shock conditions for overexpression experiments 50

3.4.3 Images of fluorescent tissue 51
3.4.4 Extraction of genomic DNA 51
3.4.5 Methylation Assay with larvae 51
3.4.6 Translation Assay with larvae 52
3.4.7 Neuroblast type II tumors 52

4 Results 53

4.1 Myc binds and regulates genes involved in ribosome biogenesis 53
4.1.1 DNA-library preparation for ChIPseq 53
4.1.2 Myc binds a core set of sites 56
4.1.3 Investigation of Myc binding sites identified by Yang *et al*. 58
4.1.4 Myc binds to Uhgs 61
4.1.5 Ribosome biogenesis and ribosome protein genes are the core Myc targets 64
4.1.6 Myc binds promoter-proximal sequences 66
4.1.7 Myc regulates Uhgs and snoRNAs 68
4.1.8 Biological effects of Uhg genes 71
4.1.9 Uhg genes affect growth *in vivo* and tumor formation 74
4.2 Myc and Chinmo interact in growth control 78
4.2.1 Chinmo controls growth via cell number 78
4.2.2 Myc and Chinmo interact directly 79
4.2.3 Tumor induction of Chinmo and Ras^{V12} is Myc-dependent 84

5 Discussion 87

5.1 Characterization of direct Myc target genes in *Drosophila melanogaster* 87
5.1.1 Myc binds a core set of target genes in *Drosophila* 87
5.1.2 snoRNAs are new Myc targets 89
5.1.3 snoRNAs play an important role in tumor formation 91
5.1.4 Myc controls all levels of ribosome biogenesis 94
5.2 Analysis of Chinmo and Myc interaction 97
5.2.1 Chinmo and Myc function in partial redundant pathways 97
5.2.2 Chinmo and Myc interact physically 98
5.2.3 Chinmo directly activates Myc target genes 100
5.2.4 Myc is important for Chinmo's role in tumor induction 101

References 104

6 Appendix 119

6.1 List of abbreviations 119
6.1.1 Prefixes 119
6.1.2 Units 119
6.1.3 Proteins, protein domains and other biomolecules 120
6.1.4 Chemicals and solutions 121
6.1.5 Other abbreviations 121
6.2 Acknowledgements 122
6.3 Curriculum vitae 123

6.4 Affidavit 124

List of figures

Figure 1-1: Schematic diagram of the Myc protein 4
Figure 1-2: Schematic diagram of the vertebrate and the *Drosophila* Myc protein 6
Figure 1-3: Myc controls growth in *Drosophila* 7
Figure 1-4: Schematic diagram of insulin/TOR signaling in *Drosophila* and the proposed relationship to Myc 8
Figure 1-5: Structure and function of box C/D and box H/ACA snoRNAs 11
Figure 1-6: Myc controls several components of ribosome biogenesis 13
Figure 1-7: Schematic overview of the different *chinmo* transcripts 14
Figure 1-8: Schematic diagram of the different *chinmo* alleles referring to Figure 1-7 16
Figure 1-9: Chinmo and Myc interact in growth control 17
Figure 4-1: Process of DNA-library preparation for ChIPseq 54
Figure 4-2: Myc binding sites in *Drosophila* cells[3] 57
Figure 4-3: Analysis of Myc binding sites published by Yang *et al*.[3] 60
Figure 4-4: Myc binds U-snoRNA host genes[3] 61
Figure 4-5: Binding of Myc to Uhgs is Max dependent[3] 63
Figure 4-6: Myc binding sites in *Drosophila*[3] 67
Figure 4-7: Myc directly regulates snoRNAs[3] 69
Figure 4-8: Northern blot analysis[3] 71
Figure 4-9: Loss of Uhg1 does not affect its neighboring genes[3] 72
Figure 4-10: Loss of Uhg1 leads to decreased O'-ribose-methylation of 28S rRNA 74
Figure 4-11: Uhg genes affect growth and tumor formation *in vivo*[3] 77
Figure 4-12: *Chinmo* alleles reduce ommatidial number 79
Figure 4-13: Myc and Chinmo interact physically; the BTB-POZ domain and the zinc finger domain are not important for this interaction 81
Figure 4-14: Chinmo and Myc bind to the same target genes 84
Figure 4-15: Chinmo cooperates with Ras^{V12} in the induction of tumors 86
Figure 5-1: Myc acts as a master regulator for ribosome biogenesis[3] 96
Figure 5-2: Model of genetic interactions between Myc and Chinmo 98
Figure 5-3: Model of molecular interactions of Chinmo and Myc 101

List of tables

Table 2-6: List of oligonucleotides 21
Table 2-7: List of primary antibodies 26
Table 2-9: Fly strains 35
Table 3-1: Restriction digest mix 38
Table 3-2: Ligation mix 39
Table 3-3: miScript II RT Kit 40
Table 3-4: Omniscript RT Kit 40
Table 3-5: Standard PCR setup 41
Table 3-6: Standard PCR thermal cycle profile 41
Table 3-7: qRT-PCR/qPCR setup 42

Table 3-8: qRT-PCR/qPCR thermal cycling profile 42
Table 3-9: Megascript T7 kit 44
Table 3-10: Oligo labeling 44
Table 3-11: Effectene transfection mix 46
Table 3-12: Cellfectin transfection mix 46
Table 3-13: Amount of antibodies used for western blot 48
Table 3-14: Reverse transcription mix 52
Table 4-1: ChIP-sequencing reads of S2 cells chipped with mouse α-Myc. 56
Table 4-2: ChIP-sequencing reads of S2 and KC 167 cells chipped with rabbit α-Myc and called binding sites using MACS software 56
Table 4-3: ChIP-sequencing reads of wing imaginal disc cells 58
Table 4-4: Enrichment over IgG in control and Myc depleted cells 62
Table 4-5: Directly Myc-activated genes, sorted by biological category[3] 65
Table 6-1: abbreviations for prefixes and multiplication factors 119

Summary

The correct regulation of cell growth and proliferation is essential during normal animal development. Myc proteins function as transcription factors, being involved in the control of many growth- and proliferation-associated genes and deregulation of Myc is one of the main driving factors of human malignancies.

The first part of this thesis focuses on the identification of directly regulated Myc target genes in *Drosophila melanogaster*, by combining ChIPseq and RNAseq approaches. The analysis results in a core set of Myc target genes of less than 300 genes which are mainly involved in ribosome biogenesis. Among these genes we identify a novel class of Myc targets, the non-coding small nucleolar RNAs (snoRNAs). *In vivo* studies show that loss of snoRNAs not only impairs growth during normal development, but that overexpression of several snoRNAs can also enhance tumor development in a neuronal tumor model. Together the data show that Myc acts as a master regulator of ribosome biogenesis and that Myc's transforming effects in tumor development are at least partially mediated by the snoRNAs.

In the second part of the thesis, the interaction of Myc and the Zf-protein Chinmo is described. Co-immunoprecipitations of the two proteins performed under endogenous and exogenous conditions show that they interact physically and that neither the two Zf-domains nor the BTB/POZ-domain of Chinmo are important for this interaction. Furthermore ChIP experiments and Myc dependent luciferase assays show that Chinmo and Myc share common target genes, and that Chinmo is presumably also involved in their regulation. While the exact way of how Myc and Chinmo genetically interact with each other still has to be investigated, we show that their interaction is important in a tumor model. Overexpression of the tumor-suppressors Ras and Chinmo leads to tumor formation in *Drosophila* larvae, which is drastically impaired upon loss of Myc.

Zusammenfassung

Die korrekte Regulation von Zellwachstum und Proliferation ist von entscheidender Bedeutung für die Entwicklung von Tieren. Myc-Proteine fungieren als Transkriptionsfaktoren, die in die Funktionskontrolle vieler Gene eingebunden sind die eine Rolle bei Zellwachstum und Proliferation spielen. Fehlregulierung von Myc ist ein Hauptfaktor menschlicher Tumorbildung.

Der erste Teil dieser Dissertation beschäftigt sich mit der Identifizierung direkt regulierter Myc Zielgene in *Drosophila melanogaster* durch Kombination von ChIPseq und RNAseq Analysen. Insgesamt wurde eine Hauptgruppe von weniger als 300 Myc Zielgenen identifiziert, von denen der Großteil eine Funktion in der Ribosomen Biogenese hat. Unter diesen Genen haben wir eine neue Klasse an Myc Zielgenen identifiziert, die nicht-codierenden „small nucleolar RNAs“ (snoRNAs). *In vivo* Experimente zeigen, dass der Verlust der snoRNAs nicht nur das Wachstum während der natürlichen Entwicklung beeinträchtigt, sondern auch, dass Überexpression verschiedener snoRNAs die Tumorbildung in einem neuronalen Tumormodel begünstigt. Zusammenfassend zeigen die Daten, dass Myc maßgeblich Ribosomen Biogenese steuert und dass der transformierende Effekt, den Myc in der Tumorentwicklung inne hat, zumindest teilweise durch die snoRNAs gesteuert wird.

Im zweiten Teil der Arbeit wird die Interaktion von Myc und dem Zink-Finger Protein Chinmo beschrieben. Co-Immunoprezipitationen der zwei Proteine die unter endogenen und exogenen Bedingungen durchgeführt wurden zeigen, dass sie physisch miteinander interagieren und dass weder Chinmos Zf-Domänen noch seine BTB/POZ-Domäne für diese Interaktion verantwortlich sind. ChIP-Versuche und Myc abhängige Luciferase-Assays zeigen weiterhin, dass Chinmo und Myc gemeinsame Zielgene besitzen und dass Chinmo darüber hinaus wahrscheinlich auch an ihrer Regulation beteiligt ist. Während der genaue Zusammenhang der genetischen Interaktionen von Myc und Chinmo noch ungewiss ist und weiterer Untersuchungen bedarf, kann gezeigt werden, dass die Interaktion der beiden Proteine in einem Tumormodel eine Rolle spielt. Die Tumorbildung die durch Überexpression des Tumorsuppressors Ras zusammen mit Chinmo hervorgerufen wird, wird durch den Verlust von Myc stark reduziert.

1 Introduction

1.1 Transcription factor Myc

The transcription factor Myc is one of the best characterized genes in the field of biomedical research. Nearly 40 years ago, the first Myc gene was identified as a transforming oncogene in retroviruses leading to *myelocytomatosis* in birds (Sheiness *et al.*, 1978). Since then, more than 26,000 primary and review articles have been published, dealing with Myc (Pubmed, June 2015). In the following years, the cellular homologs in vertebrates, c-, N- and L-Myc, were identified (Vennstrom *et al.,* 1982; Kohl *et al.*, 1983; Nau *et al.*, 1985). Two additional Myc variants, B-Myc and s-Myc, were described in rodents (Ingvarsson *et al.,* 1988; Sugiyama *et al.,* 1989). The different Myc genes encode transcription factors that play essential roles in cell growth, proliferation, apoptosis, cell cycle progression and differentiation (Dang *et al.,* 2006; Vita and Henriksson, 2006). The deregulation of Myc contributes to genomic instability, uncontrolled cell proliferation, immortalization and escape from immune surveillance, leading to the formation of tumors. In the following sections, the vertebrate system is referred to, where not otherwise stated.

1.1.1 **Functional domains of Myc**

The Myc protein contains several domains with various functions that are highly conserved between c-, N- and L-Myc (Meyer and Penn, 2008), and show a moderate to high conservation between different vertebrate species (Atchley and Fitch, 1995; Tansey, 2014). The Myc boxes I and II are located at the N-terminus, whereas Myc box IV is located centrally; the DNA binding domain (basic region) and the dimerization domain (helix-loop-helix and leucine-zipper (bHLH-LZ)) are located at the C-terminus. Myc box III is located centrally (Figure 1-1 A). The Myc boxes I-IV mediate important functions such as Myc-induced apoptosis (Evan *et al.,* 1992), transformation (Stone *et al.,* 1987) and inhibition of differentiation (Freytag *et al.,* 1990). More precisely, Myc box I is essential for Myc's destabilization as it contains two phosphorylation sites, threonine 58 and serine 62 that control ubiquitination (Sears *et al.,* 2000). Myc box II mediates the interaction with partners such as Trrap (McMahon *et al.,* 2000) and TIP48/49 (Wood *et al.,* 2000), and is needed for transformation as well as for transcriptional activation and repression by Myc. The Myc boxes III and IV are essential in modulating Myc-induced apoptosis and transformation (Cowling *et al.,* 2006; Herbst *et al.,* 2005). The basic region (BR) mediates sequence specific binding to DNA (Prendergast *et al.,* 1991), while the HLH-LZ-domain is responsible for interaction between Myc and cofactors such as Max (*Myc associated factor X*) (Blackwood and Eisenman, 1991). In addition, Myc contains a nuclear localization sequence (NLS) which is important for the subcellular localization (Dang and Lee, 1988).

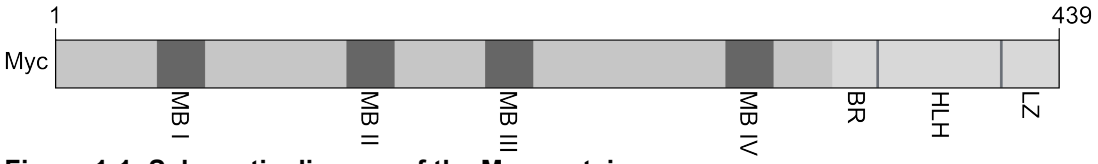

Figure 1-1: Schematic diagram of the Myc protein

A. Myc protein contains several conserved regions, the Myc boxes I, II, III and IV (MB I, II, III, IV), a nuclear localization sequence (NLS), a basic region (BR), a helix-loop-helix motif (HLH) and a leucine zipper (LZ). The human c-Myc consists of 439 amino.

1.1.2 **Transcriptional regulation by Myc**

Several ChIPseq analysis performed in various cell lines (Zeller *et al.,* 2006; Raha *et al.,* 2010; Seitz *et al.,* 2011) revealed that the human genome contains thousands of Myc binding sites and it is assumed that around 15% of all human genes are regulated by Myc (Dang *et al.,* 2006; *Li et al.,* 2003). As described earlier (1.1.1), Myc contains a basic region in the C-terminus which mediates interactions between protein and DNA. This interaction is mainly achieved via a palindromic DNA-sequence (CACGTG) called canonical E-box (enhancer-box) (Blackwell *et al.,* 1990) but Myc can also bind to non-canonical (CANNTG) E-boxes with a lower affinity (Blackwell *et al.,* 1993). In order to bind E-box sequences, Myc needs to heterodimerize with Max via its bHLH-LZ domain. The heterodimer binds to DNA and recruits different co-activator complexes, such as, histone acetyltransferases or ATPases, which can directly bind to Myc via the adaptor protein Trrap (Adhikary and Eilers, 2005). Acetylation of the nucleosomes results in an open chromatin structure and therefore enables the transcription of target genes (Lee and Workman, 2007). Another Myc-dependent mechanism of transcriptional activation works via binding of Myc to the mediator complex and to the transcription elongation factor P-TEFb (*positive transcription elongation factor b*) which enables recruitment of RNA Pol II to the promoter and elongation of the nascent mRNA, respectively (Bouchard *et al.,* 2004; Eberhardy and Farnham, 2001; Rahl *et al.,* 2010).

The process of transcriptional repression by Myc has been less well studied than the process of activation. Myc represses genes by getting recruited to the promoters via further transcription factors such as Sp-1 (*specificity protein-1*) (Gartel *et al.,* 2001) and Miz1 (Wanzel et al., 2003). The best described mechanism involves Miz1 (Peukert *et al.,* 1997). Miz1 activates negative cell cycle regulators such as *CDKN2B, CDKN1A* and *CDKN1B* by binding to their core-promoters (Herold *et al.,* 2002; Staller *et al.,* 2001; Seoane *et al.,* 2002). The expression of these Cdk-inhibitors (*cyclin dependent kinase*) is repressed by binding of Myc-Max complexes to Miz1, leading to the recruitment of repressing co-factors and the displacement of activating co-factors (Lüscher and Vervoorts, 2012).

In recent years, microarrays and next generation sequencing technologies were used to identify Myc regulated genes. It was shown that Myc, when expressed at high levels, sits at nearly all promoters with open chromatin and also binds to many enhancers, independent of E-boxes (Chen *et al.,* 2008; Lin *et al.,* 2012). This is consistent with

earlier studies where it was shown that promoters targeted by Myc are associated with an active chromatin profile, including methylation marks at H3K4 (Guccione *et al.,* 2006). In agreement with these data, Nie *et al.* (2012) and Lin *et al.* (2012) suggested a model where Myc functions as an amplifier of active transcription rather than as a regulator of specific sets of genes. In this model, the transcriptional repression by Myc would be indirect via activation of repressors which are recruited to Myc target genes (Nie *et al.,* 2012). However, Sabo *et al.* (2014) and Walz *et al.* (2014) were able to show that induction of Myc resulted in changes of promoter binding, which correlated with changes of gene expression. Furthermore, stoichiometric binding of Myc and Miz1 (*Myc interacting zinc-finger-protein 1,* see below) at the same promoter suppresses target gene expression (Walz *et al.* 2014), and consequently, transcriptional repression by Myc is not an indirect process. Consistent with earlier publications (van Riggelen *et al.,* 2010; Lee *et al.,* 2012), it was shown that a large fraction of genes regulated by Myc play a role in ribosome biogenesis, RNA-processing and translation while the regulation of other gene sets (e.g. involved in cell adhesion, apoptosis or angiogenesis) depends on Myc levels and promoter affinity (Walz *et al.,* 2014; F. Lorenzin, pers. com.).

1.1.3 **Myc-Max network**

The dimerization between Myc and Max is essential for different biological functions of Myc, such as transcriptional activation and repression of genes. As well as binding to all Myc family members, Max can also homodimerize and interact with proteins of the Mxd-family (Maxd 1-4; Ayer *et al.*, 1993; Hurlin *et al.,* 1995; Zervos *et al.,* 1993), Mnt (Hurlin *et al.,* 1997), and Mga (Hurlin *et al.,* 1999). All of these proteins contain a bHLH-LZ domain and form heterodimers with Max which recognize the same E-box sequences as Myc-Max heterodimers. In contrast to Myc-Max, Max-Mxd and Max-Mnt do not activate but repress the corresponding target genes and they effectively compete with Myc for interactions with Max.

In *Drosophila melanogaster* Myc is represented by a single protein. *Drosophila* Myc (dMyc) is equally similar to all vertebrate Myc paralogs with an overall sequence identity of 26%. In fact, the first *Myc* mutant was described in the 1930's by Calvin Bridges who isolated the mutant and called it *diminutive* (*dm*) for its smaller body size (Bridges 1953). In 1996, *dm* was shown to correspond to a hypomorphic mutation of *Drosophila* Myc (Gallant *et al.,* 1996). Even when dMyc shows only a moderate sequence identity to the vertebrate Myc family, all the domains characterized, including the C-terminal bHLH-LZ-domain, Myc box II and Myc box III (Figure 1-2 B), are highly conserved. The N-terminus of dMyc is considerably longer than that of c-MYC and, like Myc box I, shows poor sequence conservation (Gallant *et al.,* 1996). Not only the domains of Myc are conserved from insects to vertebrates but c-MYC and dMyc proteins can partially substitute each other. *Drosophila* Myc can rescue proliferation defects in murine embryonic fibroblasts that lack endogenous c-MYC (Trumpp *et al.,* 2001); it can cooperate with human Ras^{V12} in transforming rat fibroblasts (Schreiber-Agus *et al.,* 1997) and

substitute for c-MYC in transactivation assays in human cell culture (Gallant *et al.,* 1996). Alternatively, a human c-MYC variant can rescue a lethal dMyc mutant allele (Benassayag *et al.,* 2005).

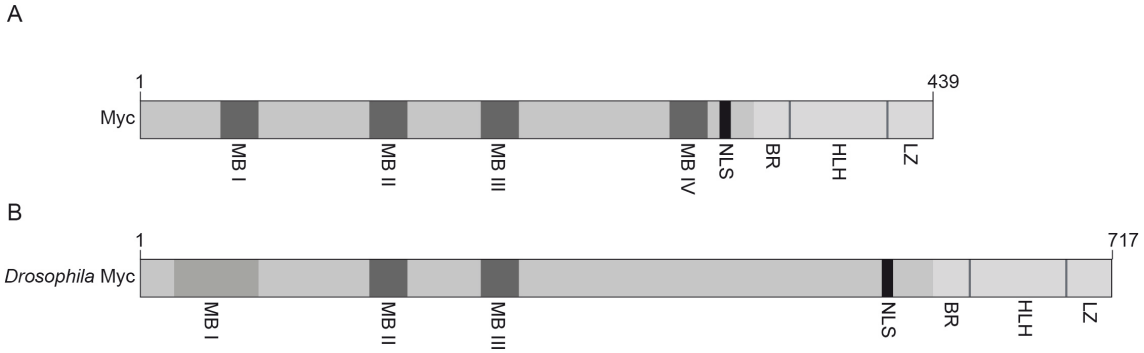

Figure 1-2: Schematic diagram of the vertebrate and the *Drosophila* Myc protein

A/B. Myc proteins contain several conserved regions, the Myc boxes I, II and III (MB I, II, III), a nuclear localization sequence (NLS), a basic region (BR), a helix-loop-helix motif (HLH) and a leucine zipper (LZ).
A. Human c-Myc consists of 439 amino acids and contains additionally Myc box IV (MB IV).
B. Drosophila Myc consists of 717 amino acids.

In *Drosophila* only one homolog for Max (dMax; Gallant *et al.,* 1996; Schreiber-Agus *et al.,* 1997) and one homolog for Mnt (dMnt; Loo *et al.,* 2005) exist. Like dMyc, they show sequence similarity to their vertebrate homologs. dMnt shares the same domains with vertebrate Mnt and Mxd proteins with a higher sequence similarity towards Mnt. These domains are the bHLH-LZ and an N-terminally located Sin3- Interaction domain (SID) (Gallant, 2009). With an overall amino acid sequence identity of 52% and the identical genomic organization, dMax shares the highest conservation with its human counterpart (Gallant *et al.,* 1996; Gallant, 2006).

1.1.4 Growth control in *Drosophila*

One of the most prominent functions of Myc in *Drosophila* is the regulation of growth. Flies carrying the Myc null allele dm^4 show severe growth defects. The mutant larvae hatch at the same time as wildtype animals but fail to undergo normal growth and die early in development (Figure 1-3 B; Pierce *et al.,* 2004). Hypomorphic mutant animals (dm^1, dm^{P0}) undergo normal development, but the resulting normally proportioned adult flies are smaller and carry thin and short bristles (Figure 1-3 A; Johnston *et al.,* 1999). The size reduction in Myc-mutants is based on smaller but not fewer cells (Johnston *et al.,* 1999; Steiger *et al.,* 2008). This stands in contrast to vertebrates, where Trumpp *et al.* (2001) incrementally reduced the *c-myc* expression in mice to zero and observed a reduced body mass due to mulitorgan hypoplasia. Elevated Myc levels on the other hand lead to an increase in cell size by accelerating cellular growth (Johnston *et al.,* 1999). This is accompanied with an increase of nucleoli size and therefore an increase in ribosomal RNA levels (Grewal *et al.,* 2005). Furthermore, overexpression of Myc leads to an augmented adult body size of almost 30% (de la Cova *et al.,* 2004). Myc,

therefore, promotes cell-autonomous growth in part by modulating ribosome biogenesis (0). Another observation which suggests a link between dMyc activity, cell growth and ribosomal proteins are the so-called *Minute* mutations. These ribosomal gene mutations also lead to a smaller body size due to smaller cells and exhibit a thin bristle phenotype comparable to *dmyc* mutants (Marygold *et al.,* 2007).

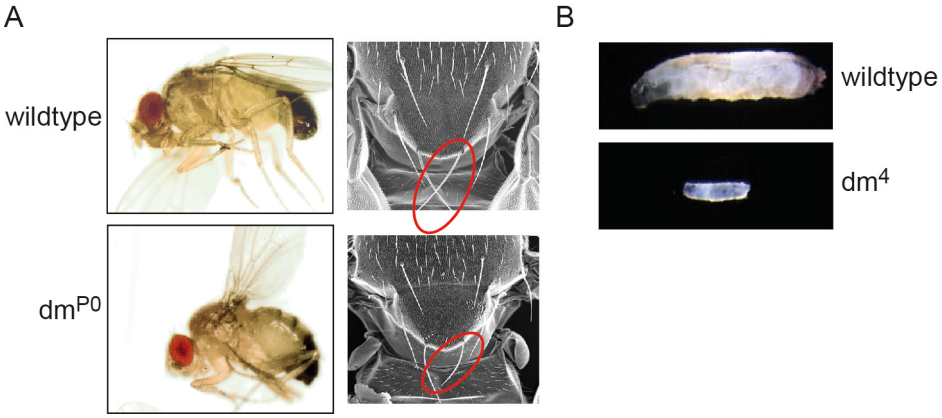

Figure 1-3: Myc controls growth in *Drosophila*

A. Differences in whole body size (left column) and bristle size and structure of an adult wildtype male (upper row) and a hypomorphic Myc mutant male (lower row). Wildtype animals are bigger and their bristles thicker and longer compared to mutant animals (modified from Johnston *et al.,* 1999).
B. Comparison of a wildtype male larva (upper row) with a Myc null mutant larva (lower row) (modified from Pierce *et al.,* 2004).

Myc interacts with other pathways known to control growth, like the TOR and the insulin signaling pathways. The insulin receptor (Inr) and the target of rapamycin (TOR) signaling pathway have been shown to mediate nutrient dependent growth and both pathways have been shown to influence Myc levels in the cell (Parisi *et al.,* 2011; Li *et al.,* 2010). In contrast to vertebrates, *Drosophila* has a single insulin receptor (InR), which is bound by a group of *Drosophila* insulin-like peptides (DILPs) in response to dietary proteins. These DILPs trigger growth by recruitment of Chico, the *Drosophila* insulin receptor substrate (IRS) protein, and initiate a conserved phosphorylation cascade that activates the phosphatidylinositol 3-kinase (PI3K) and Akt kinase signaling pathway (Böhni *et al.,* 1999; Brogiolo *et al.,* 2001; Edgar, 2006). One downstream effector is dFOXO (*forkhead transcription factors of the O class*), which is active under starvation conditions (Puig and Tjian 2006) and represses Myc mRNA expression in muscle cells, whereas it is required in the fat body to maintain constant myc levels (Teleman *et al.,* 2008). The target genes of FOXO are involved in various processes such as cell cycle arrest, DNA repair, cellular differentiation and apoptosis (Salih and Brunet, 2008). Mutations in components of the InR pathway lead to a change in cell size and number (Brogiolo *et al.,* 2001).

The TOR signaling pathway acts in parallel with the PI3K/Akt signaling pathway (Jacinto and Hall, 2003) and is activated in a cell autonomous manner in response to extracellular nutrients and amino acids. Additionally, TOR can be activated as a downstream target of the PI3K/Akt pathway. Akt activates TOR by phosphorylating the tumor sup-

pressor genes TSC1 and TSC2 which inhibit the TOR activator Rheb (de Virgilio and Loewith, 2006). TOR regulates growth through downstream effectors including the ribosomal protein kinase S6K (*p-70-S6 ribosomal protein kinase*) and the eIF4E (*eukaryotic initiation factor-4E*) inhibitor 4E-BP (*initiation factor 4E binding protein*) which is a common target of the PI3K/Akt signaling pathway (Jünger *et al.*, 2003). S6K balances Insulin and TOR activities by a negative feedback mechanism which is activated when TSC1 is highly activated (Kockel *et al.,* 2010). The TOR pathway regulates TIF-IA (*transcription initiation factor-1A*) recruitment to ribosomal DNA (rDNA) (Grewal *et* al., 2007) and induces the activation of several Myc targets which are involved in ribosome biogenesis (Li et al., 2010). Furthermore, TOR stabilizes Myc, probably through inhibition of GSK3β (Glycogen synthase kinase 3 beta) via S6K and the same was found for the InR/PI3K pathway (Parisi *et al.,* 2011). Additionally a strong correlation between TOR pathway and Myc target genes exist (Parisi *et al.,* 2011), suggesting that Myc acts downstream of InR/PI3K and TOR signaling. Loss of TOR or S6K leads to a reduction in body size which is based primarily on the reduction in cell size and impairment in cell proliferation (Oldham *et al.,* 2000; Zhang *et al.,* 2000). Figure 1-4 shows a schematic overview of the insulin/TOR signaling pathway in *Drosophila*.

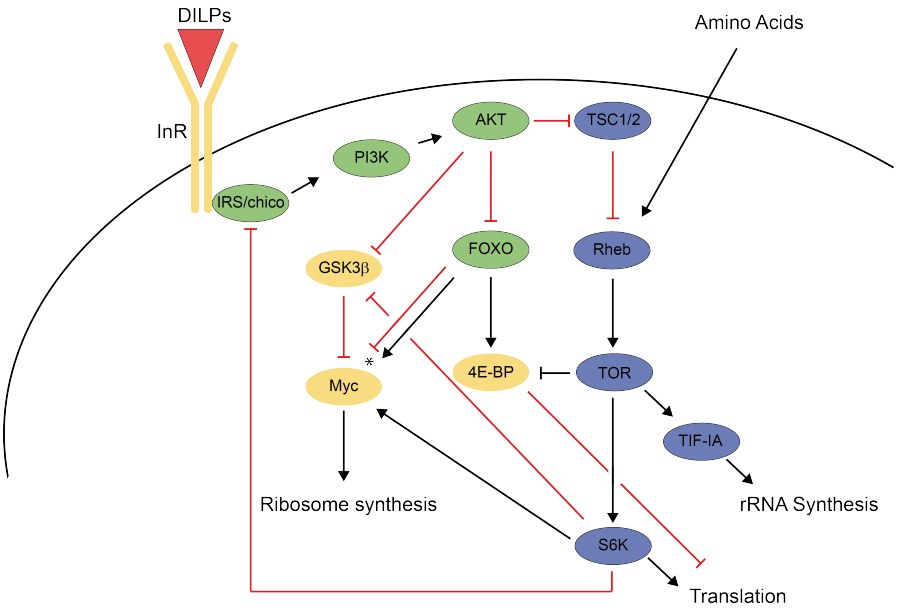

Figure 1-4: Schematic diagram of insulin/TOR signaling in *Drosophila* and the proposed relationship to Myc

The insulin/TOR signaling pathway controls growth via transcriptional effects through the nuclear factors Myc, FOXO and TIF-IA, which together regulate the expression of ribosome biogenesis and protein synthesis genes. Arrows and bars indicate positive and negative regulation, respectively. DILPs: *Drosophila* insulin-like peptides; InR: insulin receptor; IRS: insulin-receptor substrate; PI3K: phosphatidylinositol-3 kinase; TSC1/2: tuberous sclerosis 1/2; Rheb: Ras homolog enriched in brain; S6K: p-70-S6 ribosomal protein kinase; TOR: target of rapamycin; GSK3β: Glycogen synthase kinase 3 beta; FOXO: forkhead transcription factors of the O class
*tissue specific activation/repression

1.2 Ribosome biogenesis

The cellular processes of growth and cell division are tightly linked to ribosome biogenesis as the ribosomes provide the basis for protein production (Lempiäinen and Shore, 2009). The process of ribosome synthesis requires a lot of energy and the coordinated regulation of all three RNA polymerases. Ribosomes consist of four structural RNA components, 5S, 5.8S, 18S and 28S rRNAs which are associated with more than 70 ribosomal proteins (Tschochner and Hurt, 2003). The 5.8S, 18S and 28S rRNAs are encoded by ribosomal DNA (rDNA) in the nucleolus (Roeder and Rutter, 1970) and are transcribed by RNA polymerase I (Pol I), while the 5S rRNA is encoded outside the nucleolus by RNA polymerase III (Pol III) (Weinmann and Roeder, 1974). Together with approximately 80 different ribosomal proteins and over 200 additional proteins and non-coding RNAs (ribosome biogenesis, or RiBi factors) (Lempiäinen and Shore, 2009) which are transcribed by RNA polymerase II (Pol II), a pre-mature small (40S) and a pre-mature large (60S) ribosomal subunit are assembled in the nucleus and transported into the cytoplasm. After dissociation of the non-ribosomal factors, the mature 40S and 60S subunits form the 80S ribosome together with mRNA (Tschochner and Hurt, 2003). The RiBi factors are important for processing, assembly, modification and nuclear import-export reactions and can consist of simple proteins, heteromers or large complexes of molecules like the snoRNPs (Loewith, 2010).

1.2.1 Function of snoRNPs

Before the pre-rRNAs are further processed to mature rRNA, and undergo a complex pattern of nucleoside modifications, the 3'-end is cleaved by endo- and exonucleases allowing the addition of the poly(A) tail. The two main types of modifications are methylation of the 2'-O-ribose and pseudouridylation (Figure 1-5 A). In humans, there are around 100 pseudouridines and 100 2'-O-methyl groups in 5.8S, 18S and 28S rRNAs together (Kiss, 2001).These modifications are directed by two major classes of small nucleolar ribonucleoprotein particles (snoRNPs). Each snoRNP consists of a set of proteins, common to each class of family, and a small nucleolar RNA (snoRNA). The snoRNPs are divided into so-called box C/D and box H/ACA snoRNPs. Box C/D snoRNPs guide methylation of the 2'-O-ribose, whereas box H/ACA snoRNPs are responsible for pseudouridylation. Fibrillarin, Nop56p, Nop58p and 15.5 kDA are essential partner proteins for box C/D snoRNPs (Kiss, 2001) with Fibrillarin being the methyltransferase enzyme that is responsible for the addition of a methyl group to the 2'-O-ribose of the target nucleotide. Dyskerin, Gar1p, Nhp2p and Nop10p are common to box H/ACA snoRNPs (Henras *et al.,* 1998; Watkins *et al.,* 1998). The pseudouridine synthase Dyskerin catalyzes the conversion of uridine to pseudouridine. The associated snoRNAs, which range from 60 to 300 nucleotides in length, guide the modification of one or a maximum of two sites, and therefore one rRNA is predicted to associate with approximately 150-200 snoRNAs (Kiss, 2001; Bachellerie *et al.,* 2002). As stated above, snoRNAs are divided into two classes, box C/D (SNORA) and box H/ACA (SNORD) snoRNAs, which specify the modified sites. Box C/D snoRNAs are responsi-

ble for directing 2'-O-ribose-methylation and contain two conserved sequences, box C (RUGAUGA, R stands for any purine) and box D (CUGA), which are located close to the 5' and 3' ends, respectively (Figure 1-5 B). Additionally the box C/D snoRNAs contain less conserved copies of both boxes, box C' and box D' which are located centrally (Kiss-László *et al.*, 1998). The box C/D snoRNAs contain one or sometimes two elements of 10-21 nucleotides which are complementary to a site of rRNA 2'-O-ribose-methylation (Bachellerie *et al.,* 1995). The group of box H/ACA snoRNAs is required for pseudouridylation of target RNAs. They consist of two hairpins and two short single-stranded regions (Figure 1-5 B) which contain the conserved box H (ANANNA, N indicates any nucleotide) and box ACA (a trinucleotide, located always three nucleotides away from the 3' end) (Ganot *et al.,* 1997b). The guide sequences are located in one or both of the hairpin loop domains and by forming two helix structures with the target rRNA, the snoRNA guides the conversion from an unpaired uridine residue of the rRNA sequence to pseudouridine (Ganot *et al.,* 1997a). The distance between the target uridine and the location of the H or ACA box of the snoRNA (14-16 nucleotides) is important in determining the correct pseudouridylation site (Bortolin *et al.,* 1999).

Besides their function in rRNA modification, snoRNAs have been found to modify segments in small nuclear RNAs (snRNAs) involved in intermolecular RNA-RNA as well as RNA-Protein interactions. This suggests that the snoRNAs play an important role in splicing control (Bachellerie *et al.,* 2002). Additionally, snoRNAs modify and process tRNAs (Zemann *et al.,* 2006; Clouet d'Orval *et al.,* 2001) and probably even mRNAs (Cavaillé *et al.,* 2000). Bioinformatic approaches identify a growing number of so-called "orphan" snoRNAs which lack complementarities to rRNAs, snRNAs, tRNAs or any other known stable RNAs (Hüttenhofer *et al.,* 2001). This might indicate that novel roles for nucleotide modifications mediated by snoRNAs have yet to be discovered. Furthermore individual snoRNAs were described as having a function in mRNA editing (Bachellerie *et al.,* 2002) and miRNA production (Ender *et al.,* 2008; Taft *et al.,* 2009).

The mode of expression of the snoRNAs is uniquel. In yeast and plants, most snoRNAs are cleaved from mono-, di- or polycistronic RNA transcripts which are processed by exo- and endonucleases. In metazoans No polycistronic transcripts have been detected (Tollervey and Kiss, 1997) and independently transcribed snoRNAs are rare. The vast majority is encoded within introns and processed from pre-mRNA introns by exonucleolytic digestion of the debranched lariat. Many snoRNAs are embedded within introns of genes that encode for proteins which themselves are involved in ribosome biogenesis (Tollervey and Kiss, 1997). Some snoRNA host genes contain multiple snoRNAs in their intronic sequences but do not code for proteins (Tycowski *et al.,* 1996). In *Drosophila* seven of those non-protein coding host genes exist, numbered 1-5, 7, and 8, the so-called Uhgs (from the originally identified *U22 host genes*) (Tycowski *et al.,* 1996; Tycowski and Steitz, 2001; Huang *et al.,* 2005). The gene formerly called Uhg6 is now known as Nop60B. Up to 16 snoRNAs can be encoded in one Uhg, resulting in a total number of 48 snoRNAs for the previously described Uhg genes.

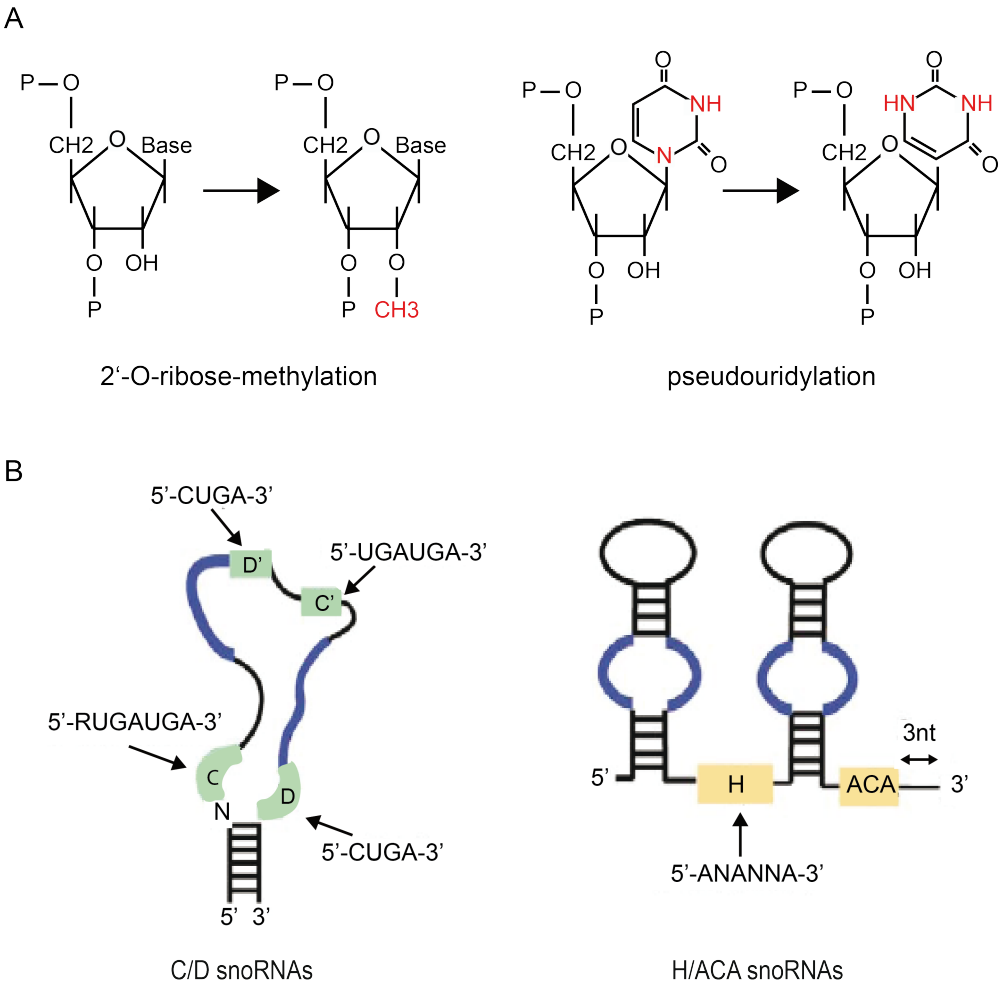

Figure 1-5: Structure and function of box C/D and box H/ACA snoRNAs

A. 2'-O-ribose-methylation: a methyl group is added to the 2' hydroxyl group of the ribose moiety of a nucleoside. Pseudouridylation: pseudouridine is synthesized from uridine via tha action of pseudouridine synthases.
B. Schematic secondary structures of the C/D and H/ACA classes of eukaryotic snoRNAs. The conserved motifs of boxes C, D, C', D', H and ACA are indicated (in green and orange boxes, respectively). The sequence tracts complementary to the specific RNA target (thick blue lines) are shown. R is a purine and N stands for any nucleotide (adapted from Bachellerie *et al.*, 2002).

1.2.2 The role of snoRNAs in cancer

For many years snoRNPs have been considered to be important elements in the protein synthesis machinery fulfilling exclusively housekeeping functions. Recent publications, however, point to a possible role for snoRNAs in controlling cell behavior, and argue that snoRNA dysfunction might contribute to oncogenesis (Williams and Farzaneh, 2012; Martens-Uzunova *et al.,* 2013). The box H/ACA snoRNA h5sn2, which is significantly downregulated in human meningiomas compared to normal brain tissue, was the first snoRNA that was linked to cancer (Chang *et al.,* 2002). Some years later, the box C/D snoRNA U50 was found to be transcriptionally downregulated in prostate cancer (Dong *et al.,* 2008) and breast cancer cells (Dong *et al.,* 2009). On the other hand, certain snoRNAs were shown to be elevated in tumor tissue compared with their normal counterparts. SNORA 42, a box H/ACA snoRNA, for example, is frequently

overexpressed in non-small-cell lung cancer (NSCLC) and SNORA 42 expression levels are inversely correlated with survival (Liao *et al.,* 2010; Mei *et al.,* 20012). In other studies, several snoRNAs (e.g. SNORA 17C and SNORD 116) were found to be overexpressed in neuroblastomas with N-Myc amplification (Schramm *et al.,* 2013), in acute leukemias (Valleron *et al.,* 2012), and metastatic prostate cancer (Martens-Uzunova *et al.,* 2012). Together, these studies show that snoRNAs might be of functional importance in cancer since they could either promote tumor development or act as tumor suppressors.

1.2.3 **Control of protein production by Myc**

One of the most important evolutionarily well-conserved functions of Myc is the process of cellular growth (0). Myc affects cell growth, but also other processes like cell cycle progression and differentiation, partially by increasing protein synthesis. Therefore, Myc stimulates a number of genes essential for ribosomal biogenesis and protein translation, including ribosomal proteins. In vertebrates, heterodimers of c-Myc and Max are associated with E-box binding sites in the ribosomal DNA (rDNA) promoter and terminator regions. Myc recruits the cofactor Trrap, which leads to an increase in histone acetylation (Arabi *et al.,* 2005) and might, therefore, activate the transcription of rRNA. Additionally, Myc recruits the RNA Pol I cofactors *upstream binding transcription factor* (UBF) and *selectivity factor 1* (SL1) which are both essential for enhancement of rDNA transcription (Poortinga *et al.,* 2004; Grandori *et al.,* 2005). While UBF stimulates the transition from transcriptional initiation to elongation and thus activates RNA Pol I transcription (Panov *et al.,* 2006), SL1 stabilizes UBF binding and directs RNA Pol I pre-initiation complex formation on the rDNA (Friedrich *et al.,* 2005). UBF itself is a Myc target gene and is regulated in a RNA Pol II dependent manner (Poortinga *et al.,* 2004). In contrast to vertebrates, the *Drosophila* rDNA locus contains no canonical E-boxes, but dMyc is an important regulator of rRNA synthesis as well. However, the Myc-dependent regulation of rRNA synthesis by RNA Pol I is most probably indirect since dMyc induces an increase in levels of the RNA Pol I transcriptional machinery, for example of TIF-1A and RpL135 (Grewal *et al.,* 2005; Grewal *et al.,* 2007).

Apart from the regulation of RNA Pol I, Myc activates transcription of ribosomal protein genes as well as of non-ribosomal protein genes involved in ribosome biogenesis via RNA Pol II (Coller *et al.,* 2000). These include small ribosomal subunit (RPS) and large ribosomal subunit (RPL) proteins, as well as proteins required for ribosome assembly and processing, like nucleolin (NCL1) and nucleophosmin (NPM1). Also proteins that modify ribosome activity like the upstream growth signaling factor S6 kinase (S6K) or proteins involved in nucleolar functions such as fibrillarin (fib) (van Riggelen *et al.,* 2010) are among Myc's target genes. The transcription of ribosome components by RNA Pol II is stimulated by Myc-Max heterodimers (van Riggelen *et al.,* 2010).

In addition to RNA Pol I and Pol II, Myc enhances transcription of 5S rRNA, transfer RNA (tRNA) and other small RNA genes via the RNA Pol III transcription apparatus (Gomez-Roman *et al.,* 2003). In *Drosophila* it was shown that RNA Pol III transcribed

target genes, such as 5S rRNA, snoRNA U3 and $tRNA^{Leu}$, are activated by dMyc and that this regulation is Max-independent (Steiger *et al.,* 2008). Activation of Pol III is achieved through binding of Myc to the transcription factor IIIB- (TFIIIB) component Brf, which is responsible for recruiting Pol III to its target promoters (Gomez-Roman *et al.,* 2003; Steiger *et al.,* 2008). Besides Myc's function in the regulation of ribosomal proteins, RNA and cofactors Myc influences mRNA translation by regulating the transcription of elongation and translation initiation factors (Boon *et al.,* 2001). The translation initiation factors eIF4E and eIF4A are required for CAP-dependent translation (Schmidt, 2004), whereas eIF5A was shown to act as a translation elongation factor (Gregio *et al.,* 2009; Saini *et al.,* 2009). By regulating translation and ribosome biogenesis, Myc controls protein production. Figure 1-6 summarizes Myc's control of ribosome biogenesis commonly accepted in 2010 when I commenced this work. It remains to be discussed if the regulation of the previously specified factors involved in ribosomal biogenesis completely explains the influence of Myc on ribosome biogenesis and translation.

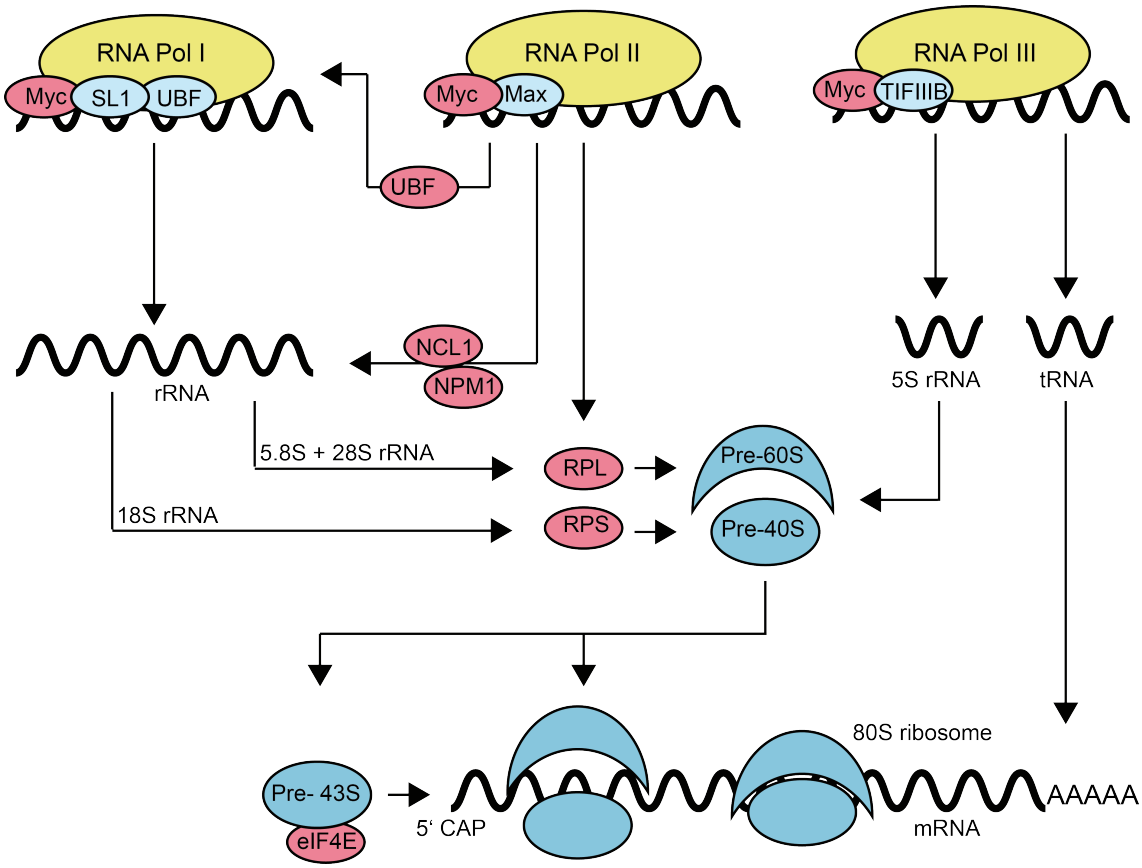

Figure 1-6: Myc controls several components of ribosome biogenesis

In vertebrates, Myc enables the transcription of rDNA via RNA Pol I, by recruiting cofactors such as UBF (*upstream binding transcription factor*) and SL1 (*selectivity factor*). The Myc-Max heterodimer stimulates transcription of ribosomal protein genes and other genes essential for rRNA processing and export via RNA Pol II, such as nucleolin (NCL1), nucleophosmin (NPM1) or UBF. Independently of Max, Myc activates transcription of 5S rRNA and tRNAs through RNA Pol III by recruiting TFIIIB (*transcription factor IIIB*) (modified from van Riggelen *et al.,* 2010).

1.3 Myc-interactors: The BTB-Zf protein Chinmo

One objective of this work was to understand how Myc fulfills its functions and what other factors are involved in these mechanisms. This was attempted by characterizing a previously identified Myc-interacting protein, Chinmo (*chronologically inappropriate morphogenesis*). The BTB-zinc finger (*Broad complex, Tramtrack, Bric à Brac*) protein Chinmo was described for the first time by Zhu *et al.* (2006) who found it in a screen for genes required for temporal identity of mushroom body neurons in *Drosophila*. It was also found to be an effector of the JAK/STAT pathway and involved in the proliferation of mature hemocytes (Flaherty *et al.,* 2010). Additionally, it was shown to regulate neoplastic tumors in *Drosophila* together with Ras^{V12} (Doggett *et al.,* 2010). Furthermore it was characterized in two independent screens performed in the Hafen and the Gallant laboratories (Sulzer, 2003; Schwinkendorf, 2008) aimed to identify genes involved in growth control and novel Myc interacting proteins, respectively.

The Chinmo gene spans a total length of 45,368 base pairs. Four transcripts (RH; RD; RG; RA) code for a protein of 604 amino acids, while two other transcripts (RE; RF) give rise to a protein of 840 amino acids (flybase.org, FB release 2015_03; Figure 1-7). A BTB/POZ- (*Broad complex, Tramtrack, Bric à Brac* / *poxvirus and zinc finger*) domain is located at the N-terminus and at the C-terminus, two C_2H_2 zinc-fingers (Zf) are present. BTB-domains mediate protein-protein interactions, including dimerization, recruitment of transcriptional repressors to DNA and protein degradation (Bardwell and Treismann, 1994; Stogios *et al.,* 2005). Zinc fingers are involved in DNA binding but can also bind to RNA and proteins (Razin *et al.,* 2012). Classical zinc-fingers contain an α-helix where a single zinc atom is hold in complex by two cysteines and histidines (C_2H_2). Based on the presence of BTB-Zf domains and the nuclear localization (Zhu *et al.,* 2006) Chinmo is likely to be a transcriptional regulator.

Figure 1-7: Schematic overview of the different *chinmo* transcripts[1]

The transcripts RD, RG, RH and RA contain the same ORF, coding for a protein of 604 amino acids. The transcripts RE and RF contain an ORF, which codes for a protein of 840 amino acids. Numbers indicate nucleotides (nt) and amino acids (aa). Purple boxes show the open reading frame (ORF) and black boxes the untranslated region (UTR). The black line represents introns.

[1] flybase.org; FB release 2015_03

1.3.1 **The role of Chinmo in brain development**

As mentioned above, Chinmo was first described to play a role in brain development (Zhu *et al.,* 2006). In the EMS (*ethyl methanesulfonate*) screen which was performed to identify genes that alter temporal identity in mushroom body neurons, a mutant was found which was called chronologically inappropriate morphogenesis (*chinmo*) due to the observed phenotype. Wildtype neuroblasts of the fly brain mushroom body produce four different types of neurons: γ, α'β', late-born pioneer-αβ (pαβ) and αβ neurons (Lee *et al.,* 1999). Mosaic animals, whose mushroom bodies are mutant of Chinmo have fewer early-born γ and α'β' neurons and more late-born pαβ and αβ neurons, which fits the expression profile of Chinmo in neurons. While Chinmo is strongly expressed in early-born γ neurons, the expression level dwindles along the lineage and is undetectable in the latest-born pαβ− and αβ− neurons (Doe*,* 2006).

Chinmo was shown to be a functional effector of the JAK/STAT pathway in eye development and stem cell self-renewal. In a genome-wide expression study on eye discs with elevated Stat92E levels, *chinmo* was identified as a new Stat92E target gene (Flaherty *et al.,* 2009). Additionally, it was found in a micro-array screen for JAK/STAT target genes in adult testis (*CG31666*; Terry *et al.,* 2006). Further studies confirmed that *chinmo* is a cell-autonomous downstream mediator of Stat92E. Loss of either Stat92E or Chinmo in the eye-imaginal disc, combining ey-FLP and *Minute* techniques (Morata and Ripoll, 1975) leads to defects in eye progenitor cells, which results in malformed head capsules and eyes, whereas overexpression of either of them in eye-imaginal discs (ey-FLP) results in blood cell tumors (Flaherty *et al.,* 2010). Chinmo as well as Stat92E are expressed in GSCs (*germline stem-cells*) and in CySCs (*cyst stem-cells*) in gonads and Chinmo is required for the self-renewal of CySCs, but not of GSCs. Furthermore, it plays an important role in the inhibition of CySC differentiation and in the signal transduction form CySCs to GSCs. This process requires the BTB and the Zf domains of Chinmo, suggesting that Chinmo's main functions in this process are transcriptional repression and protein degradation (Flaherty *et al.,* 2010). Recent publications additionally stated that transformation of testis somatic stem cells into their ovarian counterparts is prevented by Chinmo (Ma *et al.,* 2014).

1.3.2 **Chinmo regulates growth**

Chinmo was already identified in a screen for growth-defective mutants (Sulzer, 2003). Stocks of flies with bigger (bigheads) or smaller (pinheads) heads were established and mapped. One complementation group with three alleles was shown to affect the CG31666/ chinmo gene, resulting in pinheads. The three alleles have either a mutation in the zinc finger domain (*chinmo*^{110}) or lack it completely (*chinmo*^{108}*, chinmo*^{134}). The mutation 110 is a base substitution from cytosine to thymine leading to an amino acid alteration from histidine (CAT) to tyrosine (TAT) at the first histidine of the first zinc finger domain. The *chinmo*^{108} allele has a deletion of 11bp which leads to a frame shift and a stop after 247 amino acids. *Chinmo*^{134} has again a base substitution from cytosine to thymine leading to an alteration from glutamine (CAG) to a stop codon (TAG),

resulting in a protein of only 126 amino acids (Figure 1-8). Sections of adult heads, being homozygous mutant for one of the alleles, using ey-FLP, showed that the reduction in head size is based on a cell number reduction and not on cell size reduction. In another screen Chinmo was found to interact with Myc. This screen was performed to search for novel components of the “Myc pathway” and was based on the dominant genetic interaction between the hypomorphic allele *dm*^{P0} and the transcription cofactor Tip49/Pontin (Bellosta *et al.,* 2005). Animals carrying *dm*^{P0} are normally patterned and display only moderate growth defects, whereas heterozygosity for the Myc cofactor Pontin shows no effect in a wildtype background. Flies being heterozygous mutant for Pontin in a *dm*^{P0} background are characterized by delayed development, poor survival and, in particular, reduced size and irregular shape of the eye. In total, 605 deficiency lines were tested in the *dm*^{P0} background (*w dm*^{P0} *tub*-FRT-dMyc-FRT-GAL4 *ey*-FLP) and the deficiency [Df(2L)Exel6005] was found to cause the characteristic eye defects (Schwinkendorf, 2008). Further investigations revealed chinmo as the responsible gene. The effects on developmental timing and eye size were also observed with the three different Chinmo alleles and were even more dramatic in a Myc null-mutant background (*dm*^{4}).

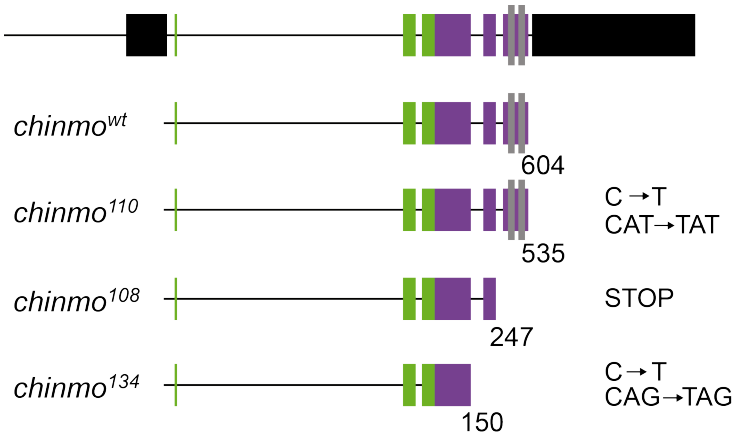

Figure 1-8: Schematic diagram of the different *chinmo* alleles referring to Figure 1-7

The diagram refers to the Chinmo ORF containing 604aa (RD, RG, RH, RA). *Chinmo*^{110} has a C-T transition in the first zinc finger that changes the first conserved histidine to a tyrosine. *Chinmo*^{108} carries a deletion after the BTB/POZ domain, followed by a frame-shift and a premature stop codon and the allele *chinmo*^{134} contains a C-T transition, which leads to a premature STOP. The BTB/POZ domain is shown in green and the two zinc finger domains in grey. The numbers indicate the amino acid coordinates of the mutant codons (modified from Schwinkendorf, 2008).

Developmental delay and eye size reduction are even enhanced when both Myc and Chinmo are completely eliminated. While loss of either Myc or Chinmo protein in the eye discs allows normal development that results in normal shaped eyes, the double mutants are fully lethal and generate only rudimentary heads (Figure 1-9 A; Schwinkendorf, 2008). Ubiquitous expression of Chinmo by *armadillo* or *tubulin* promoters, or overexpression in specific tissues under the control of *GMR* or *apterous* (eye and dorsal compartment of the wing disc), results in the death of the fly. Most animals died at early pupal stages (Schwinkendorf, 2008). Overexpression of Chinmo in the head using ey-FLP in a *dm*^{4} or *dm*^{P0} background, however, leads to an increase in

survival rate, indicating that Chinmo requires Myc to be fully active. The harmful effect of Chinmo overexpression can also be seen on the cellular level, where overexpression of Chinmo reduces clone area which is presumably a consequence of apoptosis. Therefore, it seems that Chinmo's ability to induce apoptosis is dependent upon Myc on the cellular as well as the organismal level. Chinmo is not only dependent on Myc for its full activity. Overexpression of Myc in cells normally leads to an increase in cell size, however, Myc cannot induce growth in clones mutant for Chinmo (Figure 1-9 B, B'). Since part of Myc's activity requires the association with Chinmo, and vice versa, it is very likely that Myc and Chinmo fulfill partially redundant functions in growth and development of the head. In summary, the genetic data by D. Schwinkendorf indicate a close functional interaction between Chinmo and Myc, indicating that both proteins might be transcription factors and might share common target genes.

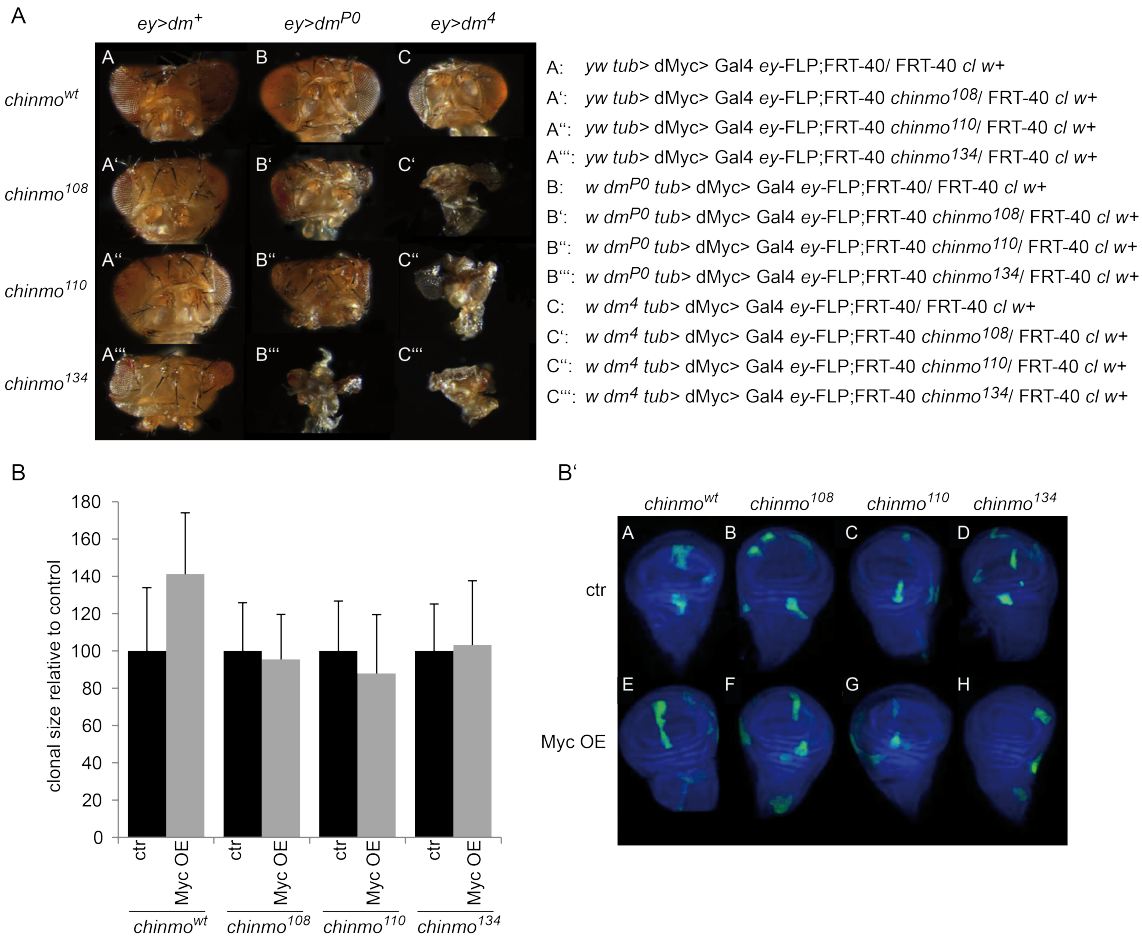

Figure 1-9: Chinmo and Myc interact in growth control

A. Phenotypes of homozygous *chinmo* mutant eyes in dm^{+} (A-A'''), dm^{P0} (B-B''') or dm^{4} background (C-C'''). The corresponding genotypes are depicted on the right.
B. Size of clones overexpressing dMyc relative to control clones. Clonal size is increased upon overexpression of dMyc (2nd bar) in $chinmo^{wt}$ clones; however dMyc cannot induce growth in a Chinmo mutant background.
B'. Clones homozygous mutant for the different *chinmo* alleles (shown in green) in a Myc wt (B, C, D), and in a Myc overexpression background (F, G, H). Size of clones was measured and the ratio to control clones is shown in B.
Modified from Schwinkendorf, 2008

1.4 Objectives of the thesis

Growth control is one of the most essential processes in animal development. It is dependent on the correct regulation of the transcription factor Myc. Similarly, enhanced activation of Myc is one of the main driving factors in human tumors. To understand how Myc regulates growth in normal and pathological situations, it is essential to know Myc's target genes and partner proteins. While three different proteins of the Myc family of proto-oncogenes, c-, N- and L-MYC, exist in vertebrates, only a single Myc protein exists in insects, qualifying *Drosophila* as an easier model organism to study Myc's function.

(1) Several publications have shown that Myc is capable of controlling a large number of genes in vertebrates, but the number of Myc targets in *Drosophila* is still unclear. Myc regulated genes in *Drosophila* have been described in the past, but these studies do not include non-protein coding genes or address which genes are regulated by direct Myc binding. The first aim of this thesis was to establish ChIPseq analysis for *Drosophila* cells to get a comprehensive list of direct Myc targets. To investigate, which of the Myc bound genes are also regulated by Myc, the results of the ChIPseq analysis will be combined with data sets obtained from RNAseq analysis. RNAseq was performed by M. Stauch and will be briefly addressed in this thesis for completeness of content. After validating direct Myc regulated genes, the role of interesting new candidates should be studied in growth control *in vivo*.

(2) The transcriptional regulation by Myc involves the interaction with different co-activators and co-repressors. D. Schwinkendorf found a new potential co-activator of Myc in a genetic screen searching for Myc interacting proteins. Chinmo was shown to be involved in growth control and is likely to act with Myc in partially redundant pathways. To study whether Chinmo and Myc physically interact, co-immunoprecipitations are performed, including Chinmo mutants lacking its interaction domains, the zinc-finger and the BTB/POZ domains. Furthermore, it will be investigated if Chinmo and Myc share common target genes and if Chinmo and Myc also interact in tumor development.

2 Materials

2.1 Strains and cell lines

2.1.1 Bacterial strains

DH5α	*Escherichia coli*; chromosomal Genotype: F^-, φ80d*lacZ*ΔM15, Δ(*lacZYAargF*) U169, *deoR*, *recA*1, *endA*1, *hsdR*17(rk^-, mk^+), *phoA*, *supE*44, λ-, *thi*-1, *gyrA*96, *relA*1; for generation of plasmids
XL1 blue	*Escherichia coli; recA1, endA1, gyrA96, thi-1, hsdR17, supE44, relA1, lac* [*F' proAB lacIqZΔM15 Tn10(Tetr)]*; for generation and amplification of plasmids
BL21	*Escherichia coli*; chromosomal Genotype: B, F^-, *dcm, ompT, hsdS* ($r_B^-m_B^-$) gal [$malB^+$] $_{K-12}$ (λ^S) ; for expression of GST fusion proteins

2.1.2 *Drosophila melanogaster* cell lines

Drosophila Schneider 2 cells	S2 cells (Schneider, 1972)
Kc167	Kc cells (Echalier and Ohanessian, 1969) Kindly provided by Aurelio Teleman
S2pmt Myc	S2 cells, containing a metallothionein promoter and a HA-Myc construct; inducible upon $CuSO_4$ addition Kindly provided by Laura Johnston

2.2 Cultivation media and supplements

2.2.1 Media and antibiotics for bacterial cell culture

LB-medium	10% (w/v) bacto trypton 0.5% (w/v) yeast extract 1% (w/v) NaCl

LB-agar	LB-medium
	1.2% (w/v) Bacto-Agar
	autoclaved, cooled down to 50°C, 20 ml poured into 10 cm dishes

The following antibiotics were added to the LB-medium or the LB-agar depending on the resistance gene of the used DNA-plasmid

Ampicillin	100 µg/ml

2.2.2 **Media for cell culture**

The basal Schneider's insect medium was purchased from Sigma.

Fetal bovine serum (*fetal bovine serum*, FBS; PAN Biotech) was heat inactivated for 30 min at 56°C before use.

Schneider's insect medium	10% (v/v) FBS
	1% (v/v) Penicillin/Streptomycin (100.000 U/ml, PAN Biotech)
Freezing medium	45% (v/v) full medium
	45% (v/v) conditioned medium
	10% (v/v) DMSO

2.2.3 **Further supplements**

Blasticidin S (InvivoGen)	5-10 µg/ml
	Selection of stably transfected cell lines
$CuSO_4$	1 mM
	Induce expression of the stable transfected plasmids

2.3 Nucleic acids

2.3.1 **Oligonucleotides**

DNA-oligonucleotides were synthesized by Sigma (for = forward; rev = reverse). Oligonucleotides for ChIP and quantitative RT-PCR were designed with the help of the Primer3 (http://bioinfo.ut.ee/primer3-0.4.0/). Quantitative RT-oligonucleotides are all intron-spanning to avoid amplification of genomic DNA.

Table 2-1: List of oligonucleotides

Name	Application	5‘ to 3‘
Myc_qPCR-2 for	qRT PCR	CAACGATATGGTGGACGATG
Myc_qPCR-2 rev	qRT PCR	CACGAGGGATTTGTGGGTAG
Uhg1_qPCR for	qRT PCR	AGAAATGCGGTCAAGTTTGG
Uhg1_qPCR rev	qRT PCR	CCTGCGTTCCCGTTTAACTA
Uhg2-2_qPCR for	qRT PCR	GTTGAGACACCTTGGGCACT
Uhg2-2_qPCR rev	qRT PCR	TGCAGCTGGACCCATACATA
Uhg3_qPCR for	qRT PCR	GGGACCAACCAGCATGGGAA
Uhg3_qPCR rev	qRT PCR	ACCATTCTTTCGTCGGTTTTC
Uhg4_qPCR for	qRT PCR	ACCGCATTGGAAACGATTAA
Uhg4_qPCR rev	qRT PCR	ACAAATGCCAGCGCTTTAAC
Uhg5-2_qPCR for	qRT PCR	ATCAATCTCATGCAACTGCA
Uhg5-2_qPCR rev	qRT PCR	CATCGCGTGCAATGCCGGCT
Uhg7_qPCR for	qRT PCR	CTTTCAGATTGGATACTTCA
Uhg7_qPCR rev	qRT PCR	AAGCTTCCCATTTAAAGACA
Uhg8_qPCR for	qRT PCR	CGTATGGGCTCGTCTCCTTT
Uhg8_qPCR rev	qRT PCR	CGTTCTGGTGCGGTATGTGT
Me28S-A3407a for	qRT PCR	TGAAACATTTACCCAGCTCGC
Me28S-A3407a rev	qRT PCR	TGCGTTGGATATGGAACAGT
Me18S-A1576 for	qRT PCR	AATTCTCGACTTGGCGCTGT
Me18S-A1576 rev	qRT PCR	CATCAGATCGCCGAATCATCT
U14_30Ea for	qRT PCR	CCTTTTGCGGTTTCCACCAG
U14_30Ea rev	qRT PCR	GTCAGACGCCTTAGACCATCA
Me28S_C2645a for	qRT PCR	TGAAATCGTTAGATGGGGACA
Me28S_C2645a rev	qRT PCR	ATCGAGATGAATCAGTCACAGTAATC
Psi28S_2949 for	qRT PCR	TTGTGATGCGCAGGGAAATG
Psi28S_2949 rev	qRT PCR	TGGAATCTCGACCACGTGAC
Or_CD2 for	qRT PCR	GTCAAGCGCTGGCAATCTTC
Or_CD2 rev	qRT PCR	CAGGGCCCATAACCAGTCAA
Me28S_G2703 for	qRT PCR	CCGTGGTTTTACACTGAGACAA

Me28S_G2703 rev	qRT PCR	TGTATCAGTTGGGGAAAAATGA
Me18S_U1356a for	qRT PCR	TGACAACTTCATACCCAAATCAG
Me18S_U1356a rev	qRT PCR	TTCAGATGGTGATGCATGTT
Or_CD11 for	qRT PCR	TGTGAAGAGCATTCCACGTAA
Or_CD11 rev	qRT PCR	ATACGGAATAGTCAAGCACACTT
αTub84B for	qRT PCR	GCCAGATGCCGTCTGACAA
αTub84B rev	qRT PCR	AGTCTCGCTGAAGAAGGTGTTGA
rab6 for	qRT PCR	TGCACGTGGCCAAGTCCTA
rab6 rev	qRT PCR	CAGCGAACGCGACTGCTA
snm158 for	qRT PCR	CACTCTACCCAAGGCCAAGA
snm158 rev	qRT PCR	CACTGGCTGCTATCCCATCT
Fibrillarin for	qRT PCR	ACGACAGTCTCGCATGTGTC
Fibrillarin rev	qRT PCR	ATGCGGTACTTGTGTGGATG
Nop60B for	qRT PCR	CCGGCAAGCTAGACAAGTTC
Nop60B rev	qRT PCR	ACATAACCGGTCAGCCACTC
Chinmo RNAi for	dsRNA	TAATACGACTCACTATAGGGAGACGGATCTAC TGGCCGATGTC
Chinmo RNAi rev	dsRNA	TAATACGACTCACTATAGGGAGACAAGATGCC AGTGGATCCGC
Myc RNAi for	dsRNA	TAATACGACTCACTATAGGGAGACCACCCGGC TCTGATAGTGACTCC
Myc RNAi rev	dsRNA	TAATACGACTCACTATAGGGAGACCACCCGGC TCTGATAGTGACTCC
GFP RNAi for	dsRNA	TAATACGACTCACTATAGGGAGAAGTGGAGAG GGTGAAGGTGA
GFP RNAi rev	dsRNA	TAATACGACTCACTATAGGGAGAAAAGGGCAG ATTGTGTGGAC
Max T7 for	dsRNA	TAATACGACTCACTATAGGGAGATTTGCGCGC AATCCGTG
Max T7 rev	dsRNA	TAATACGACTCACTATAGGGAGATAAGG TCGATTGGGTGGG
Uhg1-E2 for	ChIP	CGATTCTTGGAACTACCCTCT
Uhg1-E2 rev	ChIP	GTGACCGCACTACGATTCTG
Uhg2-ES1 for	ChIP	CCGCCATCTTTTCACAGAAT

Uhg2-ES1 rev	ChIP	CGAAGAGCACACAACTTACCA
Uhg4 for	ChIP	TGGCTTGTTTGCAGAACTCA
Uhg4 rev	ChIP	TTTGAATTGCAATCGGTGAA
Uhg5 for	ChIP	AAAATGCAATTGTGGGAAGC
Uhg5 rev	ChIP	GCTGTCCCTCTCTTTTCACC
Cluster2R for	ChIP	CGGTTTATTGCTCGTGGAGA
Cluster2R rev	ChIP	AGCACTCTGCTACCCTGGAA
Hoip for	ChIP	TTTAAGCTAGGGCTGCAGAG
Hoip rev	ChIP	CGCAGGTGGTTCGGAAATAC
Nop5 for	ChIP	CAGCCAGCAGCAACTTAACC
Nop5 rev	ChIP	TGTTATGCGCGAACCAAGTG
Pka-C1-cod for	ChIP	CATGACACGGCCAAAGGAGC
Pka-C1-cod rev	ChIP	GGACAAGTGGCGACGCAATC
Fibrillarin for	ChIP	GCAACCAAAACGCTTGAAAA
Fibrillarin rev	ChIP	TCTTGGTATTTTCGCCTTTG
Nop60B	ChIP	TCACGATGACATATCGCAAGA
Nop60B	ChIP	GGACGAAAAACACGTGGAGT
Y1476 for	ChIP	TCCAAAAGGTTCGTGTCCAT
Y1476 rev	ChIP	CTTGGGTCTGGGTTCGTCT
Y1421 for	ChIP	ATTTAGTTGGACCGCACGAC
Y1421 rev	ChIP	CTGATTCGAAGAGAGGACAGC
Y724 for	ChIP	CATTCGGGGTTTATTGCTGT
Y724 rev	ChIP	CTCCGGATTTACAGCTCAGG
Y683 for	ChIP	GCCCTCAAGTCCACTCGTC
Y683 rev	ChIP	CGGGTCTGTTGTTCTTCCAT
Y1601 for	ChIP	ACCGTTTCACTGCTTCAACC
Y1601 rev	ChIP	GCGCCCTGATTTGAAATACT
Y2679 for	ChIP	GCTACCAACACCACCCCTTA
Y2679 rev	ChIP	AATGGAATCAGTGTGCGTGA
Y3421 for	ChIP	CGTATGGGAGTTTCGCTCTC

Y3421 rev	ChIP	CGCAGTTCAACAGCATTGAT
Y3304 for	ChIP	TCGATTGTGGCGAACATTTA
Y3304 rev	ChIP	ATTGCGAAAGCATCGAAAAA
Y505 for	ChIP	CCTTATCGCCGCAGAAGTAA
Y505 rev	ChIP	CATCACCACTCATCGTCCAG
Y2248 for	ChIP	ACACTCCGCCCCATTTTTAT
Y2248 rev	ChIP	TCTTAGCCACCTCCTTTTGG
Y1503 for	ChIP	GAAGAGTGGCAAAGGAATGG
Y1503 rev	ChIP	GCCATTTGATTGACTGACGTT
Y193 for	ChIP	ATGTAGAATTCTCCTAGTCGTGCT
Y193 rev	ChIP	ACAGTGACATCAAGGATCCATCT
Y340 for	ChIP	CCGCATTAGTTTTCCGATTC
Y340 rev	ChIP	ATGGCGAGCAGAGTGAGC
Y2613 for	ChIP	CGAATGGCTCGCATTAAAGT
Y2613 rev	ChIP	TTTTGTTGTTCGTTCGTTCG
Y429 for	ChIP	CAGAGGCAACCGACTCTTTC
Y429 rev	ChIP	TCTTCCGCGATTCGATATTC
Y1764 for	ChIP	GTTAGGCGTTGCCAGACAAG
Y1764 rev	ChIP	GCAGTGTGACCGTAATCGAG
Y1234 for	ChIP	GCAGTGTGACCAAGTGTACCA
Y1234 rev	ChIP	GGTTTCGGTCACCGCTAATA
A1666	Methylation	GCCTTGAACTTAGGACCGACT
G3081	Methylation	ACACCGAGATCAAGTCAGCA
G3277	Methylation	GCTTGGTGAATTTTGCTTCA
Me18S-A1576	Northern	GTCGAGAATTTGTTCCTTCAGTCTCGTCATCT GTTTCATC
Me28S-C2645a	Northern	CACAGTAATCAGTTGTCCCCATCTAACG-ATTTCATCATGG
Me28S-G2703c	Northern	GTCTCAGTGTAAAACCACGGACTGTATTGTCA TCATTTCG
GFP for2	Cloning	GATCGAATTCCAAAATGAGTAAAGGAGAAGAA C

GFP rev	Cloning	GATCGGTACCTTACTCGAGACGCGTTTTGTATAGTTCATCCATGCC
Chinmo for	Cloning	GTACCTCGAGATGGATCCGCAGCAGCAGTTC
Chinmo rev	Cloning	GTACCTCGAGATGGATCCGCAGCAGCAGTTC
Chinmo-Zf rev	Cloning	GTACCTCGAGATGGATCCGCAGCAGCAGTTC
GST-Chinmo for2	Cloning	GCCACAGATCTCTCGAGCAACAACACATGGG
GST-Chinmo rev2	Cloning	CCAGTGAATTCCTCGAGCTACTTCTTACCGTCGG
2R-Cluster_for ≙ Cluster2R for (ChIP)	Cloning	CGGTTTATTGCTCGTGGAGA
2R-Cluster_rev1	Cloning	AATGGGTTAAGCACGTTCCA
2R-Cluster_rev2	Cloning	CCTCAAAACGCAAAGCTTCTT
UAS-Uhg1 for	Cloning	GAGGGCGGCCGCCACTTCTTTTTTTCGTTCAAA
UAS-Uhg1 rev	Cloning	ACGTGGTCTAGAGAAATGGCGTTGTTCGATCT
UAS-Uhg4 for	Cloning	GAGGAGATCTTTAAAGAACGTGGAGCGAAC
UAS-Uhg4 rev	Cloning	CCTCGCGGCCGCAAGAACACATATGAATTTTATTTATTCGTGA
UAS-Uhg5 for	Cloning	GAGGGCGGCCGCTTCTTGGCGAGCTGTGGTGT
UAS-Uhg5 rev	Cloning	CTTCGGTACCTTTTAGTTTTAGTACTTGAA

2.3.2 **Plasmids**

2.3.2.1 Empty vectors

pGEX 4T1 — Bacterial expression vector with tac-promoter expression of GST-tagged proteins (GE Healthcare)

pUAST — *Drosophila* expression vector, P element-based vector for Gal4-regulated expression of genes in *Drosophila*

2.3.2.2 Expression vectors

pGEX-Chinmo — pGEX 4T1 expression vector with CDS of Chinmo

pUAS- GFP — pUAST expression vector with CDS of GFP

pUAS-GFP-Chinmo-wt	pUAST expression vector with CDS of GFP and Chinmo-wt
pUAS-GFP-Chinmo-ΔBTB	pUAS-GFP with CDS of Chinmo lacking BTB/-POZ-domain
pUAS-GFP-Chinmo ΔZf	pUAS-GFP with CDS of Chinmo lacking Zf- domain
pRL-CG5033-wt	$CG5033^{wt}$-Renilla-luciferase
pGL-CG5033-ΔEbox	$CG5033^{\Delta EBox}$-Firefly-luciferase

2.4 Antibodies

WB = Western-Blot; ChIP = Chromatin-Immunoprecipitation

m = mouse; r = rabbit; mono = monoclonal; poly = polyclonal

2.4.1 Primary antibodies

Table 2-2: List of primary antibodies

Protein	Application	Type	Company
AU1	WB	r, poly	Biomol (A190-125A)
Chinmo	IP, ChIP, WB	r, poly	Group Gallant Production ImmunoGlobe
GFP	WB	m, mono	Santa Cruz (sc-9996)
Crude GST-Chinmo	IP, WB	r, poly	Group Gallant Production ImmunoGlobe
HA	ChIP, WB	m, mono	Sigma (H3663)
IgG	ChIP	m, poly	Sigma (I5381-10MG)
IgG	ChIP	r, poly	Sigma (I5006-10MG)
Myc	ChIP, WB	r, poly	Group Morata Production, provided by G. Morata; Martín *et al.,* 2009
Myc	ChIP, WB	m, mono	Group Gallant Production Prober and Edgar, 2000
Myc-N	ChIP, WB	r, poly	Santa Cruz (sc-28208)
α-Tubulin	WB	m, mono	Sigma (T-5168)

2.4.2 **Secondary antibodies**

α-rabbit-HRP	donkey-anti-rabbit- immunoglobulin, coupled with horseradish peroxidase (GE Healthcare)
α-mouse-HRP	goat-anti-mouse- immunoglobulin, coupled with horseradish peroxidase (Jackson)

2.5 Chemicals

All chemicals were purchased from the companies Sigma, Merck, Roth, Invitrogen and AppliChem and used without further purification. Radioactively marked products were purchased from Hartmann Analytics.

2.6 Enzymes, standards and kits

2.6.1 **Enzymes**

Absolute qPCR SYBR Green Mix	Thermo Scientific
AMV reverse transcriptase	Promega
Antarctic phosphatase	New England biolabs
Mini Protease inhibitor cocktail tablets	Roche
Omniscript reverse transcriptase	Qiagen
Proteinase K	Roth
Q5-polymerase	New England biolabs
Rnase A	Roth
Rnase free Dnase I	Qiagen
Rnasin® Ribonuclease inhibitor	Promega
Taq-polymerase	New England biolabs
T4-polynucleotide kinase	New England biolabs
Turbo Dnase	Life technologies

2.6.2 **Standards**

GeneRuler 1 kb DNA Ladder	Thermo Scientific
GeneRuler 100 bp DNA Ladder	Thermo Scientific
GeneRuler 50 bp DNA Ladder	Thermo Scientific
PageRuler Prestained Protein Ladder	Thermo Scientific

2.6.3 **Kits**

Cellfectin II Reagent	Life technologies
dNTPs	Roche
ddNTPs	Roche
Effectene® Transfection Reagent	Qiagen
GenElute Plasmid MiniPrep Kit	Sigma Aldrich
GeneJET Gel Extraction Kit	Thermo Scientific
MEGAscript® T7 Transcription Kit	life technologies
miRNeasy Mini-Kit	Qiagen
Omniscript RT Kit	Qiagen
Plasmid Midi Kit	Qiagen
Quant-iT PicoGreen dsDNA Assay Kit	Invitrogen
Random Hexamers	Roche
Rnase-Free Dnase Set	Qiagen
Absolute qPCR SYBR Green Mix	Thermo Scientifc
Qiaquick PCR Purification Kit	Qiagen

2.7 Buffer and solutions

Annealing buffer (2x)	500mM KCl 50mM Tris pH 8.3 aliquot and store at -20°C
Blocking solution	5% (w/v) skim milk powder in TBS-T
Bradford solution	8.5% (v/v) phosphoric acid solution 4.75% (v/v) ethanol 0.01% (w/v) Coomassie G250 stain stir overnight, filter with filter paper keep away from light
BSA-PBS	0.5% (v/v) BSA in PBS
Blue DNA loading Dye (6x)	0.2% (v/v) Bromphenol blue 60% (v/v) Glycerin

	60 mM EDTA
Coomassie destaining solution	10% (v/v) Acetic acid
	20% (v/v) Methanol
Coomassie staining solution	25% (v/v) Isopropanol
	10% (v/v) Acetic acid
	0.05% (w/v) Coomassie G250 stain
ChIP Lysis buffer I	5 mM PIPES, pH 8
	85 mM KCl
	0.5% (v/v) NP-40
ChIP Lysis buffer II	10 mM Tris-HCl, pH 7,5
	150 mM NaCl
	1% (v/v) NP-40
	1% (w/v) DOC
	0.1% (w/v) SDS
	1 mM EDTA
ChIP Wash buffer I	20 mM Tris pH 8,1
	150 mM NaCl
	2 mM EDTA
	0.1% (w/v) SDS
	1% (v/v) Triton X-100
ChIP Wash buffer II	20 mM Tris pH 8,1
	500 mM NaCl
	2 mM EDTA
	0.1% (w/v) SDS
	1% (v/v) Triton X-100
ChIP Wash buffer III	10 mM Tris pH 8,1
	250 mM LiCl
	1% (v/v) NP-40
	1% (w/v) SDS

	1 mM EDTA
ChIP Elution buffer	1% (w/v) SDS
	100mM $NaHCO_3$
Church Buffer	1 mM EDTA pH 8.0
	0.17% (v/v) Phosphoric acid
	7% (v/v) SDS
	0.5 M Na_2HPO_4 x 2 H_20
Denaturing Lysis buffer	2% (v/v) SDS
	20 mM EDTA
	50 mM Tris, pH 8
DEPC water	0.1% (v/v) DEPC in *aqua bidest.*
	Overnight at 37°C, autoclaved
Drosophila Ringer's solution	3 mM $CaCl_2$* $2H_2O$
	182 mM KCl
	46 mM NaCl
	10 mM Tris base
	Adjust to pH 7.2
Extraction buffer A	0.1 M Tris/HCl, pH 9.0
	0.1 M EDTA
	1% (v/v) SDS
Formamide loading dye	95% (v/v) formamide
	18 mM EDTA
	0.025% (v/v) SDS
	0.025% (v/v) xylene cyanol
	0.025% (v/v) bromophenol blue
GST Lysis buffer	50 mM NaCl
	50 mM Tris base
	5 mM EDTA
	1:1000 Protease Inhibitor

GST Elution buffer	50 mM Tris-HCl
	10 mM reduced Glutathion
	pH 8.0
Laemmli-buffer (2x)	3% (v/v) SDS
	10% (v/v) Glycerol
	62.5 mM Tris, pH 6.8
	0.001% (v/v) bromphenol blue
	5% (v/v) β-mercaptoethanol
NP-40 Lysis buffer	150 mM NaCl
	50 mM Tris/ HCl, pH 8
	5 mM EDTA, pH 8
	0.1% (v/v) NP-40
Orange DNA Loading Dye (6x)	0.4% (w/v) Saccharose
	10 mM EDTA, pH 8.0
	10 µl (v/v) Orange G
PBS	137 mM NaCl
	2.7 mM KCl
	10.1 mM Na_2HPO_4
	1.76 mM KH_2PO_4
SDS-Running buffer	25 mM Tris base
	250 mM Glycin
	0.1% (v/v) SDS
Separating gel 10-15%	10-15% (v/v) acrylamide/bisacrylamide
	375 mM Tris-HCl (pH 8.8)
	0.1% (v/v) SDS
	0.1% (v/v) APS
	0.1% (v/v) TEMED
SSC (20x)	3 M $Na_3C_6H_5O_7 * 2H_2O$
	0.3 M NaCl

Stacking gel 4%	4% acrylamide/bisacrylamide 125 mM Tris-HCl (pH 6.8) 0.1% (v/v) SDS 0.1% (v/v) APS 0.1% (v/v) TEMED
Stripping buffer	62.5 mM Tris-HCl, pH 6.8 2% (v/v) SDS 0.1 M β-mercaptoethanol
TAE (50x)	40 mM Tris 0.114% (v/v) acetic acid 1 mM EDTA adjusted to pH 8.0
TBE (2.5x)	10 mM Tris base 50 mM Boric acid 30 mM EDTA
TBS (10x)	250 mM Tris base 1.4 M NaCl pH 7.4
TBS-T	140 mM NaCl 25 mM Tris-HCl, pH 7.4 0.2% (v/v) Tween
TE	10 mM Tris-HCl, pH 8.0 1 mM EDTA
Transfer Buffer	48 mM Tris base 390 mM Glycine 3.5 mM SDS 20% (v/v) Methanol

2.8 Consumables and equipment

Consumables such as reaction tubes, cell culture and other plastic products were purchased from Applied Biosystems, Eppendorf, Greiner, Kimberley-Clark, Nunc, Sarstedt, B. Braun, Schleicher und Schüll, Millipore and VWR international.

2.8.1 **Equipment**

Binocular	Olympus SZ61
Chemiluminescence imaging	LAS-4000 mini (Fujifilm)
Cell culture incubator	Incu-Line (VWR)
Centrifuges	Eppendorf 5415 R (Eppendorf)
	Biofuge 15 (Heraeus)
	Avanti J-26 XP (Beckman Coulter)
Heating block	Thermomixer comfort (Eppendorf)
Heat Sealing	ALPS^{TM} 50V (Thermo)
Luminometer	Glomax 96 Microplate Luminometer (Promega)
Magnetic Stirrer	Combimag RCH (IKA)
Microplate Reader	Infinite M200 PRO (Tecan)
Microscope for immunofluorescence	DMI 6000 B (Leica)
	SP5 (Leica)
	Discovery V8 (Zeiss)
Microscope for cell culture	Axiovert 40CFL (Zeiss)
PCR thermal cycler	Vapo protect (Eppendorf)
	C1000 Thermal Cycler (Biorad)
Phosphorimager	Typhoon 9200 (GE healthcare)
Photometer	UltrospecTM 3100 pro UV/Visible (Amersham Biosciences)

Power supply	PowerPac 300 (Bio-Rad)
Quantitation of RNA and DNA	Experion Automated Electrophoresis System (Bio-Rad) NanoDrop 3000 (Thermo Scientifc)
Quantitative real-time PCR machine	MXp3000P qPCR system (Stratagene)
SDS-PAGE system	Mini Trans-Blot (Bio-Rad)
Sterile bench	Lamin Air (Heraeus)
Ultrasonifer	W-250 D (Heinemann)
UV fluorescent table	maxi UV fluorescent table (PEQLAB)
Universal shaker	SM-30 (Edmund Bühler GmbH) Titramax 101(Heidolph)
Vortex mixer	Vortex-Genie 2 (Scientifc Industries)
Waterbath	ED-5M heating bath (Julabo)
Western blot transfer chamber	Mini-PROTEAN Tetra Cell (Bio-Rad)

2.9 Fly lines

Table 2-3: Fly strains

Name	Genotype	Figure
Uhg1^{rev}	yw; Uhg1_4	Figure 4-9, Figure 4-10
Uhg1^{1}	yw; Uhg1_18/CyO,y+	Figure 4-9, Figure 4-10
Myc OE/ *Uhg1^{1}*	y w actin-FRT-CD2-FRT-GAL4 hs-FLP/y w; Uhg1_18; UAS-vito:GFP/UAS-Myc, GFP	Figure 4-11
Myc OE	y w actin-FRT-CD2-FRT-GAL4 hs-FLP/w; (Sp or CyO,y+)/+; UAS-vito:GFP/UAS-Myc, GFP	Figure 4-11
Brat-kd	w; wor-Gal4 ase-Gal80; UAS-brat-IR UAS-Fluc/ TM3, Sb tub-Gal80	Figure 4-11
Brat-wt	w; (wor-Gal4 ase-Gal80; UAS-Rluc QUAS-Fluc)/ (SM5; TM6B)	Figure 4-11
ctr	y w	Figure 4-11
Uhg4/1	y w; UAS-Uhg4 [F1b]	Figure 4-11
Uhg4/2	y w; UAS-Uhg4 [F12A]	Figure 4-11
Uhg5/1	y w; UAS-Uhg5 [F9D]	Figure 4-11
Uhg5/2	y w; UAS-Uhg4 [M3A]	Figure 4-11
Myc-kd	w; UAS-Myc-IR	Figure 4-11
Ras^{V12} + Chinmo	yw tub-FRT-Myc-FRT-GAL4 ey-FLP/Y; UAS-Ras^{V12}/+; UAS-Chinmo/UAS-GFP	Figure 4-11
Ras^{V12} + Chinmo, *Uhg1^{1}*/+	yw tub-FRT-Myc-FRT-GAL4 ey-FLP/Y; UAS-Ras^{V12}/*Uhg1^{1}*; UAS-Chinmo/UAS-GFP	Figure 4-11
Ras^{V12} + Chinmo, *Uhg1^{1}*	yw tub-FRT-Myc-FRT-GAL4 ey-FLP/Y; *Uhg1^{1}* UAS-Ras^{V12}/ *Uhg1^{1}*; UAS-Chinmo/UAS-GFP	Figure 4-11
yw ey-FLP	y w tub-FRT-Myc-FRT-GAL4 ey-FLP/Y; FRT-40 chinmo^{X}/CyO, y^{+}	Figure 4-12
yw eyFLP; FRT40 cl w^{+}	y w tub-FRT-Myc-FRT-GAL4 ey-FLP; FRT-40 chinmo^{X}/FRT-40 cl w^{+}	Figure 4-12
w dm^{P0} ey-FLP	w dm^{P0} tub-FRT-Myc-FRT-GAL4 ey-FLP/Y; FRT-40 chinmo^{X}/CyO, y^{+}	Figure 4-12
w dm^{4} ey-FLP	w dm^{4} tub-FRT-Myc-FRT-GAL4 ey-FLP/Y; FRT-40 chinmo^{X}/CyO, y^{+}	Figure 4-12

GFP	y w tub-FRT-Myc-FRT-GAL4, ey-FLP; UAS-GFP/+;	Figure 4-15
Chinmo	y w tub-FRT-Myc-FRT-GAL4, ey-FLP; UAS-GFP/+; UAS-Chinmo/+	Figure 4-15
Ras^{V12}	y w tub-FRT-Myc-FRT-GAL4, ey- FLP; UAS-GFP/ UAS- Ras^{V12};	Figure 4-15
Ras^{V12} + Chinmo	y w tub-FRT-Myc-FRT-GAL4, ey- FLP; UAS-GFP/ UAS-Ras^{V12}; UAS-Chinmo/+	Figure 4-15
Myc	y w tub-FRT-Myc-FRT-GAL4, ey- FLP; UAS-GFP/+; UAS-Myc/+	Figure 4-15
Myc + Chinmo	y w tub-FRT-Myc-FRT-GAL4, ey- FLP; UAS-GFP/UAS-Chinmo; UAS-Myc/+	Figure 4-15
Ras^{V12} + Myc	y w tub-FRT-Myc-FRT-GAL4, ey- FLP; UAS-GFP/UAS- Ras^{V12}; UAS-Myc/+	Figure 4-15
Ras^{V12} + Chinmo miRNA	y w tub-FRT-Myc-FRT-GAL4, ey- FLP; UAS-GFP/ UAS- Ras^{V12}; UAS-Chinmo-miRNA/+	Figure 4-15
dm^{4} ey-FLP, Ras^{V12} + Chinmo	w dm[4] tub-FRT-Myc-FRT-GAL4 ey-FLP; UAS-Ras^{V12}/ +; UAS-Chinmo/ UAS-GFP	Figure 4-15
dm^{P0} ey-FLP, Ras^{V12} + Chinmo	w dm[P0] tub-FRT-Myc-FRT-GAL4 ey-FLP; UAS-Ras^{V12} / +; UAS-Chinmo/ UAS-GFP	Figure 4-15

3 Methods

3.1 Molecular biology methods

3.1.1 Transfection of bacteria with plasmid DNA and plasmid amplification

To amplify a plasmid circular DNA can be transformed into bacteria. Competent bacteria were thawed on ice and mixed with 0.5-1 µg Plasmid DNA or the whole ligation mix (3.1.9). After 30 µl incubation on ice followed by a two minutes heat shock at 42°C, LB media without antibiotics was added and incubated for 45 minutes on 37°C. The bacteria suspension was then centrifuged resolved in 100 µl media and plated out on an LB agar plate containing antibiotics.

3.1.2 Isolation of plasmid DNA from bacteria

For large scale purification of plasmid DNA (midi prep), 100 ml of cultivated bacteria were used to isolate the plasmid with the Plasmid Midi Kit (Qiagen) according to the manufacturer's instructions until the isopropanol precipitation step. After removal of the isopropanol, the air dried pellet was resuspended in 400 µl aqua bidest and ethanol precipitated (3.1.3). After 30-60 µl at -20°C, the DNA was pelleted through centrifugation (13000 rpm, 30 µl, 4°C). The DNA was washed once with 70% Ethanol, then dried and resuspended in 50 µl aqua bidest or TE and stored at -20°C.

For the isolation of small amounts of plasmid DNA, 5 ml of cultivated bacteria were treated with the GenElute Plasmid MiniPrep Kit (Sigma Aldrich) according to the manufacturer's instructions. The DNA was resuspended in 50-75 µl of the included elution buffer or aqua bidest.

3.1.3 Ethanol precipitation of nucleic acids

Nucleic acids can be precipitated from aqueous solutions by addition of ethanol. Therefor 2.5 volumes of ethanol (100%) and 0.1 volumes of sodium acetate (3 M, pH 5.2) were added, vortexed and incubated for at least 30 µl at -20°C. After centrifugation (13000 rpm, 30 µl, 4°C), the precipitated nucleic acids were washed once with 1.0 volume of ice cold ethanol (70%). The nucleic acid sediment was air dried and resolved with ddH_2O in the initial volume.

3.1.4 Nucleic acid quantitation

The concentration of DNA and RNA in solution was measured with Peqlab's NanoDrop 1000. The purity of the nucleic acids was determined by assessing the ratio of absorbance at 260 nm and 280 nm. For pure DNA the ratio is ~1.8, for RNA ~2.

3.1.5 Separation of proteins from aqueous nucleic acid solutions

To remove proteins from aqueous protein-nucleic acid solutions, 1 volume of Phenol / Chloroform / Isoamylalcohol (25:24:1) was added and mixed properly. After centrifugation (13000 rpm, 5 min, RT) the upper aqueous phase containing the nucleic acids, was transferred into a new reaction tube. The remaining phenol-phase was washed once with 1 volume ddH_2O and pooled with the first aqueous phase. Afterwards the aqueous phases were extracted once with chloroform and the nucleic acids were precipitated with ethanol (3.1.3) or 2-Propanol.

For 2-Propanol precipitation an equal volume of 2-Propanol was added to the sample, put on -20°C for at least 15min and pelleted (13000 rpm, 15 min, 4°C). The nucleic acid sediment was air dried and resolved with ddH_2O in the initial volume.

3.1.6 Sequence specific hydrolysis of DNA (restriction digest)

DNA was hydrolyzed in a sequence-specific manner with restriction endonucleases from New England Biolabs (NEB) and Roche using the recommended reaction buffers. The digestions were set up according to the table below and incubated at 37°C for one hour to overnight.

Table 3-1: Restriction digest mix

DNA	1-2 µg
restriction endonuclease 1	0.5 µl
restriction endonuclease 2 (if applicable)	0.5 µl
10 x reaction buffer	2.0 µl
ddH_2O	ad 20 µl

3.1.7 Separation of DNA and RNA fragments via gel electrophoresis

Agarose gel

DNA and RNA fragments of different sizes were separated by agarose gel electrophoresis. A solution of 0.8-2% agarose was boiled in 1xTAE buffer depending on expected fragment size.

0.3 µg/ml ethidium bromide was added to the solution and poured into a gel chamber with combs to form sample wells in the gel. Loading buffer was then added to the samples which were pipetted into the wells of the polymerized gel. Different standards were separated next to the samples depending on the expected fragment size. The gel was run at 120 V for one to three hours and bands were visualized using a UV transilluminator which detects the intercalator ethidium bromide.

Acrylamide/ Urea gel

Small DNA and RNA fragments (< 100 nt) were separated on Acrylamide/ Urea gels. Depending on their size the gel consisted of 8% to 12% Acrylamide and 7 M to 8 M Urea. Samples were mixed with 2x formamide loading dye (2.7) and boiled for 2 min at 95°C prior to loading.

3.1.8 DNA extraction and purification from agarose gels

After separation the DNA fragment of interest was cut out from the agarose gel with a scalpel and purified with the help of GeneJET Gel Extraction Kit (Thermo Scientific) following the manufacturer's protocol.

3.1.9 Ligation of DNA fragments

Double stranded DNA fragments were attached to one another covalently by means of ligation. Insert and plasmid were incubated in a molar ration of 3:1 in the ligation mix according to the table below and incubated for one to three hours at RT or overnight at 16°C. To calculate the optimal amounts of backbone and plasmid the Insilico ligation calculator was used (http://www.insilico.uni-duesseldorf.de/Lig_Input.ht ml).

Table 3-2: Ligation mix

linearized plasmid	~ 100 ng
DNA fragment (insert)	X ng
T4 DNA ligase buffer (NEB)	1 µl
T4 DNA ligase (NEB)	1 µl
aqua bidest	ad 10 µl

Linearized plasmids were dephosphorylated with Antarctic Phosphatase (New England Biolabs) prior to ligation to prevent self-ligation following manufacturer’s instructions.

3.1.10 Isolation of total RNA from larvae or tissue culture

For isolating RNA from up to 10 larvae, 100 µl of Trizol (Life Technologies) were added to the larvae and homogenized with a micro pistil. After complete homogenization an-

other 600 µl Trizol were added and either frozen at -80°C or directly further processed with the miRNeasy Kit (Qiagen) according manufacturer's instructions.

Cells were harvested and pelleted by centrifugation (1200 rpm, 5 min, RT) before 700 µl Trizol were added, homogenized by vortexing for 1 min and either frozen at -80°C or directly further processed with the miRNeasy Kit (Qiagen) according manufacturer's instructions.

For isolating RNA from larvae and cells an on-column DNase digestion was performed with DNase I (Qiagen) following the instructions in Appendix B of the miRNeasy Kit (Qiagen) protocol. The RNA concentration was determined by NanoDrop measurement. The RNA was used for cDNA synthesis and stored at -80°C.

3.1.11 **cDNA synthesis**

To quantify specific mRNAs, the RNA was then transcribed into complementary DNA (cDNA) by reverse transcription, using the miScript II RT Kit (Qiagen) (Table 3-3) which allows the conversion of all RNA species or the Omniscript RT Kit (Qiagen) (Table 3-4) which converts mRNA. The cDNA synthesis mix were incubated for one hour at 37°C and stored at -20°C.

Table 3-3: miScript II RT Kit

total RNA	1 µg
5x miScript HiFlex Buffer	4 µl
10x miScript Nucleics Mix	2 µl
miScript Reverse Transcriptase	2 µl
RNase free water	ad 20 µl

Table 3-4: Omniscript RT Kit

total RNA	1 µg
10x Reverse Transcription buffer	2 µl
dNTP mix	2 µl
random hexamers (final conc: 10 µM)	0.2 µl
RNase inhibitor	10u
Reverse Transcriptase	1 µl
RNase free water	ad 20 µl

3.1.12 **Polymerase chain reaction (PCR)**

To amplify specific regions of nucleic acids for different purposes polymerase chain reaction (Mullis *et al.,* 1986) was used.

PCR to amplify cDNA for cloning or dsRNA synthesis

To generate new expression vectors, the gene of interest was amplified based on existing expression vectors. This also allowed the addition of new tags or new restriction sites. Furthermore the newly synthesized cDNA was used for dsRNA synthesis (3.1.16).

Table 3-5: Standard PCR setup

cDNA	100-500 ng
primer	30 pmol each
dNTP mix (10mM each)	2 µl
Phusion	5 u
RNase free water	ad 100 µl

Table 3-6: Standard PCR thermal cycle profile

1 cycle	94°C	120 s
25-30 cycles	94°C	15 s
	T_m-(2-4°C)	30 s
	72°C	1 kb/min
1 cycle	72°C	420 s
	4°C	Hold

Quantitative reverse transcriptase PCR (qRT-PCR)

To quantify specific mRNA levels the cDNA synthesized by reverse transcription was amplified by real time PCR. The qPCR SYBR Green Mix from Thermo Scientific was used to set up a reaction mix as described in the table below, and pipetted into the wells of a 96-well qPCR plate. Finally, 200 ng of cDNA in 10 µl was added to each well. The measurement was carried out with the Mx3000P qPCR system (Stratagene).

The quantification of the amplified transcripts can be determined by fluorescent monitoring in every cycle after the end of the elongation step.

The basis of real time PCR is fluorescent monitoring of DNA amplification, from which target DNA concentration can be determined from the fractional cycle at which a

threshold amount of amplicon DNA is produced. For normalization the housekeeping genes α-tubulin, rab6 and snm158 were used, the calculation was performed using the ΔΔ−CT method (Applied Biosystems User Bulletin 2). Every qRT-PCR was performed in triplicates for at least two biological independent samples.

Quantitative real-time PCR (qPCR)

For analyzing the expression of specific genes and the enrichment of ChIP DNA, quantitative PCR was used. Therefore, the synthesized cDNA was diluted 10 times and added to 10 µl of the qPCR setup. The measurement was carried out as described for quantitative reverse transcriptase PCR (see above).

Table 3-7: qRT-PCR/qPCR setup

SYBR Green Mix (Thermo Scientific)	5 µl
forward primer (10 pmol/ml)	0.5 µl
reverse primer (10 pmol/ml)	0.5 µl
RNase free water	4 µl

Table 3-8: qRT-PCR/qPCR thermal cycling profile

1 cycle	95°C	15 min
38 cycles	95°C	30 sec
	60°C	20 sec
	72°C	15 sec
1 cycle	95°C	1 min
	60°C	30 sec
	95°C	30 sec

3.1.13 **Chromatin immunoprecipitation (ChIP)**

To investigate the interaction between proteins and DNA chromatin immunoprecipitation (ChIP) were performed. Therefore, $40x10^6$-$120x10^6$ cells ($200x10^6$ cells for ChIPseq) were cross-linked with 1% formaldehyde at 37°C for 10 µl and the reaction was stopped with 50 mM glycine for 5 min. After washing the cells 3 times in ice-cold PBS, cells were swelled for 20 µl in 3 ml Lysis buffer I (containing protease inhibitor) and nuclei were lysed in 2 ml Lysis buffer II (containing protease inhibitor) for 10 µl or longer. Afterwards sonication with a Branson sonifier was carried out (15 min in total, amplitude 15%) until the majority of fragments showed nucleosomal size.

Protein A/G-dynabeads (30 µl (100 µl for ChIPseq), Invitrogen) were coupled to antibodies (3 µg (10 µg for ChIPseq)) of interest and their corresponding IgGs overnight. The beads were washed three times in PBS/BSA before the cross-linked chromatin was added for at least 6 hours. Before the chromatin was eluted (150 µl, 15min, RT, two combined eluates) from the dynabeads they were washed three times with Wash buffer I-III, containing increasing salt concentration to get rid of background signal due to unspecific binding. The same amount of elution buffer was added to the 1% input samples and the crosslink was reverted overnight.
To revert the crosslink, 14 µl 1 M Tris pH 6.8, 1.2 µl 5 M NaCl and 1 µl RNase A (10 mg/ml) were added and the samples were incubated for one hour at 37°C and afterwards at 65°C for six hours to overnight. Finally, 3.5 µl 0.5 M EDTA and 7 µl proteinase K (10 mg/ml) were added and incubated for another two hours at 45°C before the DNA was purified with Phenol-Chloroform followed by ethanol precipitation, diluted 1:15 in RNase free water and analyzed by quantitative real-time PCR (3.1.12).

3.1.14 **ChIP seq**

For ChIPseq experiments, ChIP DNA was end repaired and A-tailed. After ligating Illumina adaptors to the ChIP DNA fragments they were loaded on a 2% agarose gel and fractions of 175-225 bp size were cut out. After they were extracted from the gel with the Qiagen gel extraction kit they were enriched by 18 cycles of PCR amplification. The library was quantified using a picogreen assay (Invitrogen) and the library size was controlled with the Experion-system (BioRad). The library was sequenced on an Illumina GAIIx sequencer.

The resulting library DNA was analyzed by quantitative real-time PCR (3.1.12) under predetermined conditions for all oligonucleotide sets in a MX3000P (Stratagene).

3.1.15 **Bioinformatical analysis**

ChIP seq analysis

The resulting sequence data were processed with OLB_v1.9 and mapped to the *Drosophila* genome release 5 with bowtie-0.12.7. Peaks were identified with MACS14, using the same number of reads with single alignment for all conditions (6’874’000) and the default settings (with the switch “-g dm”). Only peaks called by the software as “significant” were considered, i.e. with an FDR (false discovery rate) of <10%. Subsequently, all unmapped peaks (mostly mapping to chromosome “Uextra”; 3-17 peaks per condition) and all peaks that were called in any of the ChIPs with non-immune IgGs or in Myc-ChIPs from Myc-depleted S2 cells were eliminated from the Myc-ChIP lists.

Selection of Yang peaks for ChIP

For the analysis of peaks from Yang *et al*. (2013) the data published by these authors were used. To determine the ratio of mouse α-Myc ChIPseq reads from naïve S2 cells versus Myc-depleted S2 cells for each of the 3993 peaks the program intersectBed

(bedtools v.2.17.0.) was used. 1936 regions with a ratio “naïve/Myc-depleted” ≤1.2 that did not overlap any of our peaks were retained and sorted by the number of reads that were recorded by Yang *et al*. From this sorted list, every 50th peak (for a total of 20 peaks) was selected, starting with the region with the highest number of reads in the Yang analysis. Primers were designed to cover the summit coordinate indicated by Yang *et al.,* resulting in 17 functioning primers (one region was omitted since no acceptable primers could be generated, and two primer pairs did not function, i.e. did not produce the expected product).

3.1.16 **dsRNA synthesis**

To generate specific dsRNA, linearized DNA (amplified by PCR (3.1.12)), was *in vitro* transcribed into RNA using the Megascript T7 kit (Ambion).

Table 3-9: Megascript T7 kit

Linear template DNA	2 µg
10x Reaction Buffer	4 µl
rNTPs	4 µl each
Enzyme Mix	4 µl
RNase free water	ad 40 µl

After an incubation time of 2-4 hours at 37°C, 1 µl TURBO DNase was added, mixed well and incubated for additional 15 min. DsRNA was purified with phenol/ chloroform (3.1.5) followed by isopropanol precipitation and resuspended in 50 µl RNase free water. Afterwards dsRNA was once heated up to 65°C and was then slowly cooled down to RT, before it was frozen at –80°C.

3.1.17 **Northern blot**

Total RNA was extracted from *Drosophila* S2 cells as described before (3.1.10). 20 µg were loaded per lane on a 10% Acrylamide 8 M Urea gel (3.1.7) and then transferred to a nylon membrane (Hybond N+, GE Healthcare). After UV cross-linking at 254 nm the membrane was pre-hybridized in 10 ml Church buffer for 1 hour at 62°C. As probes, DNA oligonucleotides were used, which were 5’ end-labeled with γ-P32-ATP using T4 polynucleotide kinase (NEB). Therefore, a 15 µl reaction was set up according to Table 3-10 and incubated for 1 hour at 37°. To stop the reaction 30 µl of 30 mM EDTA were added to the reaction.

Table 3-10: Oligo labeling

Oligo 100 µM	1 µl
10* PNK buffer	1.5 µl

PNK	1 µl
γ-^{32}P-ATP (10 µCi/µl)	2 µl
H_2O	9.5 µl

Unincorporated γ-P32-ATP was removed with illustra MicroSpin G-25 Columns (GE Healthcare), following manufacturer's protocol. Hybridization of the probe was performed overnight in 10 ml Church buffer at 62°C. The blot was washed for 30 µl in 2x SSC and 0.2x SSC at 62°C, dried and exposed on a Storage Phosphor Screen. 24-96 h later it was developed on the Typhoon 9200 (GE healthcare). Quantification was performed using ImageJ[2] software.

3.2 Cell biology methods

All cell culture work was performed at a sterile workbench. Cells were cultivated at 25°C.

3.2.1 **Passaging of cells**

Semi adherent cells were passaged after they completely covered the surface of the flask and started to distribute in several layers. Depending on the dilution factor, cells were taken out of the flask and transferred to one or more fresh ones. Afterwards full media was added to the maximum capacity of the flasks, 15 ml for 125 cm^2 flasks and 25 ml for 175 cm^2 flasks.

3.2.2 **Freezing and thawing cells**

For long term storage cells were harvested, counted and pelleted (800 rpm, 5 min, RT). The cells were resuspended in freezing medium (45% complete medium, 45% conditioned medium, 10% DMSO) to a final concentration of 2 x 10^7 cells/ml. 1 ml of cell suspension was always transferred to one cryo vial and slowly frozen at -80°C using MrFROSTY freezing container. After 24 hours the cells were stored in liquid nitrogen storage tank.

Cells were thawed by quickly heating them up in a 37° waterbath, washed once in full medium and resuspended in 5 ml full medium before they were plated in a 75 cm^2 falcon.

3.2.3 **Transfection of plasmid DNA**

To transfect *Drosophila* cells, one of the following transfection methods was used. An expression of the transiently transfected DNA was observed mostly 40 hours after transfection.

[2] http://imagej.nih.gov/ij/

Effectene Transfection

Cells were split 24 hours before transfection. For 6-well plates 5 x10^6 cells were plated and let adhere for 2 to 3 hours. 100 µl transfection mix was prepared according to the table below, for dishes with a lower or higher surface area the total volume of cells and transfection agent was scaled appropriately. The transfection mix was incubated for 5min at RT, then 10 µl of Effectene Reagent was added to the DNA-enhancer mixture and incubated for 5-10 µl at RT to enable transfection complex formation.

In the meantime the cells were washed once with PBS and 1.6 ml of complete medium was added. The transfection mixture was mixed with 600 µl of complete medium and dropwise added to the cells. 16h later the medium with the remaining DNA precipitates was removed and 3 ml of fresh medium was added to the cells. Cells were harvested 24-48 h later.

Table 3-11: Effectene transfection mix

plasmid DNA	0.4 µg
tub-Gal4	0.1 µg
Enhancer	3.2 µl
EC-buffer	ad 100 µl

Cellfectin Transfection

Cellfectin transfection was only used for luciferase assays. Cells were split 24 hours before transfection. For 24-well plates 1.3 x10^6 cells were plated and let adhere for 2 to 3 hours. 42 µl transfection mix was prepared according to the table below, for dishes with a lower or higher surface area the total volume of cells and transfection agent was scaled appropriately. The transfection mix was incubated for 15min at RT to generate transfection complex formation then 178 µl of serum free medium were added to the mix and directly added to the cells which were washed once with PBS during the incubation period.

30 µl later 200 µl of full medium was added to the cells. 16 hours later the medium with the remaining DNA precipitates was removed and 650 µl of fresh medium was added to the cells. Cells were harvested 24-48 h later.

Table 3-12: Cellfectin transfection mix

plasmid DNA	0.4 µg
tub-Gal4	0.1 µg
Cellfectin	21 µl
Serum free-medium	ad 42 µl

3.2.4 Transfection of dsRNA

Cells were split 24 hours before transfection. For 6-well plates 5 x10^6 cells were plated and let adhere for 2 to 3 hours. 1 ml of serum free medium was added to the cells, which were washed with serum free medium before. 10 µg of dsRNA were added and the plates were shaken smoothly. After an incubation of 30 µl at 25°C, 2 ml of full medium was added to the cells. Cells were harvested for further processing after 24-96h depending on the used dsRNA.

3.2.5 Induction of inducible fly cells

Cells which were stable transfected with constructs under the control of a metallothionein promotor were induced with $CuSO_4$ in a final concentration of 125 µM. Cells were harvested 6-8 h later and processed for RNA isolation used for qRT-PCR (3.1.10) or Western Blot (3.3.1).

3.2.6 Luciferase reporter gene assay

1.3x 10^6 cells in 24-well plates were transfected with "CG5033^{wt}-Renilla-luciferase" and "CG5033$^{\Delta EBox}$-firefly-luciferase" reporter constructs and additional expression plasmids with the Cellfectin method (3.2.3). 24 hours later, the cells were washed with PBS and disrupted in 100 µl passive lysis buffer (1x) (Promega) for 15 min at RT while shaking. The lysate was transferred into a reaction tube and cleared of the cell debris by centrifugation (1 min, 800 rpm, 4°C). To determine the luciferase activity, 10 µl of lysate was pipetted into a 96-well plate and placed into the Glomax 96 Microplate Luminometer. The device automatically added 50 µl of freshly prepared luciferase substrate solution and measured light emission at 562 nm two seconds later for an interval of ten seconds (in relative light units, RLU). To normalize the results the ratio of Firefly to Renilla was calculated.

3.3 Protein biochemistry methods

3.3.1 Generation of protein lysates for Western blot

To isolate total protein cells were harvested by rinsing out the dish with the actual medium, washed once in PBS and pelleted (800 rpm, 5 min, 4°C). The cell pellet was directly subjected to lysis by resuspending cells in NP 40 buffer with freshly added proteinase inhibitors (1:100). 5x10^6 cells were lysed in 50 µl lysis buffer respectively. The cells were incubated for 30 minutes on ice, then the cell debris was pelleted (13000 rpm, 15 min, 4°C) and the supernatant transferred to a fresh tube. The lysates were mixed with Laemmli Buffer in an equal volume and were directly used for Western blot analysis or stored at -20°C. 25 µl (1.25x10^6 cells) were loaded per lane on a SDS-Gel (3.3.2).

3.3.2 SDS polyacrylamide gel electrophoresis (SDS-PAGE)

Discontinuous SDS-PAGE (Sodium dodecyl sulfate polyacrylamide gel electrophoresis) was used to separate proteins according to size (Laemmli *et al.,* 1970). Protein lysates as described in 3.3.1 were incubated 5 minutes at 95°C and spun down afterwards. The protein samples were then transferred into the wells of an SDS polyacrylamide gel consisting of a 10% stacking gel and a 5% resolving gel. The PageRuler Pre-Stained Protein Ladder (Fermentas) was used as a size marker. The electrophoresis was carried out using the Bio-Rad SDS-PAGE chamber with SDS running buffer, first at 80 V for 30 minutes, then at 120 V for 90-120 minutes.

3.3.3 Staining Protein gels with Coomassie Blue

The quality and quantity of GST fusion proteins (3.3.7) after bacterial expression was checked by separating the samples on a SDS-PAGE followed by coomassie staining for at least 1 hour. To remove excess dye the gel was incubated several times with fresh destaining solution until a clear background was obtained.

3.3.4 Western blot

Proteins were separated by SDS-PAGE (3.3.2), followed by blotting onto a nitrocellulose membrane using a tank blot system. A nitrocellulose membrane of the size of the SDS gel was incubated first in water for 30 sec and then equilibrated in tank blot buffer for another 30 sec. Gel and membrane were neatly layered on top of each other and fixed between Whatman filter papers in a Western blot transfer chamber (BioRad). The electrophoretic protein transfer was carried out at 215 mA for 2 hours. All following incubation steps were performed with gentle shaking. The membrane with immobilized proteins was blocked in blocking solution for at least 30 µl, and then cut into pieces if several proteins from the same membrane were visualized. The membrane pieces were incubated o./n. with a dilution of primary antibody in blocking solution (see Table 3-13), then washed (3 x 10 min in TBS-T), incubated with secondary antibody (coupled to horseradish peroxidase; dilution 1:10,000) in blocking solution for 3-4 hours at RT, and then washed again (3 x 10 µl in TBS-T). To visualize the proteins of interest a specific chemiluminescent signal was triggered by the Immobilon Western Chemiluminescent HRP Substrate from Millipore, which was used according to the manufacturer's instructions. The signal was detected with the ImageQuant LAS 400 imager (Fujifilm Global).

Table 3-13: Amount of antibodies used for western blot

Antibody	concentration	Western blot
α-AU1	1.0 mg/ml	1.0 µg/ml
α-HA	1.0 mg/ml	1.0 µg/ml
mouse α-Myc	0.015 mg/ml	0.3 µg/ml

rabbit α-Myc (SC)	0.2 mg/ml	0.4 µg/ml
α-GST-Chinmo	not known	dilution: 1:500
α-Chinmo	1.21 mg/ml	6.05 µg/ml
α-GFP	0.2 mg/ml	0.2 µg/ml
α-Tub	not known	dilution: 1:100,000

3.3.5 **Stripping antibodies from nitrocellulose membranes**

To release antibodies from a nitrocellulose membrane covered with immobilized proteins the membrane was incubated at 60°C in a water bath in freshly prepared stripping buffer for 30 µl. Afterwards the membrane was washed with TBS-T (3 x 10 µl), blocked and incubated with primary and secondary antibodies as described in 3.3.4.

3.3.6 **Immunoprecipitation**

Immunoprecipitations (IPs) were performed to detect protein-protein interactions. Cells were collected as described in 3.3.1 and lysed in 300 µl ice cold NP-40 lysis buffer with fresh proteinase inhibitors (1:100). All quantities refer to one single well from a 6-well plate, containing approximately $5x10^6$ cells. After vortexing 3 x 15 sec at full speed, samples were put on ice and shook for 30 µl.

In the meantime Protein A-Sepharose 4B (Invitrogen) and Protein G-Sepharose 4FastFlow (GE Healthcare) beads (each 150 µl) were mixed and washed 5 times with lysis buffer and finally resuspended in an equal volume of lysis buffer. For pre-clearing, 40 µl of the 50% protein A/G beads/ lysis buffer suspension was added to each sample and incubated on a rotating wheel for 45 min at 4°C. The beads were spun down and the supernatant was transferred into a new tube. A 6% input of each lysate was collected and mixed with Laemmli buffer prior to freezing.

To each IP sample 1 µg specific antibody and 40 µl of the 50% protein A/G beads/ lysis buffer suspension were added and rotated for 4 hours at 4°C. The beads loaded with protein-bound antibodies were washed three times with lysis buffer, then 40 µl of Laemmli buffer were added and the samples were frozen at -20°C until they were further processed by SDS-PAGE and Western Blot, using the input as a reference for IP efficiency.

Endogenous Immunoprecipitation

For endogenous IPs of Chinmo and Myc $260*10^6$ naïve cells were harvested and precipitated with 9.6 µg of rabbit α-Chinmo antibody or rabbit-IgG and 100 µl of a 50% suspension of protein A/G beads.

In contrast to exogenous IPs, samples were sonicated (5 sec, 59 sec pause; in total 1 min, amplitude 15%) directly after lysis and ethidium bromide was added after sonification (20 µg/ml; incubate 30 µl before pre-clearing).

3.3.7 Bacterial expression and purification of GST fusion proteins

The gene of interest was cloned into the pGEX 4-T1 vector, which enables expression of GST fusion proteins in E.coli B21 cells upon induction with Isopropyl-®-D-thiogalactopyranosid (IPTG). A clonal overnight culture of 5 ml was diluted 1:50 and incubated shaking at 37°C until it reached an optical density of A600 nm = 0.6. IPTG was added to a final concentration of 1 mM and the culture was grown for another 3 hours at 37°C. The bacteria were pelleted (460 rpm, 10 µl, 4°C) and either stored at -80°C or directly lysed in 7.5 ml lysis buffer containing fresh proteinase inhibitors. The lysate was sonicated (10 x 10 sec, pausing 1 min in between, 20% amplitude) and centrifuged (4600 rpm, 30 µl, 4°C) to pellet bacterial cell debris and insoluble proteins. The pellet was solubilized in 7.5 ml lysis buffer and a fraction of the solubilized pellet and the supernatant was mixed with Laemmli buffer and analyzed on a coomassie gel to verify the expression of the GST fusion protein and to determine its solubility.
For the purification of the GST fusion protein, 0.67 ml Glutathione Sepharose 4B beads (GE Healthcare) were used. After washing the beads three times with cold PBS (1000 rpm, 5 min, 4°C) 0.5 ml PBS was added to the beads, resulting in a 50% suspension. 0.3 ml of the suspension was added to the supernatant and incubated shaking for 30 µl at RT. The beads were sedimented (800 rpm, 5 min, 4°C) and washed three times with cold PBS. The GST fusion proteins were eluted in elution buffer (10 µl, shaking, RT) centrifuged (800 rpm, 5 min, RT) and the supernatant was transferred into a new tube. This step was repeated twice and the eluates were pooled.

3.3.8 Protein determination by the Bradford method

Protein concentrations were determined according to Bradford (1976). Bradford dye reagent was mixed in a ratio of 1:1 with H_2O and pipetted into 1 ml cuvettes. 1 µl of the protein sample solution was added and mixed. After incubation of 5 min at RT the absorption was measured at a wavelength of 595 nm using an appropriate reference. The measured values were compared to a previously obtained standard curve to calculate the protein concentration of the sample solution.

3.4 Fly specific methods

3.4.1 Fly culturing

Flies were kept on standard *Drosophila* medium. If not indicated otherwise crosses were performed in climate chambers at 25°C.

3.4.2 Heat shock conditions for overexpression experiments

Fly vials were incubated in a water bath for 1 hour at 37°C the evening before the experiment. Afterwards the flies were transferred back to 25°C.

3.4.3 Images of fluorescent tissue

Larvae which expressed GFP plus another transgene ubiquitously or in a tissue of interest were immobilized on ice and placed on a cover lid of a 24-well plate. The size and shape of the fluorescent tissue was observed and documented using the binocular microscope (Discovery V8, Zeiss) with the GFP filter (475 nm).

3.4.4 Extraction of genomic DNA

To extract genomic DNA from adult flies or larvae, 1-5 flies were collected in a tube and homogenized with 100 µl extraction buffer A using a pestle to crash the carcasses. For higher number of flies 200 µl of buffer were used. After incubating the flies for 30 µl (70°C, shaking 350 rpm) 14 µl 8 M Sodium acetate was added and put on ice for 30 µl. To pellet fly debris samples were centrifuged twice (1300 rpm, 15 min, 4°C) and the supernatant was transferred to a new tube. To precipitate the nucleic acids, ½ volume isopropyl alcohol was added to the tube, inverted and centrifuged (13000 rpm, 5 min, RT). The pellet was washed once with cold Ethanol (100%) centrifuged as before and the pellet was eluted in 40 µl TE.

To remove genomic RNA, RNase digest was performed. Therefore 1 µl RNase A was added and incubated for 15 min at 37°C.

3.4.5 Methylation Assay with larvae

For measuring methylation activity, total RNA was isolated from larvae being mutant or wildtype for Uhg1. 2'-O-ribose-methylation was determined by reverse transcription under limited nucleotide concentrations as previously described (van Nues, 2011).

First of all, primers specific for the methylated region of interest were labeled with γ-^{32}P-ATP. Therefore, a 15 µl reaction was set up according to Table 3-10 (3.1.17) and incubated for 1 hour at 37°C before the labelled oligos were purified through a G50 column (GE Healthcare) and diluted twofold.

In the following hybridization reaction 8 µg of total RNA were annealed to 10 ng kinased oligo in a 30 µl reaction with 2x Annealing buffer, incubated for 2min at 95°C and for 10 µl 65°C before it was put on ice until the reverse transcription mix was prepared.

Reverse transcription was performed under three different dNTP concentrations, 10 mM, 1 mM and 0.5 mM or 0.1 mM. Table 3-14 shows the ingredients of the reverse transcription mix, of which 4 µl were mixed with 6 µl of the hybridization reaction and incubated for 45 min at 42°C. Each sample was mixed with formamide loading dye and separated on a 10% acrylamide/ 7 M urea gel and then visualized using a phosphorimager.

Table 3-14: Reverse transcription mix

AMV reverse transcriptase (10 u, Promega)	0.1 µl
10x RT buffer	1 µl
RNasin	0.5 µl
dNTPs (10 mM, 1 mM or 0.5 mM)	1 µl
RNase free H_2O	ad 4 µl

The RNA sequencing ladder was carried out as previously described (Nilsen, 2013), using 0.167 µg RNA for each reverse transcriptase reaction.

3.4.6 **Translation Assay with larvae**

750 µl Ringer's solution containing 15 µCi/ml ^{3}H-Amino-Acid mix were added to 10 fully inverted larvae (in 100 µl Ringer's solution) and placed on a wheel for 1 hour at room temperature for peptide incorporation. Subsequently, the supernatant was decanted and the carcasses were washed twice with cold Ringer's solution before they were lysed in 350 µl Cell Lysis Buffer (100 mM Tris-HCl, pH 8.0, 100 mM NaCl, 0.5% Triton X-100) using a pestle to crush the carcasses. For full lysis, samples were periodically vortexed during a 10 µl sit on ice. To pellet larval debris samples were spun down for 2 min (1000 rpm, RT).

250 µl of the aqueous lysate were mixed with 15 µl suspended Strataclean Resin (Stratagene) and allowed to rest for 5 min. After removing the supernatant resins were washed with Ringer's solution and transferred to 3 ml scintillation buffer. Following a 30 min rest, 1 minute counts per vial were obtained.

With the remaining aqueous lysate protein quantification was performed (3.3.8).

3.4.7 **Neuroblast type II tumors**

Type II neuroblast tumors (NBII) were induced by knocking down the tumor suppressor brat specifically in these cells with the driver system "worniu-GAL4 asense-GAL80". Co-expression of firefly luciferase allowed the quantitative determination of tumor mass. Appropriate male adults were collected 12 hours after eclosion and frozen at -80° until use. Upon thawing, 100 µl 1x Passive Lysis Buffer (Dual Luciferase Reporter Assay System; Promega) was added to individual flies as well as some steel beads (SSB14B, Next Advance). The carcasses were crushed using a Bullet Blender homogenizer (Next Advance) before another 100 µl of buffer were added and the lysates were incubated for 10 µl at RT. Fly debris was pelleted (4 min, 1200 rpm, RT) and 10 µl of supernatant were processed for luminometry in a Glomax luminometer (3.2.6).

4 Results

4.1 Myc binds and regulates genes involved in ribosome biogenesis

4.1.1 DNA-library preparation for ChIPseq

The transcription factor Myc promotes cell growth, proliferation and other processes in part by stimulating transcription of a number of genes essential for ribosome biogenesis and protein translation including ribosomal protein genes. Furthermore it stimulates the expression of r- and tRNAs and therefore controls multiple components of ribosome biogenesis (van Riggelen *et al.,* 2010).

However, most studies were performed in vertebrates and a comprehensive list of Myc target genes in *Drosophila melanogaster*, including non-polyadenylated transcripts, is still missing. To investigate which Myc regulated genes are controlled by direct Myc binding, ChIPseq experiments were performed in *Drosophila* S2 cells. The combination of Chromatin immunoprecipitation (ChIP) followed by massively parallel DNA sequencing is used to map global binding sites for any protein of interest. Since all experiments were performed in a *Drosophila* background, Myc refers to *Drosophila* Myc if not otherwise stated.

For ChIPseq in naïve and Myc depleted cells, cells were either transfected with dsRNA against Myc or left untreated and further processed for Western blot (3.3.4) or ChIP (3.1.13). The knockdown samples were included to distinguish between specific and unspecific Myc binding sites and the efficiency of the depletion was verified via Western blot, using α-tubulin as loading control. The knockdown was highly efficient, showing a depletion by almost 100% (Figure 4-1 A). For ChIP, protein was cross-linked to DNA, and the chromatin was lysed and sheared to nucleosomal size before it was immunoprecipitated using equal amounts of mouse α-Myc antibody or non-immune mouse IgGs (2.4.1). Like the knockdown samples, the non-immune IgGs were used to check for background signals. Binding sites present in either of the controls can be considered Myc non-specific. The input control is necessary to identify significant enrichment for a ChIP-Seq signal and to control for biases in the experimental methods. After reversion of the crosslink and digestion of the protein the efficiency of the immunoprecipitation was tested. Therefore qPCR (3.1.12) was performed for one positive (Nop5) and one negative (Pka-C1) Myc target gene (Figure 4-1 B) using the immunoprecipitated DNA. Myc was already shown to bind to Nop5 in ChIP experiments whereas Pka-C1 was chosen for comparison, as it shows associated Myc-binding but does not change expression upon depletion of Myc (Furrer *et al.,* 2010).

The qPCR revealed an enrichment (22 fold) for Nop5 in the Myc ChIP over IgG control (0.03% ± 0.02% of input vs. 0.0008% ± 0.0004% of input) whereas the enrichment for Nop5 in the Myc depleted cells is reduced by almost 7 fold compared to non-treated cells (0.004% ± 0.001% of input vs. 0.001% ± 0.0003% of input; Figure 4-1 B). The negative control Pka-C1 shows only slight differences between enrichment over IgG in naïve (7 fold) versus depleted cells (4 fold). Since the enrichment over IgG was high for the positive controls in naïve cells and the α-Myc antibody did not display strong background binding, the samples were further processed for ChIPseq.

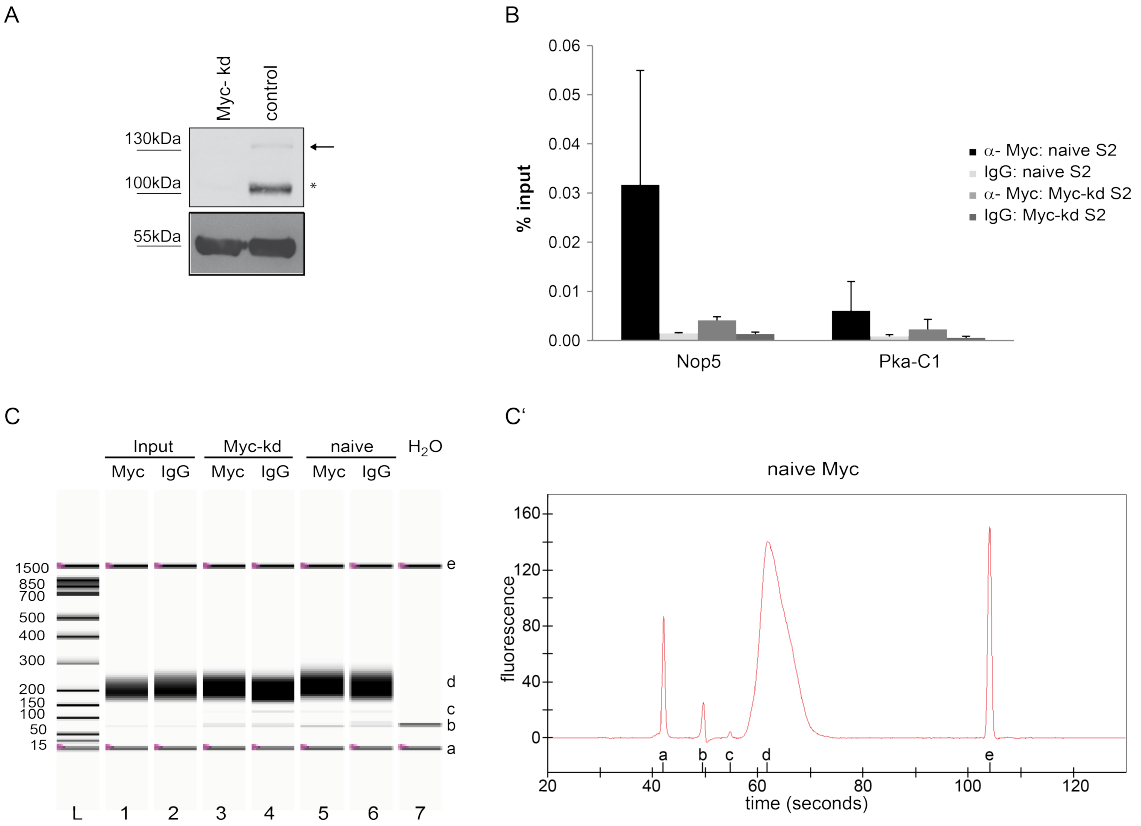

Figure 4-1: Process of DNA-library preparation for ChIPseq[3]

A. The Western blot illustrates the efficiency of Myc depletion; the asterisk points to the Myc band at ca.107 kDa, the arrow to a band presumably arising from post-translational modification of Myc. Western blot was performed with mouse α-Myc (upper panel) and mouse anti-α-Tubulin antibodies (lower panel) as loading control.
B. ChIP-qPCR of control regions. Chromatin was isolated from naïve S2 cells or from S2 cells depleted of Myc, precipitated with mouse α-Myc or control IgG antibodies and assayed by qPCR for enrichment of the indicated loci. Error bars indicate SD of technical triplicates.
C. Gel picture of a DNA 1K chip. The lanes 1-6 show size, quality and quantity of the DNA library (d) from the depicted samples plus additional gel peaks (a, e), unbound primers (b) and adaptor dimers (c) ; lane 7 contains only H_2O as negative control.
C'. Electropherogram of the DNA library of the naïve Myc ChIP (lane 5, Figure 4-1 C). The peaks, numbered a-e correspond to the bands shown in C.

The concentration of the recovered DNA was measured using a fluorescent probe (picogreen) that binds dsDNA and forms a highly luminescent complex when compared

[3] Parts of this figure were published in similar form in Herter *et al.,* 2015 (see also following pages)

to free dye in solution and can be measured with a fluorescent reader. Equal amounts of DNA were further processed for the DNA-library preparation (3.1.14). The processing of the library included end-repair of the DNA fragments to ensure that each molecule is free of overhangs and contains 5' phosphate and 3' hydroxyl groups. Furthermore, a non-templated deoxyadenosine 5'-monophosphate (dAMP) was incorporated onto the 3' end of the blunted DNA fragments to prevent concatamer formation during ligation steps. This process, also called dA-tailing, enables DNA fragments to be ligated to adaptors with complementary dT-overhangs. After ligation of the adaptors containing indexed sequences which allow discriminating between different samples, the ligation products were size selected via an agarose gel at 175-225 bp, purified and PCR-amplified to enrich for fragments containing adaptors on both ends. Quality and quantity of the resulting DNA-library were measured with an automated electrophoresis station (Bio-Rad, DNA 1K chip). Figure 4-1 C shows the gel picture of the DNA 1K chip. As expected, the lanes 1-6 show a band around 200 bp (d), which represents the DNA library. The size of the band is based on the shearing of the chromatin and addition of the adaptors and fits to the size obtained from the size selection. On the corresponding electropherogram (Figure 4-1 C') for the DNA library of the naïve Myc ChIP (Figure 4-1 C; Lane 5) a single peak is depicted for the library (d), displaying a good quality of the library. This was the case for all samples. The first and the last band/peak (a and e) correspond to the internal Experion lower 15 bp and higher 1500 bp marker. The additional bands/peaks correspond to unbound primers (b) and adaptor dimers (c) of the library processing. H_2O was loaded as a negative control (lane 7). To map the distribution of the sequences enriched by ChIP in a genome wide manner, Next Generation Sequencing was performed. Therefore, equal amounts of the different DNA-libraries were denatured and immobilized on a glass carrier plate. Individual DNA molecules were amplified using "Bridge-PCR" resulting in identical DNA-clusters, and sequenced by "Sequence by Synthesis" (SBS, Illumina) procedure. Table 4-1 summarizes the number of individual sequences (total reads), number of single aligned reads (single alignment), number of reads which were not aligned (no alignment) and called peaks (binding sites) obtained for each sample.

For each condition between 12,569,801 and 29,940,708 reads were obtained of which 54% to 70% mapped to a single position in the *Drosophila* genome. The number of total and single mapped genes fit to ChIPseq data obtained from vertebrates (Walz *et al.,* 2014). However, the number of binding sites is much lower in *Drosophila*. This was shown before by Orian *et al.* (2003). The reads with multiple or no alignment were not further considered. To identify the number of binding sites specific to Myc, the called peaks identified by MACS14 (binding sites, Table 4-1), were assigned to genes with the help of intersectBed and further processed by eliminating all peaks that were called in IgG control or after Myc depletion. This resulted in a final number of 240 Myc binding sites. The quality of the ChIP was very good, indicated by a high ratio of binding sites obtained for naïve Myc ChIP versus IgG and knockdown control (90%) and loss of very few binding sites (7%) after filtering for FDR 0.1.

Table 4-1: ChIP-sequencing reads of S2 cells chipped with mouse α-Myc.
After performing peak calling using MACS software, peaks were filtered with different false discovery rate (FDR) values and used for subsequent analyses. Input and IgG control peaks were subtracted by MACS. FDR is set to 10%.

Sample	Total reads	Single alignment	No alignment	Binding sites	Binding sites (FDR 0.1)
Naïve α Myc	12.569.801	6.874.174	2.781.777	260	240
Naïve IgG	14.848.998	9.475.215	1.630.732	27	
KD Myc α Myc	16.283.576	9.058.587	3.315.590	22	
KD Myc IgG	13.234.306	7.851.731	2.249.910	24	
Naïve Input	29.940.708	20.986.173	738.107		
KD Myc input	23.512.194	16.678.250	553.226		

4.1.2 Myc binds a core set of sites

A list of 240 peaks resulted from the ChIPseq experiment after analyzing the data (3.1.14) that were specifically bound by Myc in naïve cells but not in the Myc depleted cells and which were not recognized by control IgGs (Table 4-1). An example of a specific binding site is shown in Figure 4-2 A for Fibrillarin. A distinct peak can be seen in naïve cells, which were chipped with the mouse α-Myc antibody. The summit of the peak is located at the E-box, marked with an asterisk. No peak is present in the negative controls as well as the input sample. To exclude that binding sites were not detected due to epitope masking of the monoclonal mouse α-Myc antibody, the ChIPseq was repeated with a polyclonal rabbit α-Myc antibody (kindly provided by G. Morata) and rabbit IgG control (Table 4-2). This ChIPseq experiments resulted in 98 specifically Myc bound peaks, of which most (75) overlapped with peaks from the first ChIPseq experiment (Figure 4-2 B; Table 4-2).

Table 4-2: ChIP-sequencing reads of S2 and KC 167 cells chipped with rabbit α-Myc and called binding sites using MACS software.

Sample	Total reads	Single alignment	No alignment	Binding sites	Binding sites (FDR 0.1)
Naïve α Myc S2	17,098,819	11,317,552	1,993,197	263	98
Naïve IgG S2	11,543,400	6,867,642	2,370,948	31	
Naïve Input S2	13,314,075	9,796,752	633,339		
Naïve α Myc KC	27,884,589	19,565,700	1,646,483	308	21
Naïve IgG KC	19,316,418	9,122,683	5,944,743	187	
Naïve Input KC	33,927,814	25,567,219	823,938		

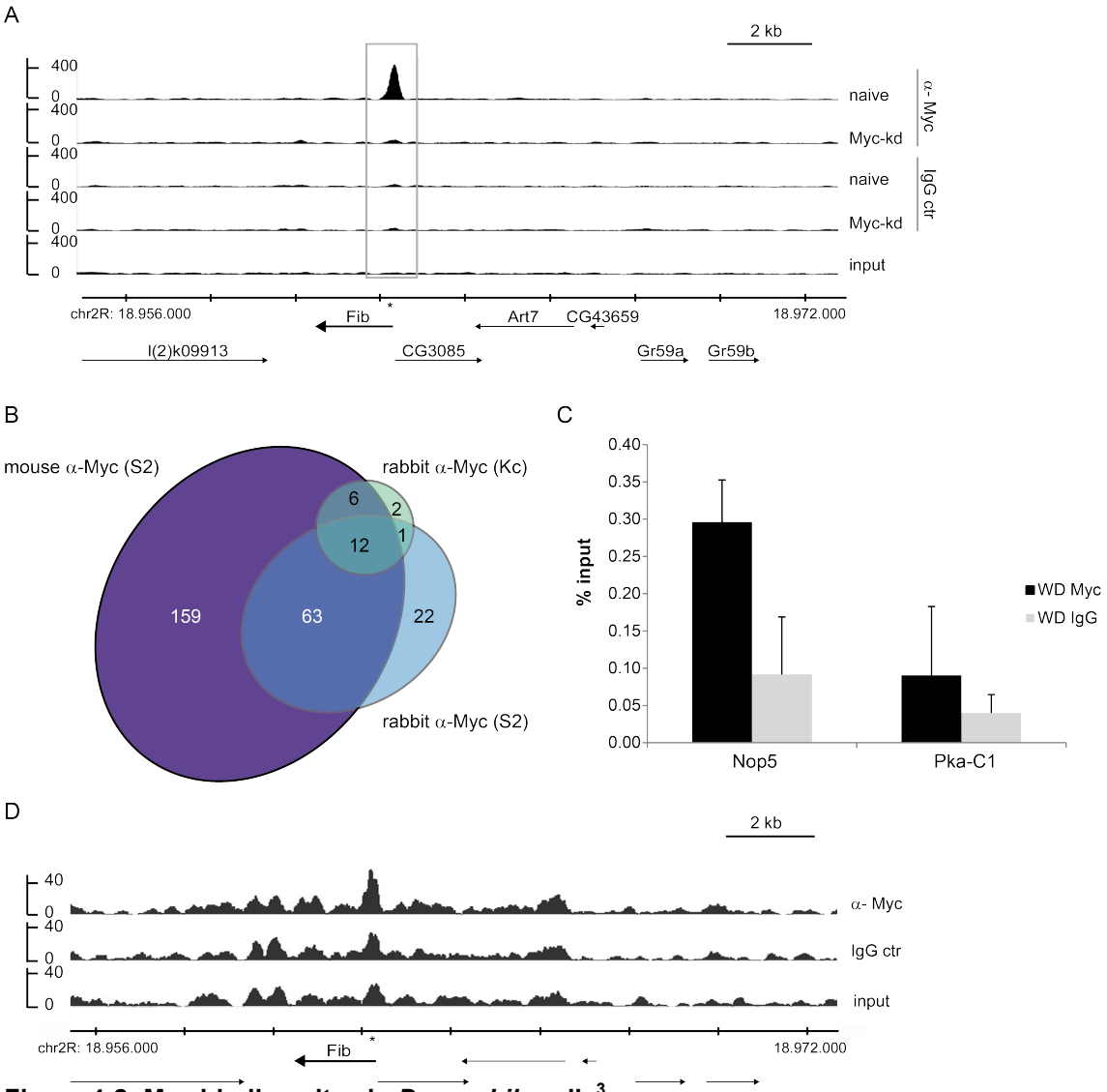

Figure 4-2: Myc binding sites in *Drosophila* cells[3]

A. As an example of a binding site in S2 cells Myc binding to the Fibrillarin locus is shown. Strong binding is observed with mouse α-Myc antibodies in naïve S2 cells (1st lane), but not upon Myc depletion (2nd lane) or with control mouse IgG (3rd and 4th lane); the grey box marks the Myc binding peak as called by the software MACS, the asterisk shows a consensus E-box. Chromosomal coordinates (on chromosome 2R) are indicated below the traces, as are the extents and orientations of genes in this region.
B. Venn-diagram of the number and overlap of binding sites resulting from three independent ChIPseq experiments in *Drosophila* S2 and Kc167 cell lines.
C. ChIP-qPCR of control regions. Chromatin was isolated from 975 wing discs, precipitated with rabbit α-Myc or control IgG antibodies and assayed by qPCR for enrichment of the indicated loci. Error bars indicate SD of technical triplicates.
D. ChIPseq profile of Fibrillarin as an example of a Myc binding site in wing imaginal discs. Weak binding is observed with rabbit α-Myc antibody as well as for control rabbit IgG and input control; the asterisk shows the consensus E-box. Chromosomal coordinates are indicated below the traces, as are the extents and orientations of genes in this region.

The 263 peaks which were found in the two different ChIPseq experiments performed in S2 cells fit to the number of Myc binding sites found in DamID experiments performed by Orian *et al.* (2003), where they identified 287 Myc binding sites in DamID experiments. On the other hand the number of binding sites is smaller than the nearly 4000 sites reported by Yang *et al.* (2013) who performed their ChIPseq in Kc167 cells

and used a different antibody (Santa Cruz, rabbit α-Myc). To exclude major differences between the different cell lines, ChIPseq with chromatin from Kc167 cells was performed, using the rabbit α-Myc antibody (G. Morata) and control IgGs (Table 4-2). Analysis of the data led to the identification of 279 Myc binding sites, of which 110 overlapped with those found in S2 cells. As the background binding in the Kc167 cells was substantially higher than in the S2 cells, only 21 binding sites were statistically significant (FDR < 10%; of which 19 overlap peaks in S2 cells, Figure 4-2 B). Since the majority of binding sites overlapped or was non-specific, major differences between the cell lines were excluded.

To get additional data about Myc binding *in vivo*, almost 1000 wing discs were isolated from wandering larvae and further processed for ChIPseq, using the rabbit α-Myc antibody or rabbit IgG control. The qPCR showed good enrichment over IgG for Nop5 (0.3% ± 0.06% of input vs. 0.09% ± 0.08% of input) but not for the negative control Pka-C1 (0.09% ± 0.09% of input vs. 0.04% ± 0.02% of input; Figure 4-2 C). Preparation of the library worked well, resulting in similar DNA concentrations after PCR enrichment as obtained for S2- and KC-cells (data not shown). The sequencing of the DNA-library had only low reads (Table 4-3), but since 68% to 76% of all reads mapped to a single position in the *Drosophila* genome, the sequencing depth was probably sufficient. However, no binding site with a false discovery rate below 0.1 was called. Even the strong Myc target genes, e.g. *fibrillarin* showed unspecific binding in input and IgG control (Figure 4-2 D). Unfortunately it is not possible to distinguish whether this is due to a lower amount of Myc in wing discs compared to S2 or Kc167 cells or if technical differences in ChIP progression led to these results.

Table 4-3: ChIP-sequencing reads of wing imaginal disc cells chipped with rabbit α-Myc.

Sample	Total reads	Single alignment	No alignment
Naïve α Myc	5,893,418	4,267,658	598,248
Naïve IgG	4,034,230	2,766,320	527,988
Naïve Input	5,683,989	4,302,615	262,376

4.1.3 Investigation of Myc binding sites identified by Yang *et al*.

To exclude that several binding sites might have been missed due to epitope masking, ChIP experiments with the Santa Cruz (SC) antibody were performed with several Myc binding sites detected by Yang (3.1.15) (Figure 4-3 A). The ChIP signals at the positive controls Nop5 and Uhg1 (4.1.4) showed a strong enrichment compared to IgG (146 fold and 176 fold) which was drastically reduced after Myc depletion (34.4 fold and 10 fold). Also several of the Yang binding sites showed a strong enrichment over IgG (e.g. 2679, 1421, and 1234). The enrichment over IgG in naïve and Myc depleted cells is stronger for the Santa Cruz antibody than for the mouse α-Myc antibody (compare

Nop5 in Figure 4-1 B and Figure 4-3 A). This might me due to a higher sensitivity of Santa Cruz antibody or a better ratio towards the rabbit IgG. Indeed, quantification (ImageJ2 software) of the western blot signals (Figure 4-3 C) reveals that the Santa Cruz antibody still detects 3% of the Myc signal after Myc-kd, whereas the mouse α-Myc antibody only detects 1.5% of residual protein. However, Yang *et al.* did not include any control ChIPs with non-immune IgGs or from Myc depleted cells and therefore we checked for the enrichment over IgG after Myc knockdown. Most of the sites exhibited only poor or no reduction after Myc knockdown (1421, 505, 1503), whereas some (2679, 193, 429, 1234) even displayed increase. Furthermore we looked at the ChIPseq traces of the selected Yang peaks (Figure 4-3 B), obtained with the mouse α-Myc antibody (4.1.1). In all the ChIPseq traces a clear peak can be seen for the α-Myc ChIP in naïve cells. However these peaks are also present in the unspecific IgG control, after Myc depletion as well as in the input sample, indicating that these regions might be enriched in the library. Since the specificity of the antibody was never shown before, western blot analysis was performed (3.3.4) with naïve and Myc-depleted cells and incubated either with the mouse α-Myc or the rabbit α-Myc (SC) antibody (Figure 4-3 C). Both antibodies detect Myc on the western blot and, as expected the Myc knockdown is highly efficient. The commercial antibody, however, detects an additional band which is unaffected by the knockdown. Hence the non Myc specific ChIP signal might correspond to this background reactivity of the Santa Cruz antibody.

Since a large fraction of binding sites, obtained by Yang *et al.*, (2013) are non Myc specific, and we only identified 265 binding sites in three different ChIPseq setups, we consider these sites to be the core set of Myc target genes.

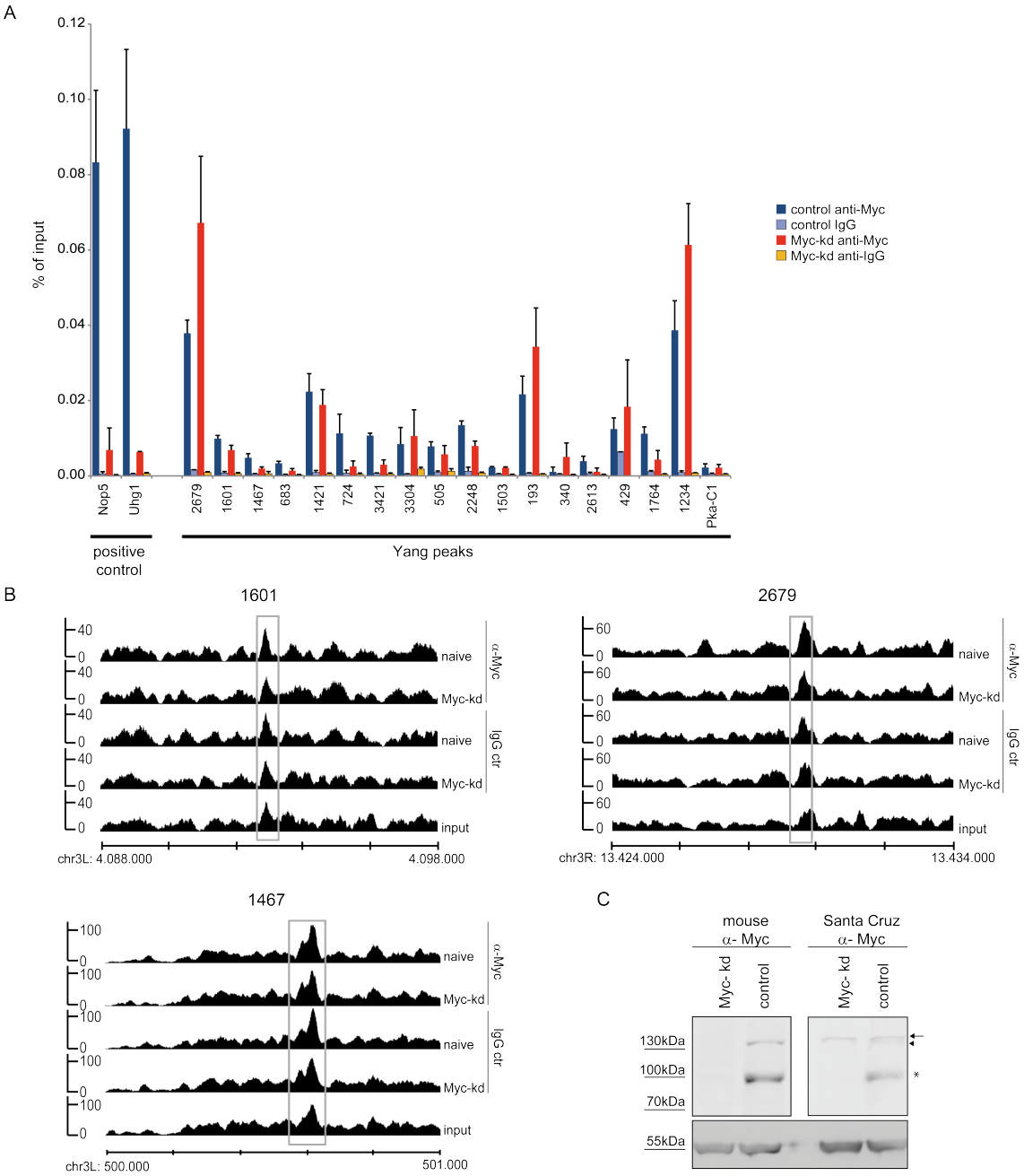

Figure 4-3: Analysis of Myc binding sites published by Yang *et al.*[3]

A. ChIP-qPCR of Yang peaks. Chromatin was isolated from naïve S2 cells or from S2 cells depleted of Myc, precipitated with rabbit α-Myc (SC) or control IgG antibodies and assayed by qPCR for enrichment of the indicated loci. Error bars indicate SD of technical triplicates.
B. ChIPseq traces obtained with the mouse α-Myc antibody or with mouse control IgG. Myc binding is observed in all lanes. The grey boxes mark the Myc binding peak as called by the software MACS. Chromosomal coordinates (on chromosomes 3L and 3R) are indicated below the traces.
C. The Western blot illustrates the efficiency of Myc depletion; the asterisk points to the Myc band at ca.107 kDa, the arrowhead to a band presumably arising from post-translational modification of Myc. The Santa Cruz antibody detects an additional band slightly above this modification of Myc which is unaffected by Myc depletion (arrow). The lower panel shows the loading control, blotted against α-Tubulin.

4.1.4 **Myc binds to Uhgs**

Amongst the Myc bound genes we found a group of targets which had not been described before. Four out of seven U-snoRNA host genes (Uhgs) and a putative novel Uhg were found to be bound (Uhg1, 2, 4, 5; Figure 4-4) and carry an E-box motif. The Myc binding sites of Uhg1, 2 and 5 are centered on the consensus E-box whereas the Myc binding site for Uhg4 is located in close proximity.It is very likely that the 2R-cluster is a novel Uhg locus, since it consists of three snoRNAs on chromosome 2R that are arranged in tandem and are flanked by a consensus E-box (Figure 4-4), which is strongly bound by Myc. However, a first trial to amplify the whole gene region failed (data not shown). It remains open if the selected oligonucleotides and the PCR conditions were not optimal for the amplification or if the 2R-cluster is no novel Uhg.

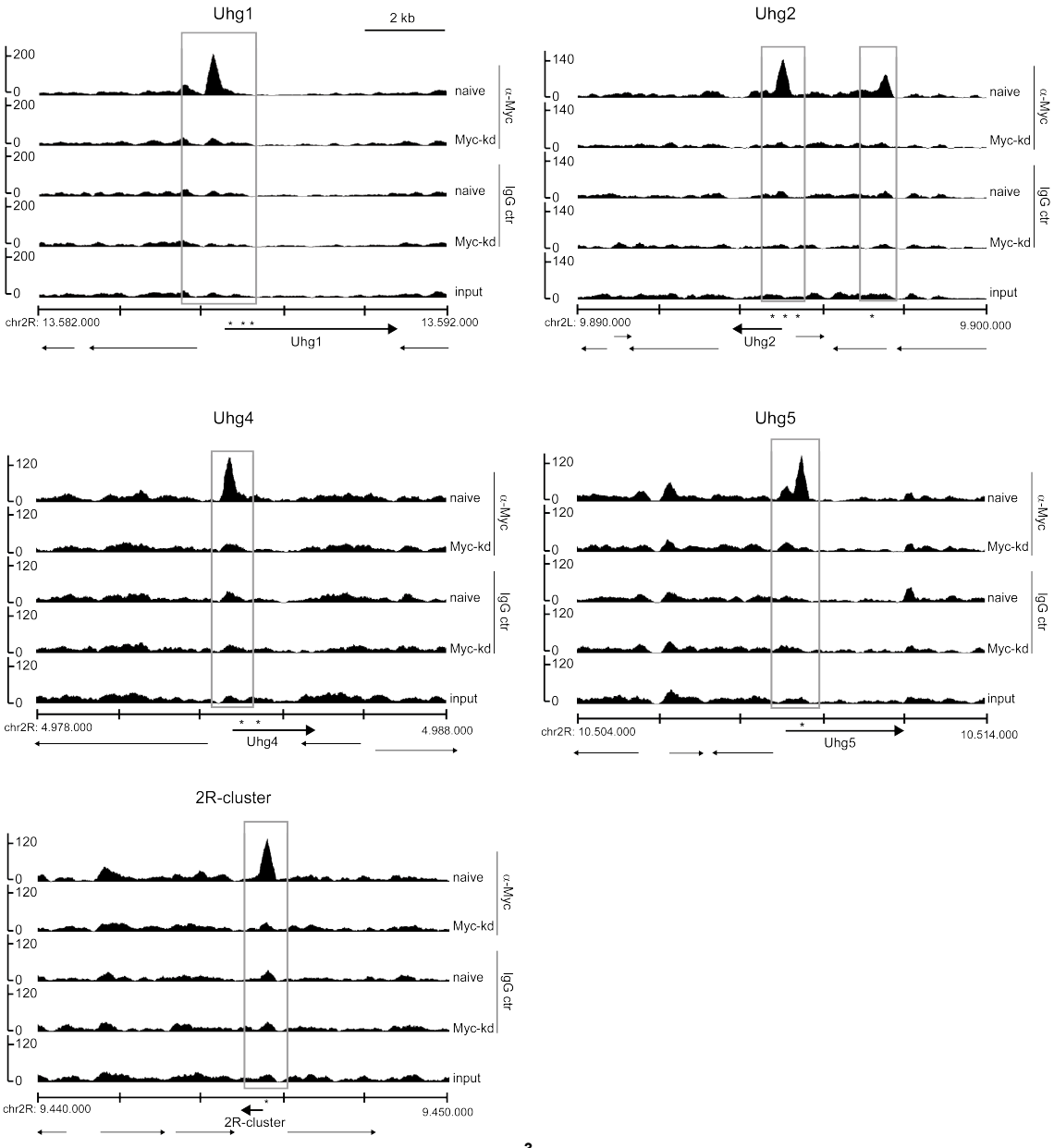

Figure 4-4: Myc binds U-snoRNA host genes[3]

ChIPseq profiles of Uhg1, Uhg2, Uhg4, Uhg5 and Uhg7 plus a putative novel Uhg, the so called 2R-cluster. Strong binding is observed with mouse α-Myc antibodies in naïve S2 cells (1st lane),

but not upon Myc depletion (2nd lane) or with control mouse IgG (3rd and 4th lane); the grey boxes mark the Myc binding peaks as called by the software MACS, the asterisk show consensus E-boxes. Chromosomal coordinates are indicated below the traces, as are the extents and orientations of genes in this region.

The binding of Myc to the E-box was confirmed by ChIP experiments including Nop5 as positive and Pka-C1 as negative control (Figure 4-5 A), using the rabbit α-Myc antibody (SC). The binding to the different Uhg genes is highly enriched over IgG in control cells but not after Myc depletion (Table 4-4, rabbit α-Myc (SC)). The negative control Pka-C1 shows no difference in enrichment between naïve and Myc depleted cells (naïve: 10.4 fold; kd: 6.4 fold). Uhg1 was used as a positive control in further experiments. The ChIP was also performed using the mouse α-Myc antibody, also showing a strong reduction of Myc binding to the Uhgs after Myc depletion (78%-94%; data not shown). The enrichment over IgG, however, is much weaker compared to the rabbit α-Myc antibody (SC), probably corresponding to a higher background binding of the mouse IgGs (Table 4-4, mouse α-My).

Table 4-4: Enrichment over IgG in control and Myc depleted cells
The enrichment data of the rabbit α-Myc (SC) antibody refer to Figure 4-5 A. The qPCR data of the mouse α-Myc ChIP are not shown.

	Naïve rabbit α-Myc (SC)	Myc-kd rabbit α-Myc (SC)	Naïve mouse α-Myc	Myc-kd mouse α-Myc
Nop5	146 fold	34.4 fold	Not done	Not done
Uhg1	176 fold	10 fold	5.2 fold	0.55 fold
Uhg2	196.3 fold	11.9 fold	3.3 fold	0.47 fold
Uhg4	35.9 fold	3.5 fold	2.6 fold	0.41 fold
Uhg5	13.5 fold	10.5 fold	1.4 fold	0.45 fold
2R-cluster	77.8 fold	10.4 fold	3.5 fold	0.5 fold

Since Myc cannot homodimerize and bind to E-boxes on its own it is likely that all E-box dependent Myc targets require the association with Max for their regulation (Steiger *et al.,* 2008). To address the question whether the binding and regulation of snoRNAs by Myc requires Max, ChIP was performed 48 hours after Max knockdown using rabbit α-Myc antibody (SC). The presence of Max had to be tested indirectly via qRT-PCR, since no α-Max antibody was available that efficiently recognizes endogenous Max protein and can be used for Western blot. The qRT-PCR was performed 24 hours after Max knockdown since Max protein has a half-life of less than 10 hours (Steiger *et al.,* 2008), and protein levels should reflect mRNA levels 12-24 hours after mRNA measurement. Rab6 and Snm158 were used as housekeeping genes and the values of the knockdown samples were normalized to the values of the naïve samples (Figure 4-5 B'). While the relative expression of the housekeeping genes is unaffected by Max depletion, Myc levels are slightly increased (114% ± 28%), testifying that the repressing effect of Max upon Myc is reduced. Max mRNA levels are strongly reduced

after 24 hours (6.1% ± 2.5%) suggesting that 24 hours later Max protein levels are also below 10% of the wildtype level.

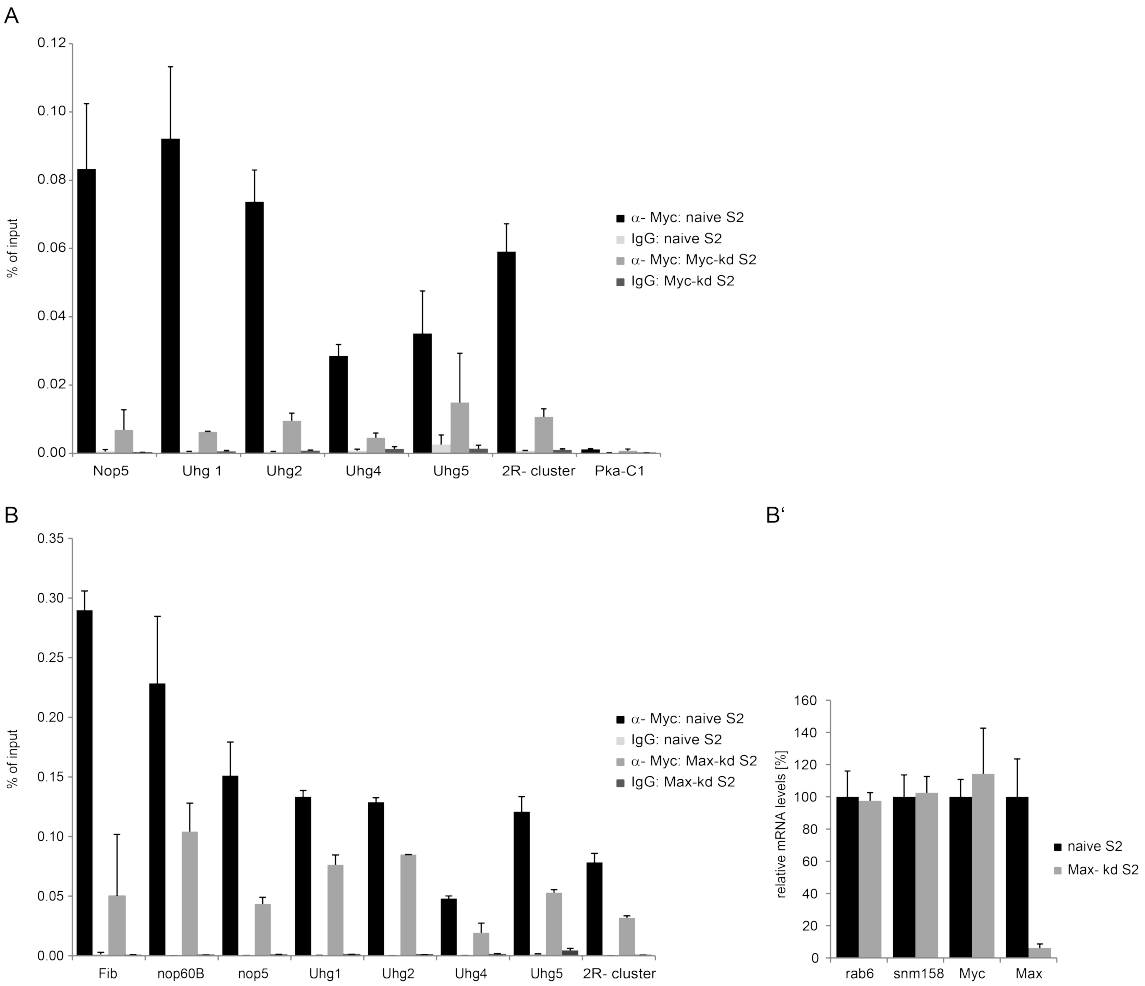

Figure 4-5: Binding of Myc to Uhgs is Max dependent[3]

A./B. ChIP-qPCR of Uhg loci. Chromatin was isolated from naïve S2 cells or from S2 cells depleted of either Myc (A.) or Max (B.), precipitated with rabbit α-Myc (SC) or control IgG antibodies and assayed by qPCR for enrichment of the indicated loci. Fibrillarin (Fib), nop60B (B.) and Nop5 were used as positive, Pka-C1 (B.) as negative control. The error bars indicate SD of technical triplicates. B. Similar results were achieved with the mouse α-Myc antibody
B'. qRT-PCR of Myc and Max after Max knockdown. Total mRNA was isolated from naïve S2 cells or from S2 cells depleted of Max and transcribed into cDNA. Rab6 and snm158 were used as housekeeping genes and the values of the knockdown samples were normalized to the values of the naïve samples. Error bars indicate SD of technical triplicates.
B./B'. Experiments are representative of biologically independent duplicates.

After Max knockdown, Myc binding to the positive controls Fibrillarin and Nop5 is strongly reduced (Fib: 82.3%; Nop5: 71.1%; Figure 4-5 B). For Nop60B (54.4%), Uhg4 (59.4%), Uhg5 (56.1%), and 2R-Cluster (59.3%) the binding is decreased by at least 50%. The binding at Uhg1 and Uhg2 is also reduced but to a lesser extent (Uhg1: 42.8%; Uhg2: 33.9%). Since loss of Max reduced the recruitment of Myc to these promoters the binding of Myc to the Uhgs presumably involves Myc-Max heterodimers.

4.1.5 Ribosome biogenesis and ribosome protein genes are the core Myc targets

The ChIPseq experiments lead to the discovery that Uhgs are a novel class of Myc target genes and the question arose whether they are directly regulated by Myc. To determine, if this is the case, Maria Stauch (pers. com.) performed high-throughput RNA sequencing (RNAseq) to globally detect Myc dependent changes in expression levels. To obtain a greater amount of less abundant transcripts, RiboMinus™ technology was used, which selectively depletes ribosomal RNA molecules, regardless of the presence of a 5'-cap structure or their polyadenylation status. M. Stauch performed RNAseq in biologically independent triplicates for naïve and Myc depleted S2 cells. Only genes were kept for final analysis, which had more than 10 reads combined in all six samples and had a predicted transcript size of more than 125 nt. A cutoff at 125 nt was chosen due to technical reasons. From the resulting 8019 genes, 281 genes were differentially expressed in naïve compared to Myc-depleted S2 cells ($p \leq 0.05$). From these 281 genes, the majority was down regulated after Myc knockdown and only a few were up regulated (240 vs. 41) (Herter *et al.,* 2015). A comparison of expression and binding data showed that 254 of the bound genes are also regulated by Myc in at least one experiment ($0 \leq p \leq 1$). After Myc knockdown, 139 of the Myc bound genes are down regulated by at least one third (fold change ≤ 0.65) whereas 59 genes are up regulated by at least one third (fold change ≥ 1.34). Since these 59 genes were not enriched for any process and showed a poor overlap between different data sets in contrast to the Myc-activated genes, they were not analyzed further. The other 56 genes were altered by less than one third in response to Myc-depletion, implying that Myc most probably has no effect on their regulation, and were not further considered in the analysis.

The 139 genes which are bound by Myc and require Myc for their full expression were considered as the core set of directly activated Myc genes. GO (Gene Ontology) term analysis (GOrilla tool) and manual analysis revealed that the majority of these genes (112; 81%) play a role in ribosome biogenesis and in translation (Table 4-5, Herter *et al.,* 2015), including synthesis of ribosomal RNA by RNA polymerase I (Pol I) (van Riggelen, 2010). Due to the depletion of rRNAs with RiboMinus™ technology, no direct binding of Myc to rRNA loci is observed. Instead components or cofactors of Pol I (e.g. Rpl135, Rbp5; Table 4-5) are bound and regulated by Myc, which confirms that the regulation of rRNA synthesis by RNA Pol I is indeed indirect in *Drosophila* (Grewal *et al.,* 2005).

Table 4-5: Directly Myc-activated genes, sorted by biological category[3]

Function	Number	Genes
RNA Pol I activity	7	Rpl135, Rpb5, CG18600, mod, vig, CG7911, CG42358
snoRNP function	15	Fib, hoip, Nop5, Nop56, Nop60B, NHP2, CG11180, CG4038, CG7637, Nopp140, Uhg1, Uhg2, Uhg4, Uhg5, Uhg7
40S subunit assembly, processing, maturation	18	Bka, l(3)07882, CG9253, CG9799, CG30349, U3-55K, l(2)k09022, l(2)34Fd, CG12050, CG5728, CG7338, bys, CG11660, l(1)G0004, CG2691, CG15027, Eap, mat89Ba
60S subunit assembly, processing, maturation	17	Nnp-1, CG8801, CG13096, CG11583, CG1785, CG32409, CG8939, RpLP0-like, Dbp73D, CG8545, CG5114, CG9630, ns1, Surf6, vas, CG8414, CG10286
processing of both subunits	1	Ip259
40S ribosomal subunit	19	RpS5a, RpS27A, RpS14a, RpS15Aa, RpS13, RpS20, RpS28b, RpS23, RpS16, RpS30, RpS27, RpS8, RpS7, RpS25, RpS10b, RpS24, RpS26, RpS4 RpS2
60S ribosomal subunit	21	RpL7, RpL13, RpL11, RpL22, RpL9, RpL29, RpL14, RpL3, RpL10, RpL23A, RpL17, RpL24, RpL21, RpL18, RpL10Ab, RpL34b, RpL6, RpL5, RpL41, RpL30, RpL24-like
Mitochondrial ribosome	2	mRpS17, mRpS14
Translation factors	6	Ef2b, Ef1beta, eEF1delta, CG7414, bic, eIF6
tRNA processing, maturation	6	La, l(1)G0045, Jhl-1, CG8097, CG1074, CG31381
Total Ribi and translation	*112*	
Metabolism	5	r, Sam, CG5599, SpdS, CG11089
Transcription, RNA processing	5	Nap1, Elp2, Elp1, Dis3, CG31759
Mitochondrial function	4	Hsc70-5, CG2059, CG3085, Spargel
Other, unknown	13	FK506-bp1, FK506-bp2, CG16833, msk, CG12909, CG6550, Ufd1-like, CG5535, CG8132, CG2003, CG42672, CG9286, CG9300

Via RNA polymerase II (Pol II), Myc controls several genes coding for components of small nucleolar ribonucleoproteins (snoRNPs), including Fibrillarin (Fib), hoi-polloi (hoip), Nop5 and various Uhgs, and therefore controls the post-transcriptional modifications in general. Furthermore, Myc targets control genes essential for the maturation of the 40S (18 genes) or the 60S subunit (17 genes) and Myc induces the expression of components of the small (19 genes) and the large (21 genes) ribosomal subunits, as well as for the mitochondrial ribosome (2 genes). Additionally, Myc induces the expression of translation factors (6 genes) and of genes involved in tRNA maturation (6 genes).

4.1.6 **Myc binds promoter-proximal sequences**

Considering the ChIPseq experiments described above, performed in different cell lines and with different antibodies (4.1.2), a core set of 265 Myc binding sites could be identified. In total, these 265 binding sites affect potentially 279 genes since some of the Myc binding sites are located close to more than one transcriptional start site (TSS). This is due to the high gene density in *Drosophila*. The majority of binding sites are located within 100 bp from the nearest TSS (58%) and 80% of the binding sites map in less than 1000 bp from a TSS (Figure 4-6 A), suggesting that Myc preferentially binds to promoter proximal sequences. This preference gets even clearer when only binding sites are considered which cover a canonical E-box (red line, Figure 4-6 A). In this case, 77% of all binding sites map within 100 bp and 93% within 1000 bp from the Myc binding summit.

To identify sequence motifs that are associated with Myc binding sites, the MEME-ChIP algorithm within the MEME suite was used (Machanick and Bailey, 2011). For this purpose a region ± 100 bp around the summit of a Myc peak was analyzed. As expected, the most highly enriched motif (46.7% ≙ 79 peaks, $E=2.3*10^{-60}$) amongst the 169 Myc bound and activated genes (4.1.5) is the extended E-box sequence "[AA]CACGTG[CG]" (Hulf *et al.,* 2005) (Figure 4-6 B). Another highly enriched motif (26.0% ≙ 44 peaks, $E=3.0*10^{-19}$) is the DNA replication element (DRE) "ATCGATA[G]" (Figure 4-6 B') which has been found to be associated with Myc target genes (Orian *et al.,* 2003). A third motif was also found to be enriched in Myc bound and down regulated genes (33.1% ≙ 56 peaks, $E=1.1*10^{-36}$), but its physiological binding partner is unknown (Figure 4-6 C). The E-box and the third motif were centrally enriched at the summit, suggesting that Myc directly binds to these motifs. Since the DRE motif is not enriched centrally around the summit of the Myc peak, it is likely that Myc binding at the DRE sites is indirect and mediated by binding partner.

For the Myc bound and up regulated genes (85 genes) a single motif was enriched (30.6% ≙ 26 peaks, $E=1.2*10^{-13}$), for which the physiological binding partner is unknown, too (Figure 4-6 D).

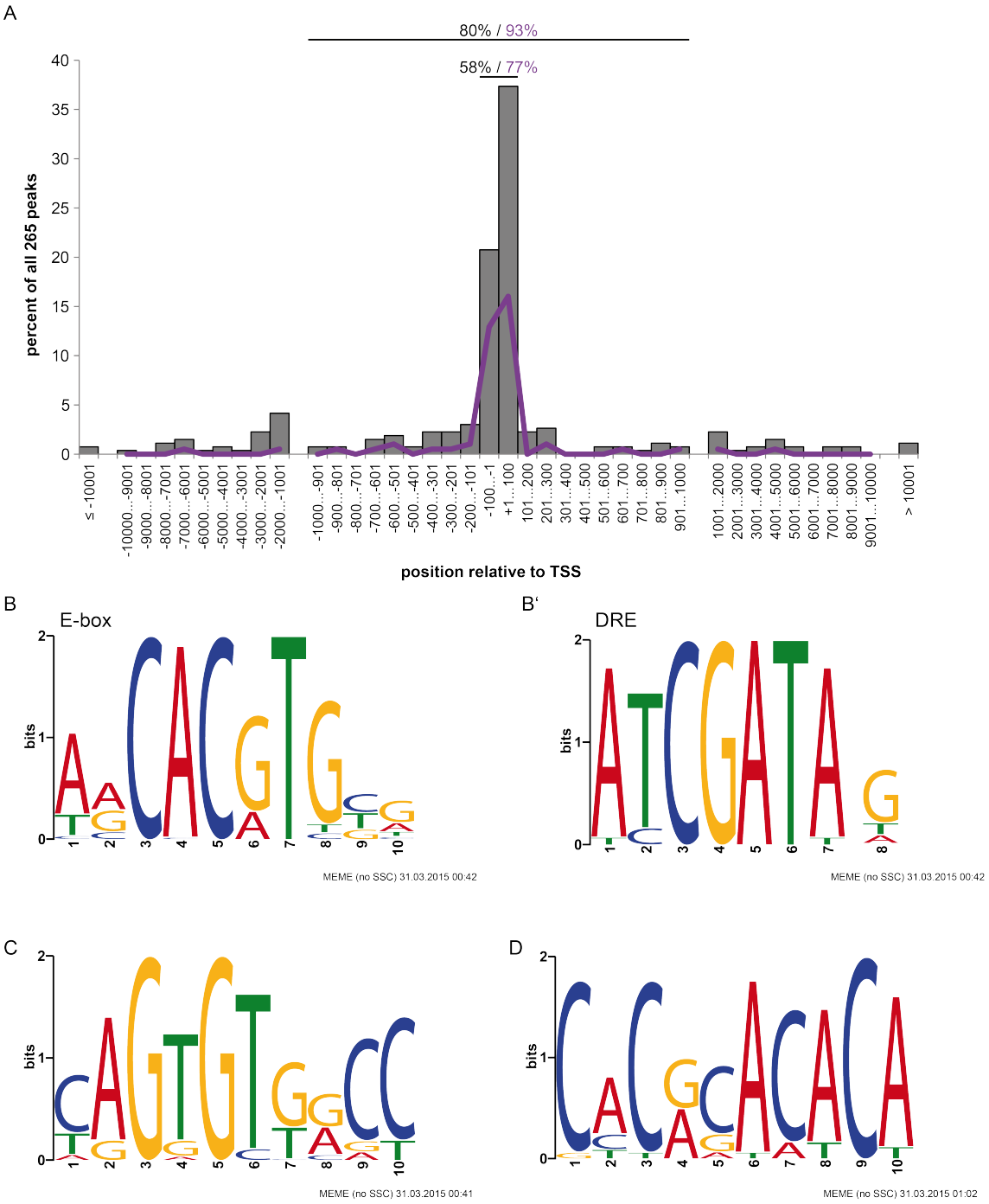

Figure 4-6: Myc binding sites in *Drosophila*[3]

A. Position of Myc binding peaks relative to the nearest transcription start site (TSS). Data are grouped in 100-nt bins for a distance of up to 1'000 nt from the TSS and in 1'000-nt bins for distances between 1'000 nt and 10'000 nt, and shown as percent of all 265 peaks. Grey bars show all Myc binding peaks, the purple line only the Myc binding peaks containing a canonical E-box. Horizontal lines above the graph illustrate windows of ± 100 nt and ± 1'000 nt around the TSS.
B./B'./C. MEME analysis showing the most strongly enriched motifs in 169 Myc bound genes which were down regulated after Myc knockdown (RNAseq data M. Stauch: 4.1.4). For the analysis, 100 bp around the summit of the Myc peaks were used.
D. MEME analysis showing the most strongly enriched motif in 85 Myc bound genes which were up regulated after Myc knockdown (RNAseq data M. Stauch: 4.1.4). For the analysis, 100 bp around the summit of the Myc peaks were used.

4.1.7 **Myc regulates Uhgs and snoRNAs**

As already shown in 4.1.5, Myc depletion led to 240 significantly downregulated genes ($p<0.05$) (Herter *et al.* 2015) amongst which 36 did not code for proteins, but for snoRNAs. The *Drosophila* genome is predicted to encode 288 snoRNA with sizes from 46 to 316nt (flybase.org[4] and Huang *et al.,* 2005). All snoRNAs which passed the cutoff of 125nt and were detectably expressed in S2 cells (103) were strongly downregulated after Myc knockdown (Herter *et al.,* 2015). Among these, most of the box H/ACA snoRNAs were found, whereas the majority of box C/D snoRNAs were not detected in the RNAseq experiments since they were smaller than the cuttoff used. The exonic Uhg transcripts, hosting 48 snoRNAs in total, were found to be downregulated after Myc knockdown in the RNAseq data sets, too (Herter *et al.,* 2015).

To analyze the effect of Myc depletion on several box C/D snoRNAs, qRT-PCR was performed. The corresponding box C/D snoRNAs host genes, Uhg1, 2, 3, 4, 5, 7 and Uhg8 were also included (Figure 4-7 A). No snoRNA hosted in Uhg7 was analyzed because I was not able to design functioning qRT-PCR primers. All selected snoRNAs, as well as the Uhg genes, were strongly downregulated after Myc depletion (40%-49% and 20%-55% of control transcripts, respectively). Nop60B which was formally known as Uhg6 also shows a strong reduction (30% of control transcripts). Fibrillarin (10% of control transcripts), a well established direct transcriptional target of Myc was used as positive control.

To determine if Myc is also able to increase the expression of the snoRNAs and the Uhg genes, Myc was overexpressed in an inducible cell line (S2pMT-Myc), stably transfected with a plasmid containing HA-Myc under the control of the *Drosophila* metallothionein (MT) promoter. The MT-promoter is inducible by addition of copper sulfate and allows transient expression of the protein of interest. Six hours after Myc induction, an increase on protein- (Figure 4-7 C) as well as on RNA-levels can be observed (75 fold; data not shown). Transient overexpression of Myc is sufficient to increase the expression of the snoRNAs and their host genes to supraphysiological levels (121%-272% of control transcripts) (Figure 4-7 B). Taken together, the qRT-PCR data confirm the results of the RNAseq experiments and show that also the short box C/D snoRNAs are controlled by Myc.

[4] flybase.org; FB release 2014_6

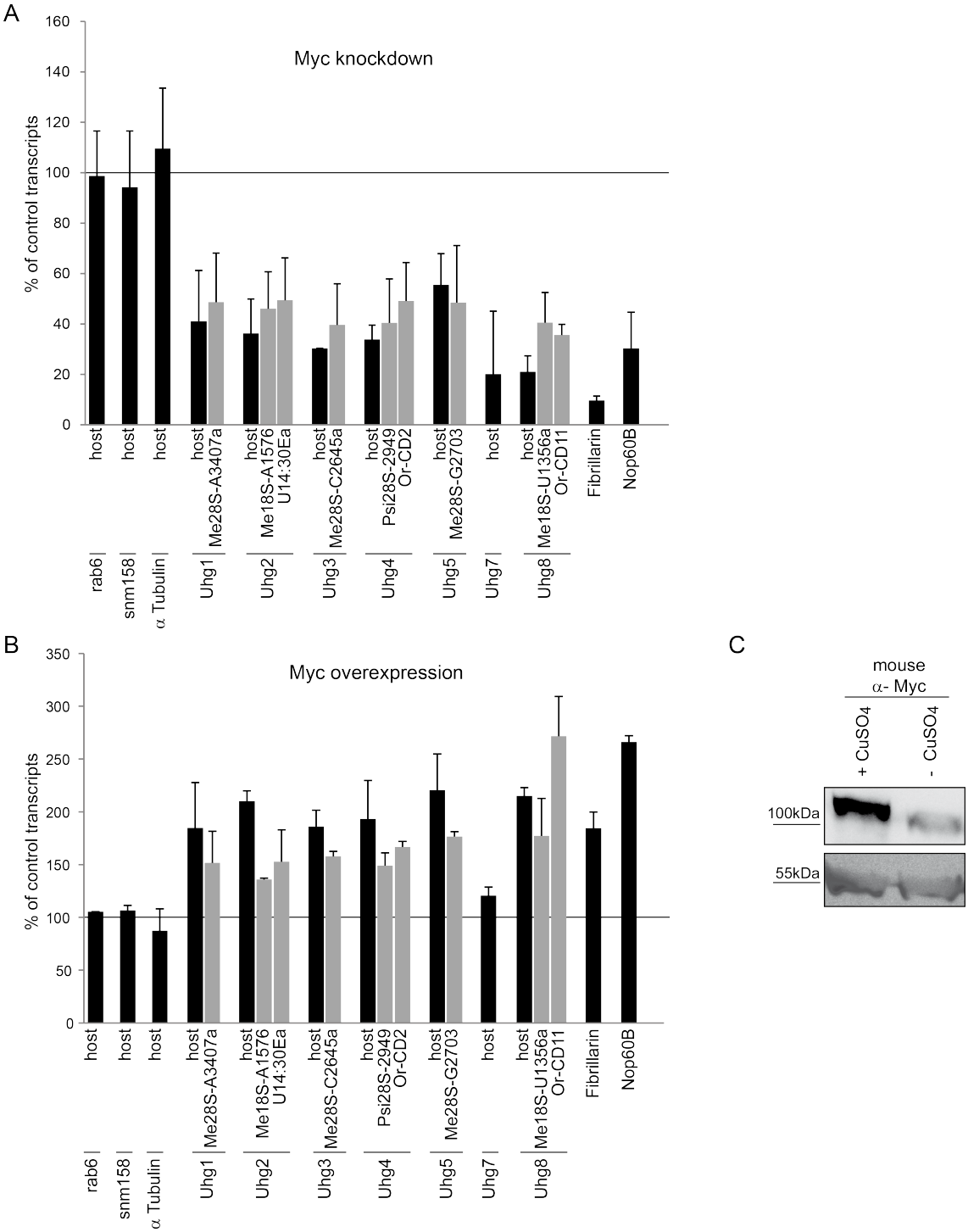

Figure 4-7: Myc directly regulates snoRNAs[3]

A./B. The averages of the three reference genes rab6, snm158 and α-Tubulin were used as housekeeping genes and were set to 100%. Error bars show standard deviations of biologically independent duplicates. Spliced transcripts from each Uhg host gene are grouped with selected snoRNA(s) hosted within the intron of the corresponding Uhg gene, except for Uhg7 where no functioning qRT-PCR primers could be designed for the intronic snoRNAs. A. qRT-PCR after Myc knockdown: RNA levels were assayed 24 hours after addition of Myc-dsRNA to S2 cells. B. qRT-PCR 6 hours after addition of 125 µM $CuSO_4$ to S2pmt-Myc cells to induce Myc over-expression.

C. Western blot of Myc (upper panel) and α-tubulin (lower panel) in control cells and cells over-expressing Myc 6 h after $CuSo_4$ induction (125 µM). The samples for western blot originate from the same transfection as the samples in B.

To show that the regulation of the host genes reflects the regulation of the mature snoRNAs and to confirm the qRT-PCR analysis of snoRNAs smaller than 125 nt, Northern blot analysis was performed (3.1.17) with wildtype or Myc depleted S2 cells. The Myc knockdown was confirmed via western blot (Figure 4-8 C). For northern blot, either control or Myc depleted RNA was loaded on the acrylamide gel and hybridized with 100 µM of the indicated γ-P^{32}-ATP labeled probes (Figure 4-8 A). The blots were exposed on a Storage Phosphor Screen (3.1.17) and the quantification of the Northern blot signals was performed using ImageJ2 software. The arrowheads point to the bands of the predicted sizes (113 nt, 75 nt and 85 nt respectively). After Myc knockdown the expression of the mRNA is reduced by 23% (snoRNA: Me18S-A1576), 43% (snoRNA: Me28S-C2645a) and 38% (snoRNA: Me28S-G2703c) (Figure 4-8 A, B), which confirms that mature snoRNAs are affected and not just their immature precursors and fits to the results obtained by qRT-PCR. On the Me28S-G2703c blot a slower migrating signal can be seen around 140 nt (asterisk). Its origin is not clear, however it possible that it is a differently spliced variant of the indicated snoRNA since the intensity of the signal is reduced to the same extent as the signal at the expected height. In total 10 snoRNAs were investigated of which one additional snoRNA showed a reduced signal after Myc knockdown (Or-CD2, data not shown). Four snoRNAs gave no (Me28S-A3407a, U14:30Ea) or a very weak signal (Psi28S-2949, Me28S-A2634c) and therefore quantification was not possible. Only one snoRNA (Or-CD11) gave a strong signal which was not obviously changed after Myc depletion upon visual inspection. However, quantification of the northern blot signal showed a reduction of 19.5% (data not shown). Since a lot of smear instead of a distinct band was present on the northern blot, it was difficult to make a clear statement about signal changes upon loss of Myc. Therefore this snoRNA was not further considered. Unfortunately it was not possible to use a RNA as loading control since no RNA being unaffected by Myc knockdown in the correct size range (50 nt to 180 nt) was detectable. Therefore the same RNA samples were analyzed by reverse transcription and quantitative RT-PCR for the reference genes *snm158* and *rab6*, as well as for the indicated snoRNAs (Figure 4-8 B). The expression levels of the depicted snoRNAs fit to the results gained from the Northern blot analysis (81.6%, 68.6% and 54.6% relative expression).

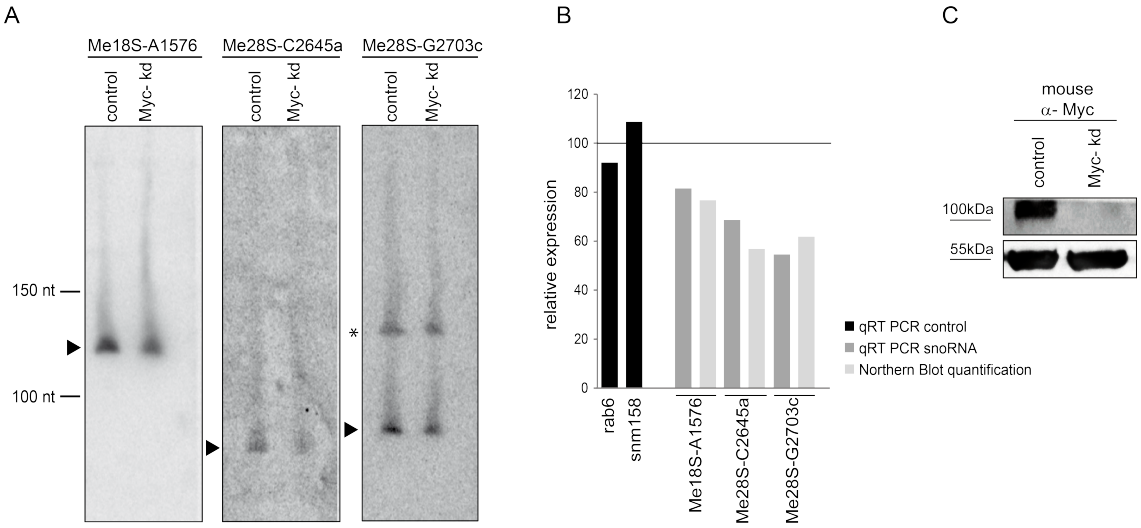

Figure 4-8: Northern blot analysis[3]

A. Northern blot for three different snoRNAs (snoRNA: Me18S-A1576, snoRNA: Me28S-C2645a, snoRNA: Me28S-G2703c). Arrowheads point to bands of the predicted sizes, the identity of the cross-reactive slower migrating band in the Me28S-G2703c blot (asterisk) is unclear. The locations of molecular weight DNA markers are indicated.

B. qRT-PCR results and quantification of the Northern blot bands. Rab6 and snm158 were used as housekeeping genes and were set to 100%.

C. Western blot of Myc (upper panel) and α-tubulin (lower panel) in control and Myc knockdown cells. The samples for western blot originate from the same transfection as the samples in A and B. The experiments shown in panels A, B and C are representative of biologically independent duplicates.

4.1.8 **Biological effects of Uhg genes**

In the previous chapters it has been shown, that snoRNAs are a novel class of Myc targets. This raises the question whether loss or overexpression of snoRNAs plays a role *in vivo*. To address this question, overexpression and loss of function studies had to be performed. The vast majority of snoRNAs are hosted in other, partially growth related genes. Therefore we focused on snoRNAs hosted in Uhg genes, since they are non-protein coding and their loss should not impair any other growth-relevant transcripts. Anan Uhg1 mutant fly line was established, since it encodes 16 out of 51 snoRNAs, the largest number of all Uhg genes (Herter *et al.,* 2015).

The Uhg1 null mutant, *Uhg1*^{1}, was established by imprecise excision of a P-element and carries a deletion from the first to the last exon (nucleotides chr2R:13'586'606 to 13'590'803, Figure 4-9 A). As a consequence the coding regions for all snoRNAs are eliminated. The attempt to establish an Uhg5 null mutant failed, while other Uhgs did not contain appropriate or available P-elements to establish a mutant. In the following experiments, a wildtype revertant, *Uhg1*^{rev}, was used as control. The genomic sequence of the Uhg1 mutant revealed that the neighboring coding regions of Uhg1 were not affected. To investigate whether their expression was affected, qRT-PCR was performed, using total RNA, isolated from wandering larvae of mutant and control animals (Figure 4-9 B). Rab6, α-Tubulin and Snm158 were used as housekeeping genes and the expression of Uhg1 and of the neighboring genes, CG6424 (77% ± 25%), RdgBβ (114% ± 23%) and CR45146 (103% ± 18%), was normalized to their average.

While the expression of the three neighboring genes is not strongly affected by the loss of Uhg1, Uhg1 expression is strongly reduced to 10.9% ± 2.5%. Since *Uhg1*^{1} is a null mutant, a weaker amplification product was expected. To investigate whether the amplification product derives from maternally deposited RNA or from an experimental background, the melting curve and the migration of the amplification product were examined (Figure 4-9 **B'** and data not shown). The melting curve and the migration behavior of the amplified product from *Uhg1*^{1} larvae differ from control, showing no clear peak for a specific temperature and a differently sized product. Thus the amplification product presumably corresponds to a non-specific product.

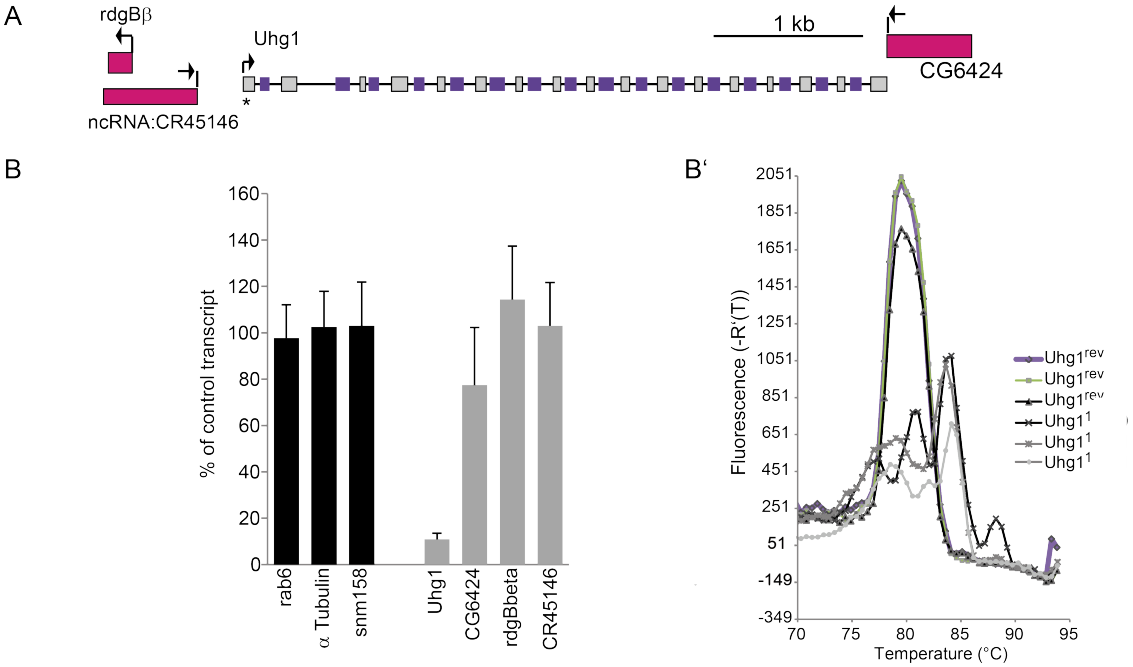

Figure 4-9: Loss of Uhg1 does not affect its neighboring genes[3]

A. Uhg1 locus with adjacent genes. Black arrows indicate direction of transcription, grey boxes correspond to exons, purple boxes to introns, respectively, and purple boxes show snoRNAs. The asterisk represents the single E-box.
B. Expression of Uhg1 and the neighboring transcripts in *Uhg1*^{1} mutant wandering larvae. Expression was normalized to the average of the 3 housekeeping genes rab6, α-Tubulin, and snm158. The graph shows the average and standard deviations of three biological replicates.
B'. The Uhg1 amplification product from mutant larvae shows an aberrant melting curve. Depicted are the melting curves of technical triplicates from *Uhg1*^{rev} and *Uhg1*^{1} samples.

Yoshihama and colleagues (2013) have predicted the target sequences for several snoRNAs, including the snoRNAs hosted in Uhg1. These snoRNAs exclusively affect 2'-O-ribose-methylation of 18S- and 28S-rRNA at five positions (18S:A28, 28S:A1666, 28S:G3081, 28S:G3277 and 28S:A3407). This implies, that these positions should not be methylated upon loss of Uhg1. Therefore methylation mapping by primer extension (3.4.5) was performed to visualize the consequences of the loss of the snoRNAs on 2'-O-ribose-methylation at the expected nucleotides. This method uses primer extension by reverse transcriptase at low dNTP concentrations (Maden 2001; Motorin *et al.,* 2007) and is based on the observation that reverse transcriptase pauses or slows down at nucleotides which are methylated at the 2'-O-ribose. With decreasing dNTP

concentration the pause should be longer and therefore a stronger signal should be detected. Because of the halt, the following methylated site should show a weaker signal. Thus it is necessary that beside the site of interest, at least one other site, methylated by an other box C/D snoRNA, not hosted in Uhg1 is visible on the gel. The sequencing gel only allows to display a sequencing product of up to 100 nt, with the best resolution at 20-60 nt after start of the reverse transcription. Therefore one or two methylated sites should flank the site of interest in this 40 nt window. Since no flanking sites are present for 18S:A28 inside the 40 nt window, it was not further analyzed. The methylation mapping (3.4.5) was performed using total RNA from larvae being mutant (*Uhg1*^{1}) or wildtype (*Uhg1*^{rev}) for Uhg1.

For 28S:A3407 the sequencing always stopped before base A3407 and no further bands could be detected. This is probably due to a long pause at C3403, which caused a lack of reverse transcriptase or of the available dNTPs (data not shown). For the other three positions the expected effect was detected (Figure 4-10 C). The band which can be seen in the *Uhg1*^{rev} samples at the indicated position (reverse letters with asteriks) is strongly reduced (A1666) or not present at all (G3277, G3081) in the *Uhg1*^{1} samples. In comparison no difference between the samples can be seen for bands which are unaffected by loss of Uhg1 (e.g. C3113). With decreasing dNTP concentrations (10 mM to 1 mM) the band intensity increases for all three methylation sites. For 28S:G3081 the intensity at 0.5 mM (dNTPs) is weaker than at 1 mM. This was expected since a methylation site which is unaffected by the loss of Uhg1 pauses the reverse transcriptase at C3113 (methylated by 28S:G3113, hosted in CG13900). With the G3277 primers, almost no signal can be seen at 0.1 mM dNTPs. Since this is the case for the mutant and the control lane it is very likely that the dNTP concentration was already too low for this sequence context. The sites being methylated by other box C/D snoRNAs, not hosted in Uhg1 (A1688, G3341) which were expected to influence 28S:A1666 and 28S:G3277 are not detectable or unchanged. At position A1688 this might be due to the long pause at C1698 which is not methylated or modulated in an other specific way at the corresponding nucleotide. Position G3341 is probably too far away to have an influence on the halt at G3277. The additional bands visible on the sequencing gel might be due to other modifications of the nucleotides or due to random stops of the transcriptase (Motorin *et al.,* 2007).

Summing up the data obtained from the methylation assay, it can be stated that loss of Uhg1 and therefore its snoRNAs indeed leads to loss of methylation at five specific ribose residues and might therefore affect ribosome assembly and activity.

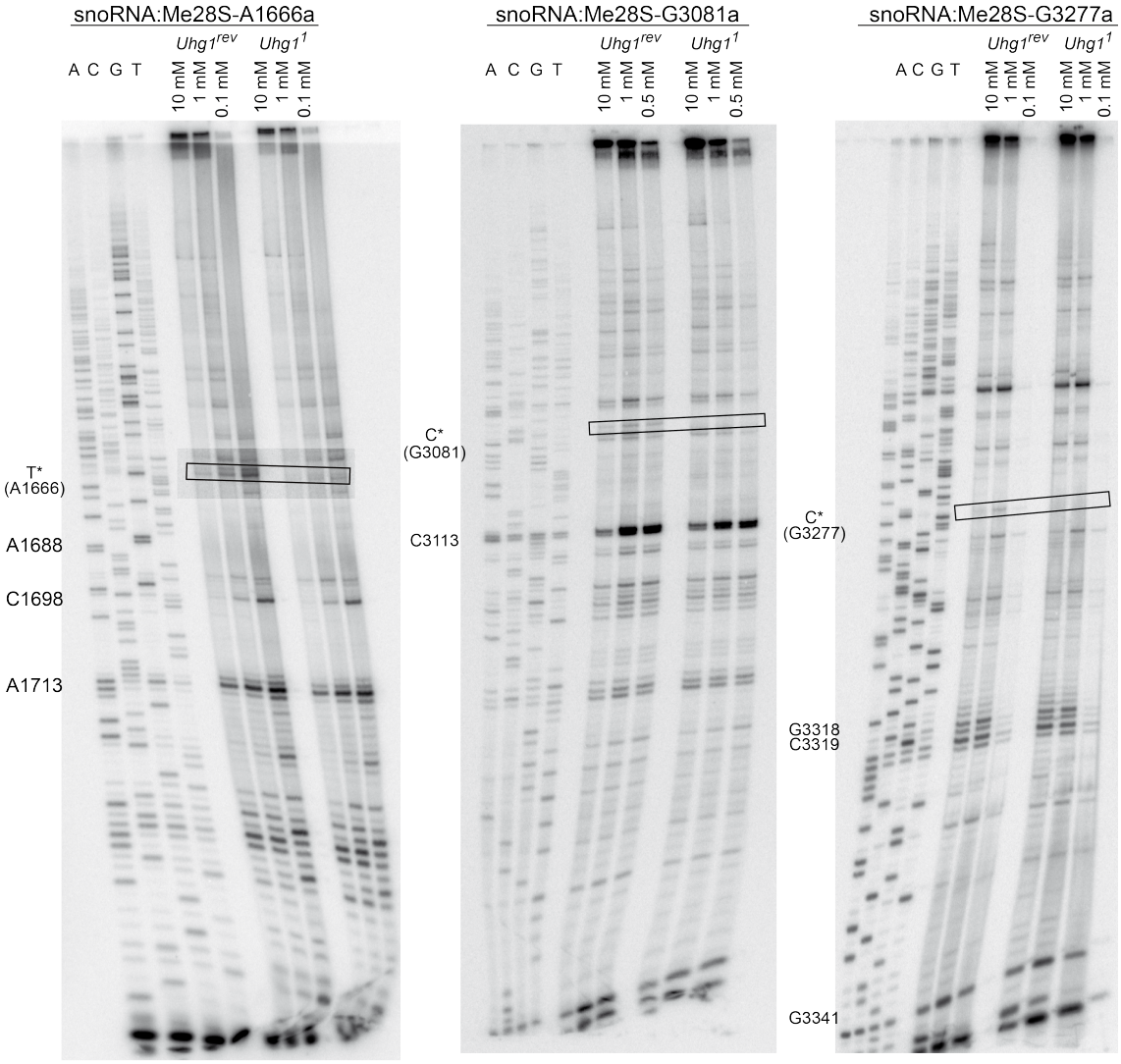

Figure 4-10: Loss of Uhg1 leads to decreased O'-ribose-methylation of 28S rRNA

Methylation mapping by primer extension for three different positions, 28S-A1666, 28S-G3081 and 28S-G3277 affected by the loss of Uhg1. For every reverse transcription reaction, 8 µg of total RNA (*Uhg1*^{rev} or *Uhg1*^{1}) were used and either 10 mM, 1 mM or 0.5/0.1 mM dNTPs. The lines A, C, G and T refer to the sequencing ladder. Here 0.167 µg of total RNA, 0.4 mM dNTPs each and 0.5 mM of ddATP, ddCTP, ddGTP or ddTTP were used. The numbers indicate the corresponding nucleotide of Uhg1; the letters with the asterisk indicate the methylation site of interest. Due to the reverse transcription, the nucleotides appear in reverse order.

4.1.9 **Uhg genes affect growth *in vivo* and tumor formation**

As shown previously (4.1.8), the Uhg1 null mutant affects 2'-O-ribose-methylation at specific positions and thus could affect ribosomal assembly and/or activity. To investigate whether the ribosomal activity is suppressed, translation assays were performed with each 10 *Uhg1*^{1} and *Uhg1*^{rev} wandering larvae (3.4.6). Following a 30 µl incubation time, the content of incorporated ^{3}H-Amino-acid-mix was measured to serve as a read out for newly synthesized protein. The animals do not differ in weight (data not shown) or protein content (cold protein *Uhg1*^{1}: 124% ± 50%; p=0.8) (Figure 4-11 A). However, the amount of newly synthesized protein in mutant larvae (Figure 4-11 A, hot protein) was reduced by 22.1% ± 3.6% compared to control animals (p=0.00045).

This significantly lower protein synthesis rate of the Uhg1 mutant animals is accompanied by a delay in development. Adult flies eclose about 12 hours later than control animals and female *Uhg1*^{1} flies show a strongly reduced fertility (Herter *et al.*, 2015). Together the developmental delay and the female specific sterility are often seen in mutations in pathways affecting growth, which have been observed before for hypomorphic mutations in Myc (Johnston *et al.,* 1999). To investigate whether Myc's function is dependent on the presence of Uhg1, Myc was overexpressed in either wildtype (*Myc OE*) or Uhg1 mutant (*Myc OE/ Uhg1*^{1}) animals using hs-Flp in combination with actin-Gal4/FRT. In this setup, the presence of a FLP-out cassette prevents the actin promoter from triggering Gal4 expression. Upon heat shock (1 h) the transcription of Gal4 in cells in which the FLP-out cassette has been excised takes place and subsequently expression of Myc (Steiger *et al.,* 2008). The different genotypes are listed in Table 2-3. For each genotype an equal number of female wandering larvae (varying between 4 and 11 for the 5 different assays) were processed as described above and in 3.4.6. Due to the developmental differences of the genotypes, *Uhg1*^{rev} and *Myc OE* larvae were collected 70 hours after egg deposition, whereas the timespan between egg deposition and collection of the *Uhg1*^{1} and *Myc OE/ Uhg1*^{1} larvae was approximately 12 to 15 hours longer. Myc overexpression was induced by a single heat shock (37°C; 1 h), 54 h (*Uhg1*^{rev} and *Myc OE*) and 69 h (*Uhg1*^{1} and *Myc OE/ Uhg1*^{1}) after egg deposition, respectively. All animals were collected and sacrificed 16 h ± 2 h afterwards and protein synthesis assay was performed (see above). To allow a better comparison between the protein synthesis rates of the different genotypes, the ratio of newly synthesized to total protein was calculated for both genotypes and normalized to the ratio measured for *Uhg1*^{rev}. Overexpression of Myc leads to a massive increase in protein synthesis (217% ± 95%; p=0.26) in a wildtype background (Figure 4-11 B). This increase is completely abolished in the absence of Uhg1 (*Myc OE/ Uhg1*^{1}: 51% ± 14%; p=0.05) and is even lower than in the mutant alone (*Uhg1*^{1}: 59% ± 17%; p=0.01). This can be due to the bad condition of the *Myc OE/ Uhg1*^{1} larvae, which were recognizable thinner than larvae from the other genotypes (pers. observation; data not shown). Why the animals were in such a bad condition is not clear. However, we were able to show that loss of Uhg1 influences protein synthesis rates.

Besides effects on wildtype cells and animal growth, the impact of Uhg genes on a Myc dependent tumor model was analyzed (Betschinger *et al.,* 2006). Loss of the tumor suppressor *brat* in type II neuroblast stem cell lineages leads to tumor formation that depends upon Myc (Figure 4-11 C). The tumor size can be compared via co-expression of firefly luciferase (Neumüller *et al.,* 2013; 3.4.7). The type II neuroblasts are selectively addressed by a combination of the worniu-Gal4 (wor-Gal4) driver which is specifically expressed in all neuroblasts and the asense-Gal80 (ase-Gal80) which blocks expression in type I neuroblasts (Neumüller *et al.,* 2011). These flies were crossed with flies either carrying an UAS-construct for overexpressing different Uhg transgenes (see below), knockdown of Myc, or *Uhg1*^{1}/ *Uhg1*^{rev} flies. Adult males were collected 12 hours after eclosion and processed for luciferase measurement (3.4.7). Luciferase values were normalized to control animals ("yw"). While luciferase values in

wildtype type II neuroblasts are not influenced by depletion of Myc (96% ± 15%), luciferase levels are highly impaired after brat knockdown (81% ± 19%, p=0.004; Figure 4-11 C). Loss of Uhg1 (*Uhg1*^{1}) does not lead to a reduction in luciferase levels (106% ± 53%) (Figure 4-11 C). It might be possible that the delay in larval development, which is caused by the loss of Uhg1, also slows down the tumor growth rate and therefore the NBII tumors develop later. In this case, a reduction in tumor growth rate would be masked by the loss of Uhg1. Therefore, overexpression of various Uhg transgenes was chosen as a different approach. To establish fly lines, the gene regions of the different Uhgs, spanning all snoRNA containing introns, were cloned into a pUAST-vector and inserted into embryos (M. Gallant and P. Gallant, pers. com.). The oligonucleotides used for cloning are listed in Table 2-1. Unfortunately, overexpression of Uhg1 does not show an effect on luciferase levels (data not shown). Since the functionality of the UAS-Uhg1 transgenes was never tested, it is possible that no effect was observed because no increase in snoRNA levels was achieved.

On the other hand, overexpression of two independent Uhg4 (Uhg4/1: 123% ± 32%, p=0.027; Uhg4/2: 113% ± 28%, p=0.13) and Uhg5 transgenes (Uhg5/1: 129% ± 21%, p=0.000; Uhg5/2: 119% ± 26%, p=0.011) leads to an increase in luciferase levels (Figure 4-11 C). No effect is measurable in a wildtype background (Figure 4-11 C; black bars).

The effects on loss of Uhg1 were also investigated in another Myc-dependent tumor model (4.2.3), where overexpression of Ras^{V12} and Chinmo in the head capsules (ey-FLP) (Doggett *et al.*, 2010) leads to severe tumor formation. Also in this tumor model neither heterozygous (27% ± 14%) nor homozygous (33 % ± 13%) loss of Uhg1 leads to a decrease in tumor size compared to control (32% ± 9%) (Figure 4-11 D). It remains open whether an effect in this model could be achieved with depletion of other transgenes. However, we were able to show that overexpression of different Uhg genes can enhance tumor formation in at least one Myc dependent tumor model.

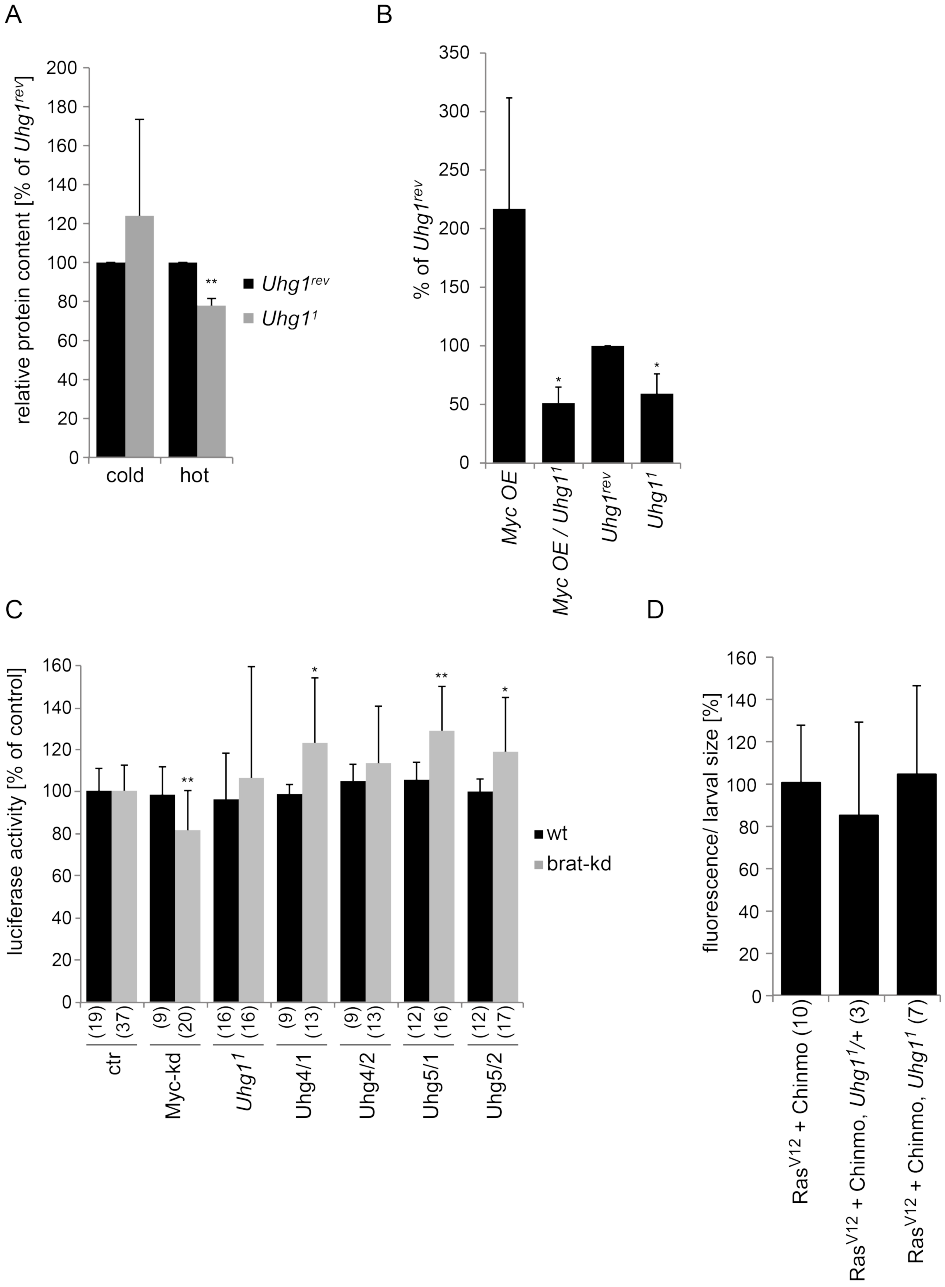

Figure 4-11: Uhg genes affect growth and tumor formation *in vivo*[3]

A. Total protein amount (cold) and amino acid incorporation rates (hot) in wandering larvae. Ratios (*Uhg1*^{1}/*Uhg1*^{rev}) and standard deviations are shown for 3 biological replicates each with 10 larvae for each genotype. Difference to control is p<0.001 (**, Student's 2-tailed t-test)
B. Ratio of newly synthesized protein (hot) to absolute protein amount in female wandering larvae, normalized to control (*Uhg1*^{rev}). Ratios and standard errors (SEM) are shown for 4 biological replicates each with 4-11 larvae for each genotype. Difference to control is p≤0.05 (*, Student's 2-tailed t-test)
C. Luciferase assays from single adult males overexpressing the indicated Uhg-transgenes under brat-knockdown (brat-kd) conditions in type II neuroblast lineages. #1 and #2 correspond to independent transgenes. Number of individually assayed flies (originating from 2-10 separate experiments) are shown in parentheses Error bars indicate SD. In addition to the indicated UAS-Uhg transgene, the flies carried "worniu-GAL4 asense-GAL80/+; UAS-brat-(inverted repeat) UAS-Luciferase/+". Difference to control is p<0.05 (*) and p<0.005 (**), respectively (Student's 2-tailed t-test).
D. Ratio of the size of fluorescent tissue to the size of whole larvae for the depicted genotypes. Ratios and standard deviations were normalized to control (Ras^{V12} + Chinmo). Error bars indicate SD of individually assayed flies shown in parentheses.

4.2 Myc and Chinmo interact in growth control

4.2.1 Chinmo controls growth via cell number

The zinc finger protein Chinmo was shown to interact with Myc in the process of tissue growth and development (Schwinkendorf, 2008) but their interaction was not fully characterized yet. Three different *chinmo* alleles were characterized, either having a mutation in the zinc finger domain (*chinmo*^{110}) or lacking it completely (*chinmo*^{108}, *chinmo*^{134}; Figure 1-8).

To investigate whether the growth defect was based on reduction of cell size or cell number, a FLP/FRT system was used which allows the generation of homozygous mutant clones by site-specific mitotic recombination (Newsome *et al.,* 2000). Expression of FLP recombinase under the control of the *eyeless* regulatory sequences (ey-FLP) restricts the recombination events to the developing head capsule. The mitotic recombination occurs between two FRT sequences on homologous chromosome arms, of which one arm carries the FRT insertion and the mutation of interest and the other arm carries a white (w^+) marker and a *cell lethal* (cl) mutation (prevents the survival of homozygous cells).

The compound eyes of *Drosophila* are made out of 600-700 single ommatidia, which themselves consist of always 20 cells. Therefore, counting the number of ommatidia and measuring the area of the compound eye is sufficient to state whether a reduction in eye size is based on differences in cell number or cell size. The eye sections were taken by D. Schwinkendorf with the help of a scanning electron microscope (SEM) and the numbers of ommatidia of four to five eyes from different adult flies were counted. In both, heterozygous (yw eyFLP) and homozygous (yw eyFLP; FRT40 cl w^+) head capsules, ommatidial number is reduced for all three alleles compared to control (yw eyFLP: 724 ± 13; yw eyFLP; FRT40 cl w^+: 711 ± 17) (Figure 4-12 A). In heterozygous animals, *chinmo*^{110} shows the strongest reduction in ommatidia number (513 ± 55) followed by *chinmo*^{108} (574 ± 49) and *chinmo*^{134} (630 ± 35). The reduction of ommatidia is highly significant for all three alleles ($p<0.001$) compared to control animals (724 ± 13). In the homozygous Chinmo mutants (Chinmo-pinheads), the number of ommatidia is reduced even more. Here, *chinmo*^{108} (329 ± 16) and *chinmo*^{134} (353 ± 30) have less ommatidia than *chinmo*^{110} (391 ± 63), which fits to the observation (Sulzer, 2003; Schwinkendorf, 2008) that *chinmo*^{108} and *chinmo*^{134} have smaller heads than *chinmo*^{110} animals. Also in the homozygous mutant animals the reduction of ommatidia is highly significant for the different alleles ($p<0.0001$) compared to control animals (712 ± 17). No difference in ommatidial size was observed (D. Schwinkendorf, unpublished data).

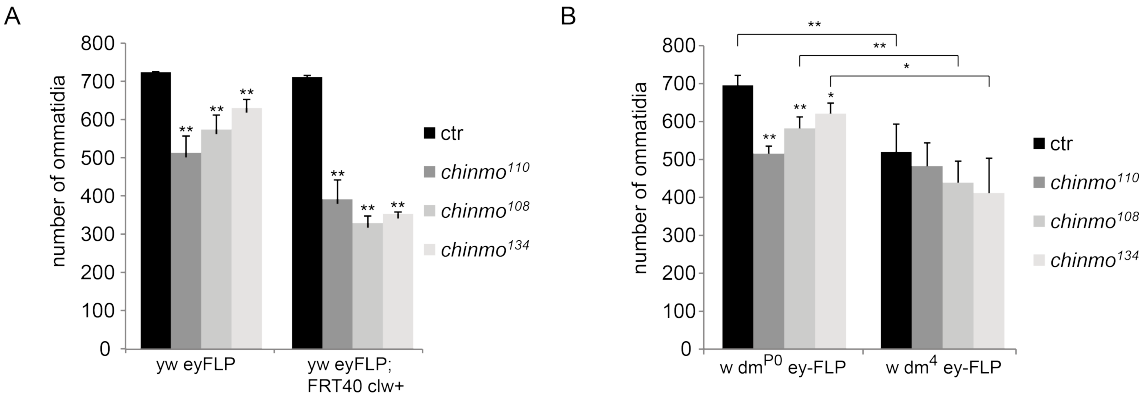

Figure 4-12: *Chinmo* alleles reduce ommatidial number

A. Number of ommatidia of different animals carrying different *chinmo* alleles in a Myc wildtype background. Average and standard deviations are shown for 4 to 5 independent fly eyes, difference to control is p<0.001 (**) (Student's 2-tailed t-test). The control chromosome is isogenic with the *chinmo* alleles, heterozygous animals have the genotype "*y w tub*>Myc>GAL4 *ey*-FLP/Y; FRT-40 *chinmo*^{X} /CyO, *y*$^{+}$", homozygous animals "*y w tub*>Myc>GAL4 *ey*-FLP; FRT-40 *chinmo*^{X} /FRT-40 *cl w*$^{+}$".
B. Number of ommatidia of different *chinmo* alleles in a Myc mutant background. Average and standard deviations are shown for 4 to 5 independent fly eyes, difference to control is p< 0.01 (*) or p<0.002 (**) (Student's 2-tailed t-test). The control chromosome is isogenic with the *chinmo* alleles, Myc null mutants have the genotype "*w dm*^{4} *tub*>Myc>GAL4 *ey*-FLP/Y; FRT-40 *chinmo*^{X}/ CyO, *y*$^{+}$", the hypomorphic mutants "*w dm*^{P0} *tub*>Myc>GAL4 *ey*-FLP/Y; FRT-40 *chinmo*^{X}/ CyO, *y*$^{+}$".

The effects of Chinmo mutation were also investigated in the Myc null mutant *dm*^{4} or the hypomorphic Myc mutant *dm*^{P0}. The defects described above are dramatically exacerbated when both Myc and Chinmo are completely eliminated, i.e. in Myc-null and Chinmo-homozygous mutant eyes. While both *ey>dm*^{4} mutants and Chinmo-pinheads allow normal survival and the development of quite normally patterned eyes, the double mutations are fully lethal and do generate at most rudimentary heads (Schwinkendorf, 2008). Loss of Myc in a Chinmo-heterozygous background leads to a strong reduction in ommatidial size, which does not differ significantly between the *chinmo* alleles (D. Schwinkendorf, unpublished data). On the other hand, a partial loss of Myc (*dm*^{P0}) has no influence of the number of ommatidia in a Chinmo-heterozygous background (compare Figure 4-12 A **"***yw ey-FLP*" and Figure 4-12 B "*w dm*^{P0} *ey-FLP*"). Interestingly the complete loss of Myc has an influence on the number of ommatidia in control animals (520 ± 82) as well as the *chinmo*-heterozygous alleles *chinmo*^{108} (439 ± 64) and *chinmo*^{134} (411 ± 103). Therefore loss of Myc not only affects cell size but also number, whereas Chinmo only affects cell number.

4.2.2 **Myc and Chinmo interact directly**

To be able to detect endogenous Chinmo and to perform immunoprecipitations independently of a tag, a Chinmo antibody had to be produced. Therefore the central part of Chinmo (aa 132-516) was cloned into the pGEX-4T1 expression vector, neither including the BTB/POZ (aa 32-128) nor the zinc finger domains (aa 517-540 and 545-568). The plasmid was expanded in BL21 bacteria, which enables expression of the

GST fusion protein upon induction with Isopropyl-D-thiogalactopyranosid (IPTG). The resulting GST-Chinmo protein was purified (3.3.7) and sent to immunoGlobe® for antibody production. The resulting antiserum was depleted from α-GST antibodies with the help of GST protein only (immunoGlobe®) and finally resulted in the purified rabbit α-Chinmo antibody (1.21 mg/ml). Both, the crude as well as the purified antibody specifically recognized Chinmo in Western blots (Figure 4-13 C, E; Figure 4-14 B) and Co-IPs (Figure 4-13 D, G).

To get further insight into the interaction of Chinmo and Myc described on a genetic base, D. Schwinkendorf performed several experiments in S2 cells. She was able to show that Chinmo overexpression does not affect endogenous and transiently transfected Myc levels. Apart from that, she was able to show that Chinmo can activate the transcription of a Myc-dependent luciferase reporter (*CG5033*; Schwinkendorf, 2008). Furthermore, qRT-PCR analysis showed that Chinmo overexpression leads to an increase in some Myc target genes associated with ribosomal biosynthesis (i.e. *fibrillarin*, *nnp1*). Thus, Chinmo might be a co-activator of Myc, necessary for its biological functions *in vivo.* This hypothesis raised the question whether Myc and Chinmo interact physically and if so, which domains are important for the interaction. Co-immunoprecipitations (Co-IPs) between transiently transfected Myc and Chinmo showed that both proteins interact physically and that the binding site for Chinmo in Myc lies between amino acid 1-403, spanning all three Myc boxes but not the basic region or the helix-loop-helix/ leucine zipper (Schwinkendorf, 2008). To locate the binding site for Myc in Chinmo, two different Chinmo mutants were established by deletion mutagenesis. In a first step, the Zf- or the BTB/POZ-domain was removed. Chinmo-ΔZf lacks amino acids 517-604, spanning the two zinc fingers, and in Chinmo-ΔBTB the BTB/POZ-domain (amino acids 32-128) are substituted by two amino acids (Thr^{32} + Arg^{33}) (Figure 4-13 A) (Schwinkendorf, 2008). The sequence of the mutant plasmids was verified (Schwinkendorf, 2008).

D. Schwinkendorf was able to co-immunoprecipitate Myc and Chinmo-ΔZf but not Chinmo-ΔBtB. This might be due to two different possibilities: first, the BTB/POZ domain is important for the interaction and second, the Chinmo-ΔBTB was unstable and could not be precipitated. To investigate these two options, S2 cell were transfected with different amounts (0.2 µg, 0.28 µg or 0.35 µg) of the AU1-Chinmo plasmids and lysed 48 hours afterwards. GFP (0.05 µg) was co-transfected to monitor the transfection efficiency. While AU1-Chinmo-wt (62 kDa) and AU1-Chinmo-ΔZf are clearly detectable for all conditions, no bands can be seen for AU1-Chinmo-ΔBTB (53 kDa, same height as AU1-Chinmo-ΔZf). The transfection worked well since clear GFP bands are detectable (Figure 4-13 B). Given that no signal for AU1-Chinmo-ΔBTB was detected, it is conceivable that a deletion in the BTB/POZ domain decreases Chinmo stability, it is not soluble or that it is not expressed by the plasmid.

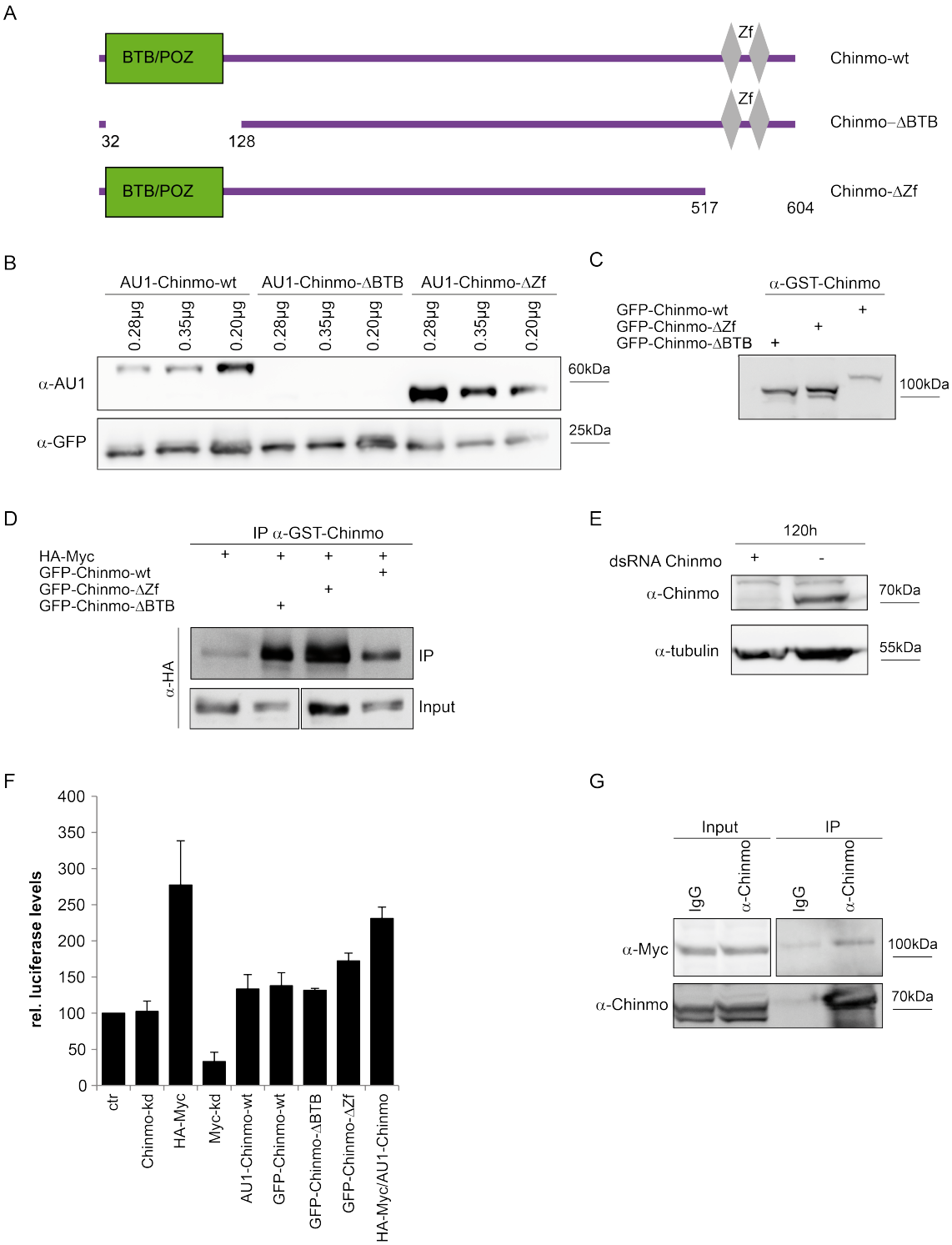

Figure 4-13: Myc and Chinmo interact physically; the BTB-POZ domain and the zinc finger domain are not important for this interaction

A. Schematic diagram of wildtype and mutant Chinmo protein. Chinmo-ΔBTB lacks the BTB/POZ domain and Chinmo-ΔZf lacks the complete C-terminus including the two zinc fingers. Numbers indicate coordinates of the corresponding deletions with the first and last deleted amino acid.
B. Western blot of AU1 tagged Chinmo variants. S2 cells were transfected with the indicated plasmids in different amounts (0.2 µg, 0.28 µg or 0.35 µg) and harvested 48 h later. The protein extracts were analysed by Western. GFP (0.05 µg) was co-transfected to monitor the transfection efficiency.
C. Western blot of S2 cells, transfected with the indicated plasmids.

D. Western blot of co-IPs between Myc and Chinmo variants. S2 cells were transfected with the indicated plasmids and harvested 48 h after transfection. Chinmo-complexes were immunoprecipitated with the crude rabbit α-GST-Chinmo antibody and Western blotted with a α-HA antibody.
E. Western blot of naïve cells and cells depleted of Chinmo. $5*10^6$ cells were either treated with dsRNA against Chinmo or left untreated and were harvested 120 h afterwards. Tubulin was used as loading control.
F. Relative Luciferase levels after overexpression of the indicated plasmids. Lysates were taken 48 h or 120 h (Chinmo-kd) after transfection. Error bars indicate SD of biological duplicates (Myc-kd, GFP-Chinmo-ΔBTB and GFP-Chinmo-ΔZf) or triplicates. Relative reporter level (ctr) was set to 100%.
G. Western blot of endogenous IP between Myc and Chinmo variant. Naïve S2 were immunoprecipitated with the rabbit α-Chinmo antibody or non-immune rabbit-IgG and Western blotted with mouse α-Myc or rabbit α-Chinmo antibody.

To easily monitor the transfection efficiency and potentially stabilize Chinmo-ΔBTB, the wildtype and the two mutant Chinmo constructs were cloned into a pUAST expression vector carrying GFP (2.3.2.2). All proteins were detectable in Western blot experiments (Figure 4-13 C). Therefore Co-IPs together with HA-Myc were performed using the crude rabbit α-GST-Chinmo antibody and immunoblotted with mouse α-Myc antibody. S2 Cells were transfected with either HA-Myc alone or in combination with one of the GFP-Chinmo constructs, harvested 48 hours later and processed for immunoprecipitation (3.3.6). Figure 4-13 D clearly shows that both mutants are still able to interact with Myc and therefore the BTB/POZ-domain is presumably not important for the physical interaction between Myc and Chinmo. The stronger signal for the mutants compared to the wildtype can be explained by the weaker intensity of Chinmo-wt in the input sample. Also a weak interaction of HA-Myc in the absence of any GFP-Chinmo construct can be seen, however the Co-IP is much stronger. To further investigate the Myc binding site in Chinmo, six more Chinmo deletions were established, lacking a different number of amino acids either at the C- or the N-terminus, which still need to be tested.

Since the BTB/POZ-domain is presumably not the Chinmo-Myc interaction domain, the luciferase assay performed by D. Schwinkendorf was repeated to investigate whether Chinmo-ΔBTB is also able to transactivate Myc target genes. S2 cells were transfected with either AU1-Chinmo-wt or the different GFP-Chinmo plasmids alone or in combination with HA-Myc and additionally with a Myc-dependent reporter plasmid (*CG5033*, 2.3.2). Cells were harvested 48 hours after transfection. To examine whether the activation is dependent upon Chinmo, S2 cells were treated with dsRNA against Chinmo or transfected with HA-Myc as control. Depletion of Chinmo is shown in Figure 4-13 E. Consistent with previous observations, Myc overexpression increases the relative reporter level almost 3 fold compared to control (277% ± 61%) and Myc depletion reduces the level to 33% ± 13% (Figure 4-13 F). Depletion of Chinmo has no effect on luciferase levels (103% ± 14%), showing that Chinmo is not required for Myc-dependent target gene activation. However, all Chinmo-plasmids are able to transactivate the Myc-dependent reporter on their own by 131% to 138%, only GFP-Chinmo-ΔZf shows a higher increase (173% ± 11%). This result is similar to experiments performed by D. Schwinkendorf, although the effects in her experiments were slightly

higher (Schwinkendorf, 2008). Combined overexpression of Myc and Chinmo transgenes even enhances luciferase activity compared to overexpression of Chinmo alone (231% ± 16%). These experiments show that Chinmo is able to hyperactivate Myc targets.

So far, physical interaction was only shown for Myc and Chinmo overexpression. Endogenous immunoprecipitations of Chinmo and Myc were performed using the rabbit α-Chinmo antibody or rabbit IgG as non-immune control. Both, the rabbit α-Chinmo as well as the non-immune IgG co-precipitate endogenous Myc (Figure 4-13 G), but to different extents. The signal obtained for the Myc immunoprecipitation with the Chinmo antibody is much stronger than the signal of the IgG control.

Since Myc and Chinmo presumably physically interact with each other and Chinmo is able to transactivate a Myc dependent reporter (Figure 4-13 D-G**)**, we were interested if Chinmo and Myc share the same target genes. Therefore, ChIP experiments were performed in naïve S2 cells with either rabbit α-Chinmo or mouse α-Myc antibody and the corresponding non-immune IgG control. While the binding of Myc to hoip and Nop5 was quite weak compared to IgG (hoip: 1.5 fold; Nop5: 1.7 fold), the Chinmo IP showed a very strong enrichment over IgG (hoip: 42 fold; Nop5: 44.8 fold; Figure 4-14 A). A weak binding of Chinmo towards Pka-C1 (10.9 fold) is observed, which is not the case for Myc (0.4 fold). The weak binding of Myc might be due to experimental problems, for example an old batch of antibody.

To investigate whether the Chinmo antibody specifically binds the Myc target genes hoip and Nop5, Chinmo was depleted in S2 cells for 72 hours (Figure 4-14 B). Quantification of the western blot signals shows a depletion of Chinmo by at least 80%. However, the antibody displays strong background binding, which is not depleted upon knockdown of Chinmo. For ChIP experiments, cells were also harvested 72 hours after transfection with dsRNA against Chinmo. The binding is reduced by more than 30% for all three genes after Chinmo knockdown (Figure 4-14 C) but the enrichment over IgG is still very high (hoip: 72.5 fold, Nop5: 109.1 fold, Pka-C1: 32.3 fold). This might be due to the non-specific binding of the rabbit α-Chinmo antibody or by some residual Chinmo protein that is not completely depleted by RNAi. Due to the strong background binding of Chinmo, the antibody is not suitable for ChIPseq experiments.

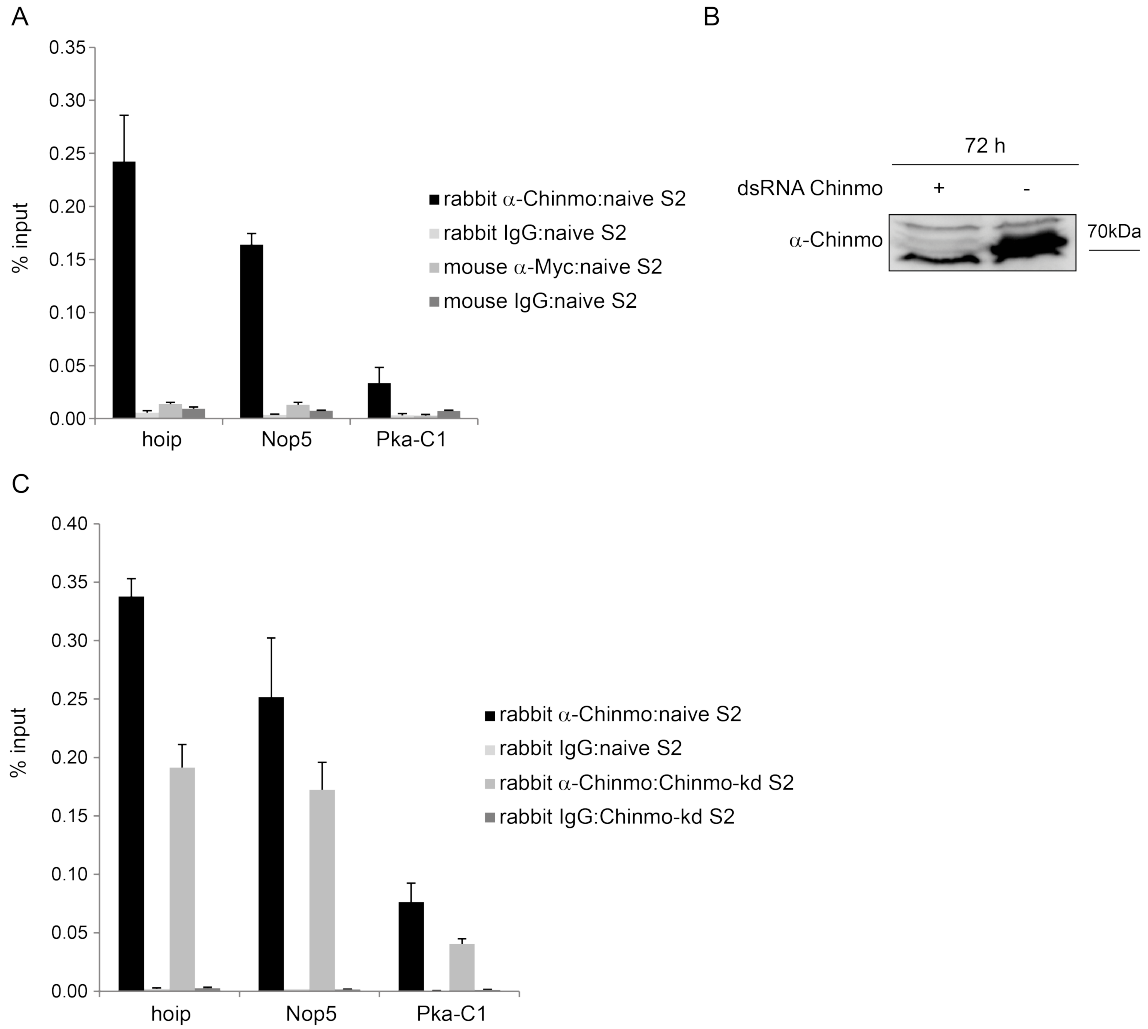

Figure 4-14: Chinmo and Myc bind to the same target genes

A./C. ChIP-qPCR of Myc control genes. Chromatin was isolated from naïve S2 cells or from S2 cells depleted of Chinmo, precipitated with rabbit α-Chinmo, mouse α-Myc or control IgG antibodies and assayed by qPCR for enrichment of the indicated loci. Hoip and Nop5 are known Myc target genes and used as positive, Pka-C1 as negative control. The error bars indicate SD of technical triplicates. Experiments were performed in biological duplicates.
B. Western blot of naïve S2 cells or S2 cells depleted of Chinmo by addition of dsRNA against Chinmo. Cells were harvested 72 h after dsRNA treatment. Western blot was performed with rabbit α-Chinmo antibody.

4.2.3 Tumor induction of Chinmo and Ras^{V12} is Myc-dependent

Chinmo has been linked to cancer by other groups previously to this thesis (Doggett *et al.*, 2010). Since Myc and Chinmo interact in the regulation of growth we wanted to investigate whether this tumor formation is dependent upon Myc. Ectopic activation of oncogenic Ras in combination with loss of the cell polarity regulator and tumor suppressor *scribble* (*scrib*) within the eye imaginal disc of *Drosophila* results in neoplastic tumors (Pagliarini and Xu, 2003). To study the global transcriptional changes of these tumors, the group of H. Richardson (Doggett *et al.*, 2010) performed a comparative microarray approach. The BTB/Zf domain containing protein family was highly enriched in their analysis, including Chinmo (Doggett *et al.*, 2010). They were able to show that overexpression of Chinmo together with Ras^{V12} leads to tumor formation. Based on

these results, experiments were performed to investigate if ectopic activation of Chinmo and Ras indeed leads to tumors. The transgenes of interest were exclusively activated in cells of eye imaginal discs (ey-FLP), combining FRT/FLP-techniques with UAS/Gal4 (yw ey-FLP, GFP; 2.9). For differentiation purposes, GFP was co-expressed with the particular transgenes. A tumor was defined as fluorescent tissue that overgrew the eye-imaginal discs. For comparing the size of the different fluorescent tissues, the size of the whole larvae was measured and divided through the size of the fluorescent tissue and normalized to wildtype control (GFP).

Overexpression of Ras^{V12} (120% ± 24%), Myc (109% ± 24%) or Chinmo alone does not increase tumor size but overexpression of Chinmo even reduces tumorous tissue slightly (83.5% ± 9.2%). This effect seems to be independent from Chinmo, since loss of Chinmo has no effect in a Ras^{V12} overexpressing system (119% ± 21%). However, the specificity of the Chinmo-kd transgenes was never tested before. The combination of Myc together with Ras^{V12} (121% ± 34%) or Chinmo (151% ± 65%) has only mild effects on tumor growth measured as fluorescent tissue (Figure 4-15 A, B). Overexpression of Ras^{V12} together with Chinmo on the other hand leads to a massive increase in tumor size (300% ± 159%, p=0.02; Figure 4-15 A, B).

To investigate Myc's role in this tumor model, flies carrying Ras^{V12} and Chinmo were crossed to flies carrying the *myc* null allele dm^{4} or the hypomorphic allele dm^{P0}, the "*tub*-FRT-Myc-FRT-GAL4 ey-FLP" transgene and GFP. Since the "*tub*-FRT-Myc-FRT-GAL4 ey-FLP" transgene drives ubiquitous expression of Myc-wt cDNA, the lethality of the *myc* mutant is fully rescued (de la Cova *et al.,* 2004; Bellosta *et al.*, 2005). Therefore Myc is slightly overexpressed in the whole animal except the head capsule. Ectopic expression of Ras^{V12} and Chinmo in a Myc mutant background leads to a strong decrease in tumor size, showing that the tumor formation indeed depends on Myc (Figure 4-15 C). Partial loss (dm^{P0}: 58.5% ± 2.8%, p=0.0026) as well as complete loss of Myc (dm^{4}: 66% ± 13%, p=0.03) shows a strong reduction in tumor growth. Therefore we can conclude that the Ras^{V12}-Chinmo tumor model is indeed dependent upon Myc.

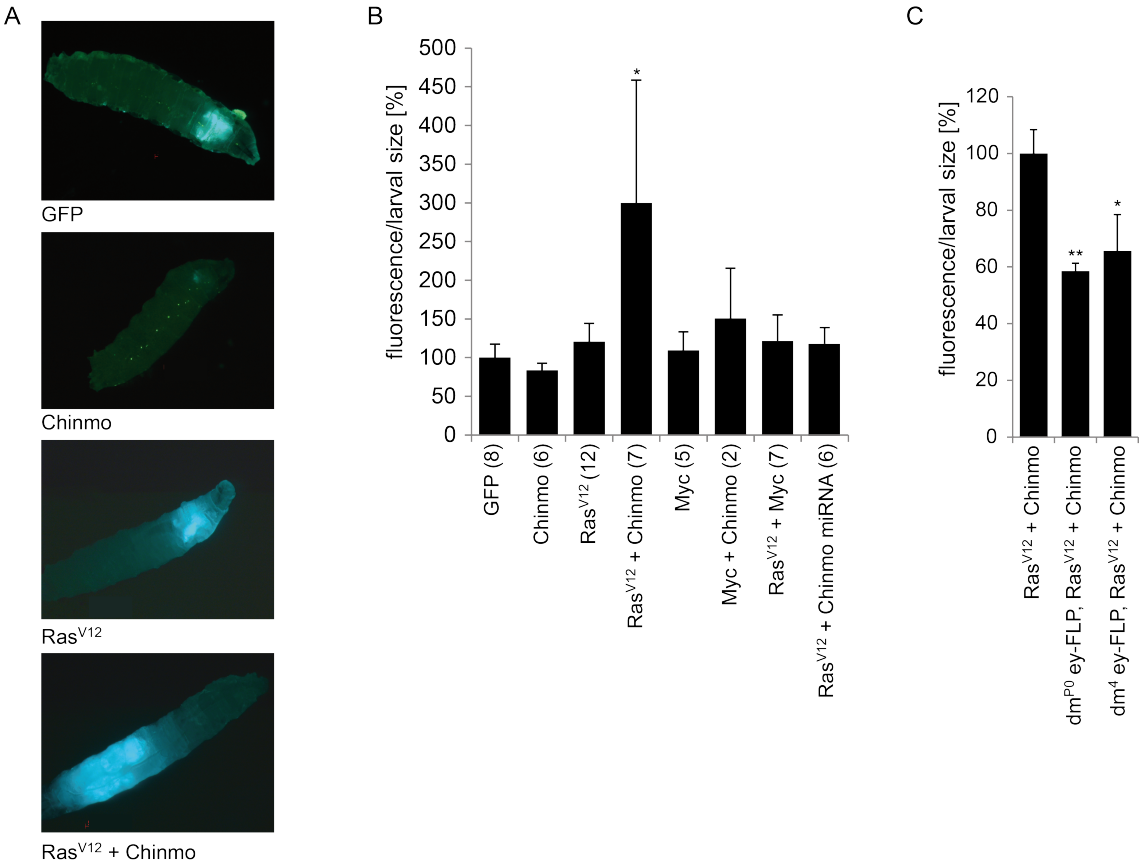

Figure 4-15: Chinmo cooperates with Ras^{V12} in the induction of tumors

A. Larvae express GFP and the depicted UAS-constructs under the control of the tub-Gal4 ey-FLP promoter.
B. Ratio of the size of fluorescent tissue to the size of whole larvae for the depicted genotypes. Ratios and standard deviations were normalized to control (yw ey-FLP, GFP). Error bars indicate SD of individually assayed flies shown in parentheses. Difference to control is $p<0.05$ (*, Student's 2-tailed t-test).
C. Ratio of the size of fluorescent tissue to the size of whole larvae for the depicted genotypes. Ratios and standard deviations were normalized to control (yw ey-FLP, DRas^{V12} + Chinmo). Error bars indicate SD of three individually assayed flies. Difference to control is $p<0.05$ (*) or $p<0.005$ (**) respectively (Student's 2-tailed t-test).

5 Discussion

5.1 Characterization of direct Myc target genes in *Drosophila melanogaster*

5.1.1 Myc binds a core set of target genes in *Drosophila*

The transcription factor Myc is known to be involved in various processes like cell growth, proliferation, cell cycle progression, cell adhesion and apoptosis (Dang *et al.,* 2006; Vita and Henriksson, 2006). New technologies such as microarray and next generation sequencing technology allowed getting an overview of the genes which are regulated and bound by Myc. While several publications focus on Myc target genes in vertebrates (Schuhmacher *et al.,* 2001; Dang *et al.,* 2006; Lin *et al.,* 2012; Nie *et al.,* 2012), less is known about direct Myc targets in other organisms. To get a comprehensive list of directly regulated genes in *Drosophila*, we performed ChIPseq and RNAseq (M. Stauch, pers. com.) analysis.

To reduce the possibility that binding sites were missed due to epitope masking, ChIPseq analysis was performed with two different antibodies, a monoclonal mouse α–Myc and a polyclonal rabbit α–Myc antibody. In addition, two different cell lines, *Drosophila* S2 cells and Kc167 cells, were used. Both cell lines are hematopoietic cells of embryonic origin, but it could be possible that they differ in their molecular characteristics. However, the binding sites of S2 and Kc167 cells showed a big overlap (Figure 4-2 B) excluding major differences between the cell lines.

All three ChIPseq experiments together led to the identification of 265 statistically significant Myc binding sites (FDR ≤ 10%; Figure 4-2 B). Due to the good overlap between the three ChIPseqs, it is very likely, that these 265 binding sites represent the core set of Myc binding sites in *Drosophila*. The number of binding sites identified in our experiments nicely matches the number of binding sites identified in DamID experiments by Orian *et al.* (2003). For DamID experiments, a fusion protein consisting of *E.coli* DNA adenine methyltransferase (Dam) and the protein of interest is created. The fusion protein is expressed in cells and Dam will be targeted to the native binding sites of the protein used for fusion. Dam marks the sequences near a binding site by methylation of adenines in the sequence GATC, which can be detected by specific restriction enzymes. The methylated DNA is amplified and labelled for hybridization to microarrays (van Steensel, 2005). Orian *et al.* identified 287 Myc bound genes under slightly increased Max levels, while they identified only 22 Myc bound genes when Max was not overexpressed. Therefore Max was probably rate limiting in their experiments. Taking into account that they identified the target genes under slightly increased Max and Myc-Dam levels, it is possible that part of their targets are overexpression artefacts. Howev-

er, the spotted microarray they have used covered only 6255 cDNAs, representing roughly half of *Drosophila* coding sequences, and they therefore probably missed several target genes. Thus the sum of 287 Myc bound genes might very well reflect the real amount of Myc target genes. However, the number of binding sites identified is tremendously smaller compared to Yang *et al*. (2013). In their study, Yang *et al.* examined the distribution of Myc during interphase and mitosis in Kc167 cells. Myc associates preferentially with paused genes and a large fraction of Myc sites persisted during mitosis. In total 3995 binding sites were identified, with the biggest fraction present at promoter-proximal regions and the corresponding genes being involved in ribosomal RNA synthesis. The big discrepancy between the number of binding sites in our ChIPseq analysis and the Yang analysis could have three reasons. First of all, the cell lines S2 and Kc167 could differ in their molecular characteristics, what has been excluded (see above). Secondly, the commercial rabbit α-Myc antibody (SC) might detect other epitopes on Myc, have a higher affinity, or the way of experimental processing led to differences in sequencing results (e.g. buffers, cross-linker). Finally, since the specificity of the Santa Cruz antibody was never shown in any publication, some of the peaks might reflect non-specific binding of the antibody to chromatin. QRT-PCR analysis of 17 randomly selected Yang peaks (3.1.15; 4.1.1) revealed that the peaks were not Myc specific, due to the fact that they showed positivity also in IgG control or were not decreased upon Myc KD. The unspecific binding might correspond to a background reactivity of the antibody which was detected in Western blot analysis, too (Figure 4-3 C). ChIPseq traces of the selected Yang peaks from our own data, obtained with the mouse α-Myc antibody also showed a non-specific Myc signal (Figure 4-3 B). Since Yang *et al.* (2013) did not include control ChIPs with non-immune IgG or from Myc depleted cells and since we were able to show that randomly chosen Yang peaks were not Myc specific (Figure 4-3 A, B), we consider the additional peaks found by Yang *et al.* to be Myc non-specific.

In agreement with data published in mammalian cells (Zeller *et al.,* 2006; Walz *et al.,* 2014), most binding sites map less than 1000 bp from a transcriptional start site also in flies, suggesting that Myc preferentially binds to promoter-proximal sequences. This preference is even enhanced when only binding sites are considered which cover an E-box binding motif, the most enriched binding motif in our dataset (Figure 4-6 A, B). Several publications have shown that Myc preferentially binds E-boxes, in vertebrates as well as in flies (Amati *et al.,* 1992; Solomon *et al.,* 1993, Gallant *et al.,* 1996). E-box presence in the promoter has also been described previously as indicative of Myc-regulated genes (Hulf *et al.,* 2005). Another highly enriched motif in our dataset, is the DNA replication element (DRE; Figure 4-6 B'), which has been recognized to be associated with Myc target genes before (Orian *et al.,* 2003). DRE sequences were reported to be present near genes involved in growth and cell proliferation (Hirose *et al.,* 1993, 2001).

RNAseq was performed in naïve and Myc depleted S2 cells (M. Stauch, pers. com.), to get insight which of the Myc bound genes are also regulated. Some non-coding RNAs

(rRNAs, tRNAs, miRNAs) had been identified in vertebrates as Myc targets before (Grandori *et al.,* 2005; Gomez-Roman *et al.,* 2003). To investigate whether these and other non-protein coding transcripts mediate biological activities of Myc, non-polyadenylated transcripts were included in our search for Myc targets. In total 240 genes were found to be activated by Myc, while only 41 Myc repressed genes were identified to be differentially expressed in all three independent RNAseq experiments. Myc-activated polyadenylated transcripts overlap nicely with previously published data (Hulf *et al.,* 2005; Grewal *et al.,* 2005; Bonke *et al.,* 2013), while the Myc repressed ones show only poor overlap (Herter *et al.,* 2015). When expression and binding data were combined, 139 genes were identified to be directly activated by Myc, while 59 genes were directly repressed. Summing up the ChIPseq and the RNAseq data, less than 300 genes are bound by Myc in *Drosophila*, and only 198 genes are regulated directly. This represents roughly 1% of all *Drosophila* genes and stands in sharp contrast to earlier published data, where Myc is assumed to regulate around 15% of all genes (Dang *et al.,* 2006). Furthermore several other groups (Nie *et al.,* 2012; Lin *et al.*, 2012; Walz *et al.,* 2014; Sabo *et al.,* 2014) propose a much higher number of genes controlled by Myc in mammals. However, we only considered genes which were differentially regulated with a fold change of at least one-third and a p-value below 0.05 for our analysis. Also other differences in data processing, e.g. the definition of the false discovery rate for the peak calling could explain this huge discrepancy. However, the organization of *Drosophila* is simpler than that of vertebrates (e.g. one instead of three Myc proteins) and Orian *et al.* (2003) found equal numbers of Myc target genes, in comparison to us. Thus it is highly probable that the 300 genes we found in our setup represent the core set of Myc target genes in *Drosophila*.

Independent on the amount of directly regulated genes, genes involved in ribosome biogenesis, translation and RNA-processing are among Myc controlled genes in all cases. Dependent on its expression levels, Myc controls genes involved in cell adhesion, apoptosis and angiogenesis, too (Lee *et al.,* 2012; Walz *et al.* 2014). Taking into account the high number of genes controlled by Myc in mammals and the various processes they play a role in, Myc may act as a general transcription factor in mammals. In *Drosophila*, on the other hand, Myc seems to act as a specific, process related transcription factor, mainly involved in growth control. In this context, the question arises if growth control represents the primordial function of Myc, having evolved to a broader functional field in higher organisms. Also the presence of a single Myc protein in flies versus three Myc family members in vertebrates might be a reason for the fewer target genes and processes Myc is involved in. In addition, the regulation of some gene sets in mammals is dependent on Myc levels and promoter affinity (Walz *et al.* 2014; F. Lorenzin, pers. com.) and might be relevant only in tumorous tissues.

5.1.2 **snoRNAs are new Myc targets**

From the 240 genes, which were significantly downregulated after Myc depletion (fold change ≤0.66; $p<0.05$), 36 genes did not code for proteins but instead for snoRNAs.

Further analysis on the snoRNAs showed that all 103 snoRNAs that passed the 125 nt cutoff and were detectably expressed in S2 cells were, downregulated upon Myc depletion (Herter *et al.,* 2015). The *Drosophila* genome is predicted to encode 288 snoRNAs (Huang *et al.,* 2005; Herter *et al.,* 2015), which divide into two major classes, Box C/D (SNORA) and Box H/ACA (SNORD) snoRNAs (Kiss-László *et al.*, 1998; Bachellerie *et al.,* 1995). SnoRNAs are quite small, consisting of only 46 nt to 316 nt. While SNORAs guide methylation of 2'O-ribose of target genes, mainly rRNAs, mRNAs and tRNAs, SNORDs are essential for pseudouridylation of target RNAs (Kiss, 2001). Many snoRNAs are hosted in protein coding genes, which themselves are bound and regulated by Myc. The biggest fraction of snoRNAs (229; 80%) is encoded in introns of 84 protein-coding genes (Dieci *et al.,* 2009), many of which are Myc targets, too (Table 4-5). Examples of hosting genes are those encoding for components of snoRNPs (Fib, hoip, nop5), translation factors (Ef2b, eEF1delta, bic) or ribosomal protein genes (RpS5a, RpL7, RpL11). To investigate whether the dramatic impact of Myc on the snoRNAs is directly via their host genes, or instead, if the regulation is indirect, for example via depletion of snoRNPs and a resulting destabilization of the corresponding snoRNAs (Lafontaine and Tollervey, 1999), Myc's transcriptional effects on Uhg genes were studied. Almost 17% of all snoRNAs (48) are not encoded in introns of protein-coding genes but in introns of non-protein-coding "U-snoRNA host genes" (Tycowski and Steitz, 2001; Huang *et al.,* 2005). In *Drosophila*, 7 Uhgs exist (Uhg1; 2; 3; 4; 5; 7; 8), which are dedicated to the synthesis of snoRNAs only. The gene formally known as Uhg6 is actually Nop60B. Our data reveal a putative novel Uhg gene (2R-cluster), since three snoRNAs were found to be arranged in tandem repeats on chromosome 2R with a single E-box flanking them upstream. Since only seven other snoRNAs are independently transcribed, it is likely that these three snoRNAs belong to another Uhg gene.

All but three of the Uhg-encoded snoRNAs are smaller than 125 nt and were therefore not detected in the RNAseq (Herter *et al.,* 2015). qRT-PCR and Northern blot analysis revealed that Myc depletion leads to downregulation of the snoRNAs and their host genes (Figure 4-7 A), confirming the RNAseq results and that also mature snoRNAs are affected and not just the immature precursors (Figure 4-7 C). Furthermore, overexpression of Myc can also increase the expression of the snoRNAs to supraphysiolgical levels (Figure 4-7 B). Consequently Myc controls all examined snoRNAs independently of their stability by direct binding to the host genes. Myc binding was shown to the E-boxes of Uhg1, 2, 4, 5 and the 2R-cluster (Figure 4-5 A, B). In addition, a peak was found close to the TSS of Uhg7. Since Uhg7 and Rpl23A overlap and the peak was closer to the TSS of Rpl23A, it was allocated to Rpl23A. However there is still the posiblility that Uhg7 is also bound by Myc. Binding of Myc to the Uhgs presumably involves Myc-Max heterodimers, since loss of Max reduced the recruitment of Myc to these promoters (Figure 4-5 C). This was expected, since Myc needs the association with Max to bind to E-boxes (Blackwell *et al.,* 1990; Blackwell *et al.,* 1993). However, loss of Max does not decrease the recruitment of Myc to the promoters to the same extent as loss of Myc. Therefore it is possible that the binding is partially independent

of Max or that the knockdown of Max was not complete. Considering that the knockdown of Max was not verifiable due to the lack of a Max antibody, it is likely that still residual Max was present. To distinguish between the possibilities, ChIP should be performed at different time points after Max depletion, to investigate if the binding further decreases.

Myc not only regulates snoRNAs in *Drosophila*, but also in mammals. The human genome encodes 745 snoRNAs, of which 419 are encoded in 232 different host genes, including 15 non protein-coding "snoRNA host genes" (SNHG) (Li *et al.,* 2010). Reanalysis of data from human U2OS cells (Walz *et al.,* 2014), showed a significant enrichment of snoRNA host genes among the highly c-Myc bound genes (Herter *et al.,* 2015). These genes can also be activated by c-Myc, as shown in murine T-cell lymphomas (Müller *et al.,* 2010; Herter *et al.,* 2015). Like in *Drosophila*, vertebrate Myc has an impact on the SNHG loci, which are dedicated to the production of snoRNAs. Myc is recruited to the majority of SNHG promoters in human and murine cells, mostly to positions containing an E-box (E. Wolf, pers. com.; Herter *et al.,* 2015). Also in neuroblastomas with high N-MYC expression, the upregulation of snoRNAs has been observed (Schramm *et al.,* 2013). Therefore, the control of non-coding snoRNA host genes and of snoRNA levels in general, is an evolutionary conserved function of Myc proteins.

5.1.3 **snoRNAs play an important role in tumor formation**

To further investigate the role snoRNAs play in vivo, we focused on the snoRNAs encoded by the Uhg genes. All snoRNAs are quite small and their integration in snoRNPs complicates to target them directly via dsRNA or mutations. Targeting their host genes has the advantage that several snoRNAs can be studied at once. Furthermore, if snoRNAs can compensate for each other, depletion of several snoRNAs might show stronger phenotypes than loss of single snoRNAs. Several sites have been shown to be targeted by more than one snoRNA, and most of these snoRNAs are clustered within the same host genes (e.g. Uhg1; Yoshihama *et al.,* 2013). In this case, depletion of a single host gene leads to loss of modification at several sites at once. It is very likely that this increases the loss of function effect in comparison to loss of a single snoRNA or a single target site. Since most of the protein-coding host genes are Myc targets themselves and play important roles in processes involved in ribosome biogenesis and translation and therefore in growth-related processes, studying the role of the encoded snoRNAs is difficult. The Uhg genes, however, do not encode potentially growth-relevant transcripts. Furthermore, they host 17% of all snoRNAs and Uhg1 alone encodes 16 different snoRNAs. An Uhg1 mutant fly line (*Uhg1*^{1}) was established (Herter *et al.,* 2015) and used to study the effects, snoRNAs have on growth-related processes. As expected, Uhg1 mutant flies did not show methylation at three (28S:A1666, 28S:G3081, 28S:G3277; Figure 4-10 C) out of five positions which are exclusively targeted by snoRNAs encoded by Uhg1 (Yoshihama *et al.,* 2013). Contrary to what had been described by Dong *et al.* (2012) and N. Watkins (pers. com.), the sites of interest

(A1666, G3277) were not influenced by the previous, Uhg1 unaffected methylation sites (Figure 4-10 C). While A1688 was not detectable at all, G3341 was not changed upon different dNTP concentrations. On the other hand, several other positions seemed to be influenced by decreasing dNTP concentrations (e.g. A1713), which are not be methylated. This fits to observations of Motorin *et al*. (2007), who states that regions exist, where the reverse transcriptase has the tendency to pause independently of mathylation (e.g. G3318, G3319). Furthermore, pauses observed at 2'-O-methylated residues are sequence dependent and no pause may occur depending on the sequence context (Motorin *et al*., 2007). Loss of Uhg1 leads to loss of methylation at 5 specific ribose residues and could therefore affect ribosome assembly and activity. The Uhg1 mutant animals did not differ in size and weight (Herter *et al.,* 2015) and also protein content was equal to control animals (Figure 4-11 A). However, in comparison to control flies, only one third of the females and half of the males survived to adulthood (M. Gallant, pers. com.). In addition, *Uhg1*^{1} females showed a strongly reduced fertility which was not observed for male flies (M. Gallant, pers. com.). While total protein content of larvae did not differ between mutant and control animals, the synthesis rate of new proteins was significantly reduced in *Uhg1*^{1} larvae (Figure 4-11 A). In agreement with slower protein synthesis, mutant animals had a delay in development and adult flies eclosed approximately 12 hours later than control animals (Herter *et al.,* 2015). Female-specific sterility together with an increase in developmental timing are typical indications of mutations in pathways affecting growth (Johnston *et al.,* 1999). Moreover, hypomorphic Myc mutations were shown to display the same defects (Johnston *et al.,* 1999). These observations could imply that loss of Myc downregulates expression of ribosomal genes and other genes involved in cellular growth, leading to defects in ribosome assembly and activity and so to female sterility and delay in development.

To investigate whether Myc can still fulfill its functions in the absence of Uhg1, flies carrying a Myc transgene were crossed with either wildtype or Uhg1 mutant animals. Overexpression of Myc resulted in a massive increase in protein synthesis rate (Figure 4-11 B), which fits to experiments performed in B lymphocytes in control and *Eμ-myc* mice (Iritani and Eisenman, 1999). B cells from *Eμ-myc* mice contained 2-fold higher protein levels than control animals, showing a correlation between Myc overexpression and increased protein synthesis. Overexpression of Myc in an Uhg1 mutant background however, did not enhance protein synthesis rate compared to *Uhg1*^{1} larvae but was even slightly decreased (Figure 4-11 B). Thus Myc's ability to increase protein synthesis is dependent on the presence of these snoRNAs and loss of methylation of only five residues leads to a massive impairment in ribosome activity that cannot be rescued by overexpression of other snoRNAs. Since *Uhg1*^{1} animals still survive and develop quite normally, snoRNAs seem to complement each other at least partially. It is very interesting that the Uhg1 mutant animals only need half a day longer for development than wildtype animals (10.5 days versus 10 days) but overexpression of Myc in *Uhg1*^{1} animals does not show any increase in protein synthesis rates. Normally, overexpression of Myc results in a 100% increase in cell size (Johnston *et al.,* 1999), which might correspond to a 100% increase in protein synthesis rates (Figure 4-11 B). There-

fore, it seems as if the *Uhg1*^{1} animals already grow with maximum achievable protein synthesis rates, not being able to further increase the rates upon Myc overexpression. One reason for the decreased protein synthesis rate of *Myc OE/ Uhg1*^{1} animals towards *Uhg1*^{1} animals might be their physical state. While animals of both genotypes started wandering the same time, the *Myc OE/ Uhg1*^{1} animals were smaller (pers. observation). Therefore the inversion of the larvae (3.4.6) was more complicated. Given no big differences within the different experiments with the *Myc OE/ Uhg1*^{1} animals (SEM < 14%), it is unlikely that the handling led to the observed differences in protein synthesis rates between *Myc OE/ Uhg1*^{1} and *Uhg1*^{1} animals. It remains open why the *Myc OE/ Uhg1*^{1} larvae were smaller and if this might for example reflect a different composition of cell types, e.g. less polyploid tissue and therefore fewer cells which can react upon overexpression of Myc. It is also not clear whether smaller animals might have a slower protein synthesis rate due to viewer cell. The differences in protein synthesis between different genotypes and between different trials could also originate from time dependent expression of the Uhgs. The interval between the heat shock and collection of the larvae was 16 h ± 2 h, but was given at different time points in the evening and therefore the light conditions in the incubator differed slightly. While our experiments show that reduction of Uhg1 leads to a decrease in protein synthesis rates, other groups were able to show that the expression levels of different Uhgs (Uhg1-5, Uhg8 and Nop60B) display a rhythmic and time dependent behavior in light/dark experiments performed in adult fly brains (Hughes *et al.,* 2012; P. Menegazzi, pers. com.). Therefore it is possible that effects on protein synthesis are differentially strong at different time points throughout the day. It would be very interesting to investigate if protein synthesis rates change throughout the day in correlation with Uhg expression. Just recently it was shown that the circadian clock influences the translation of a subset of mRNAs involved in ribosome biogenesis (Jouffe *et al.,* 2013). Furthermore it should be investigated whether Myc shows rhythmic expression, too, as it was shown for c-Myc (Fu *et al.,* 2002). Interestingly, no other snoRNA host genes besides the Uhgs were found to display rhythmic expression (Hughes *et al.,* 2012), arguing against rhythmic activity of Myc in *Drosophila*.

Since loss of Uhg1 and therefore of only 16 different snoRNAs greatly affects growth, it is very likely that different snoRNAs can only partially substitute for each other. Thus, loss of snoRNAs can lead to severe effects in development and growth and presumably enhances tumor formation and other diseases. Loss of Uhg1, however, did not reduce tumor growth in a Myc dependent brain tumor system (Figure 4-11 C). It is possible that the delay in larval development and the prolonged time, needed for metamorphosis (Herter *et al.,* 2015), which is caused by the loss of Uhg1, also slows down the tumor growth rate. In this context, the NBII tumors might develop later and a reduction in tumor growth rate would be masked by the loss of Uhg1. Also, loss of Uhg1 did not affect "Ras^{V12} + Chinmo" tumors (Figure 4-11 D), while loss of Myc has a strong effect in this tumor model as well. Loss of Myc on the other hand does not only lead to reduction of distinct but all snoRNAs and therefore a much greater impairment. It is likely that

loss of several Uhgs at once might also lead to a reduction in tumor growth in both tumor models.

On the other hand, overexpression of Uhg4 or Uhg5 led to an increase in tumor growth. How this increase is achieved is not clear, however all processes in ribosome biogenesis are coordinated with each other to sustain rapid cell growth (Warner, 1999). Overexpression of Uhg4 or Uhg5 might trigger a feedback loop, activating synthesis of rRNAs and ribosomal proteins and therefore ensure an efficient assembly of ribosomal particles. It should be tested, whether overexpression of Uhg4 and Uhg5 has an effect on protein synthesis rates, too.

SnoRNAs not only play a role in tumor formation in *Drosophila*, but deregulation of several snoRNAs was observed in human cancers (Mannoor *et al.,* 2012). The group of G. Jenster (Martens-Uzunova *et al.,* 2012) performed deep sequencing in prostate cancer samples to investigate the composition of the entire small transcriptome and found a strong differential expression of snoRNAs between metastatic and non-metastatic prostate cancer samples, linking snoRNA abundancy to poor prognosis. Furthermore the snoRNAs SNORD44, SNORD43, SNORD48 and RNU6B were found to be deregulated in breast cancer and head and neck squamous cell carcinomas, and the low expression levels of SNORD44 were associated with poor prognosis and correlated with an aggressive pathology (Gee *et al.,* 2011). The authors also mention that they noted generally lower levels of snoRNAs in association with aggressive tumors and poor prognosis and suggest that the loss of the snoRNAs and therefore a decrease in ribosome biogenesis leads to chromosomal instability, an indicator of cancer. Another set of specifically downregulated snoRNAs in tumor samples was described in acute leukemia (Valleron *et al.,* 2012). In neuroblastomas with high N-MYC expression, on the other hand, several snoRNAs were found to be overexpressed (Schramm *et al.,* 2013), raising the possibility that snoRNAs contribute to N-MYC dependent tumor growth, similar to what we have described in *Drosophila* type II neuroblast tumors. Not only snoRNA sets have been found to be deregulated in human cancers, but also distinct snoRNAs have been shown to have an impact on cellular proliferation or transformation. A SNORD114-1 variant promotes cell growth through cell cycle modulation, where it is involved in the G0/G1 to S phase transition (Valleron *et al.,* 2012). SNORA42 was shown to be overexpressed in lung tumors, where it enhances cell growth and colony formation and is inversely correlated with survival of patients (Mei *et al.,* 2012). Our data together with published data in humans show evidence that snoRNAs play a role in tumor formation. Since it is possible that they contribute to Myc dependent tumor growth, the connection between snoRNAs and Myc should be studied further, to better understand the mechanism of their interaction, which might enable new therapeutic approaches in cancer therapies.

5.1.4 **Myc controls all levels of ribosome biogenesis**

It was shown before that Myc plays an important role in ribosome biogenesis (Grandori *et al.,* 2005; Grewal *et al.,* 2005; Arabi *et al.,* 2005) and influences mRNA translation by

regulating the transcription of translation initiation factors, like eIF4E and eIF4A (Schmidt, 2004). Our data, however, reveal a new set of Myc target genes involved in ribosomal biogenesis, the snoRNAs. In higher eukaryotes, most snoRNAs are encoded in introns of other genes, many of which code for translation- or ribosome-related proteins. In *Drosophila*, more than 50% of all host genes belong to these groups of proteins, while in humans still more than a quarter does (Dieci *et al.,* 2009). It is convincing that this arrangement helps to adapt snoRNA production to the cell's biosynthetic needs. Not only snoRNAs are direct Myc targets, but also the partner proteins which are essential to form snoRNPs (small nucleolar ribonucleoprotein particles). These targets are, for example the box C/D snoRNP components Fibrillarin, Nop58/ Nop5, Nop56,15.5kDa/ hoi-polloi, with Fibrillarin being the methyltransferase responsible for methylation of the 2'O ribose of the target nucleotide (Kiss, 2001; Reichow *et al.,* 2007). Dyskerin/ Nop60B, GAR1, NHP2, NOP10/ CG7637 are the box H/ACA components, with Dyskerin/ Nop60B being the pseudouridine synthase (Henras *et al.,* 1998; Watkins *et al.,* 1998). All of these components are included in our list of bound and regulated genes (Table 4-5). Furthermore, several other factors required for the correct assembly and functionality of the snoRNPs are established Myc targets. Nopp140, a nucleolar phosphoprotein, functions as a molecular link between the nucleolus and the coiled bodies (Isaac *et al.,* 1998) and is associated with box C/D and box H/ACA snoRNPs (Bachellerie *et al.,* 2002). Also the nucleoplasmic helicases Tip48/ reptin and Tip49/ pontin were shown to be required for the production of box C/D and box H/ACA snoRNAs as well as for the localization of snoRNP proteins (Bachellerie *et al.,* 2002; King *et al.,* 2001). Both proteins are no direct Myc targets, but show a close physical and genetic interaction with Myc (Bellosta *et al.,* 2005). Also *Modulo* (*mod*), a *Drosophila* homolog of nucleolin (Mikhaylova *et al.,* 2006), which was shown to be directly controlled by Myc (Perrin *et al.,* 2003), was found in our dataset. By controlling all snoRNAs and the core proteins essential to form snoRNPs, Myc acts as a master regulator of snoRNP production. Besides its role in snoRNP production, Myc controls several other steps in ribosome biogenesis, such as induction of components of the small (e.g. RpS5a, RpS27a, RpS14a) and the large (e.g. RpL7, RpL13, RpL11, RpL22) ribosomal subunits and genes essential for their processing and maturation (Table 4-5). In agreement with earlier publications, stating that rRNA synthesis by RNA Pol I in *Drosophila* is indirect (Grewal *et al.,* 2005), no direct binding to rRNA loci was observed in our data. Instead some components or cofactors of Pol I were found to be directly activated by Myc, for example Rpl135, a Pol I subunit (Grewal *et al.,* 2005). Due to the small transcript size of tRNAs, they were not included in the RNAseq analysis, but it has been shown that Myc increases the amount of tRNAs and other RNA polymerase III (Pol III) products (Gomez-Roman *et al.,* 2003; Steiger *et al.,* 2008). Since no significant enrichment of Myc at the 306 annotated tRNA loci was observed (data not shown), it is likely that Myc does not contact DNA directly at these sites. In fact, Myc does neither need Max nor its DNA binding domain to activate Pol III (Steiger *et al.,* 2008) and 96% of all tRNAs (295 of 306) do not contain E-boxes. Therefore it is very likely that Myc does not contact these sites directly. Myc not only encodes proteins

involved in translation and ribosome biogenesis, but also proteins involved in metabolism, RNA processing and transcription as well as in mitochondrial function (Table 4-5).

Put in a nutshell, Myc not only stimulates transcription of ribosomal proteins and rRNA, but also regulates snoRNAs and therefore all components to build snoRNPs. By controlling all these components, Myc can be considered as a master regulator of ribosome biogenesis (Figure 5-1).

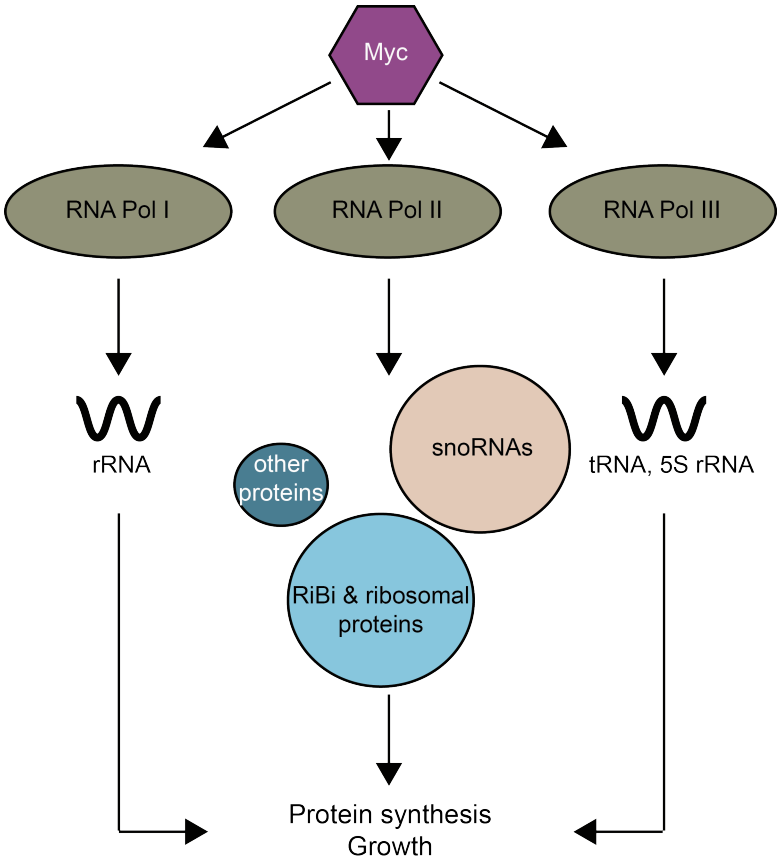

Figure 5-1: Myc acts as a master regulator for ribosome biogenesis[3]

Myc has been shown previously to activate RNA Polymerases I and III and therefore the transcription of rRNAs and tRNAs. The majority of direct Myc target genes code for ribosomal proteins or control ribosome biogenesis (RiBi genes). SnoRNAs are a new class of Myc targets and are considered to be direct if their host genes are bound by Myc.

Myc repressed genes were not significantly enriched for any process (GOrilla tool). In contrast to the Myc activated genes, they also showed only a poor overlap between different data sets. Among these targets, two genes were found which are involved in ecdysone response, *Eip75* and *Kr-h1* (*Ecdyson-induced protein 75B; Krüppel homolog 1*) and two other ones which play a role in the JAK/STAT pathway, *Socs36E* and *nej* (*Suppressor of cytokine signaling at 36E; nejire*). *Eip75* is the only Myc repressed target gene, which hosts a snoRNA (snoRNA:Me28S-A30). Other repressed genes are for example *brk* (*brinker*), a negative factor in Dpp signaling, *Snx3* (*Sorting nexin 3*), a positive factor in Wnt signaling, *Indy* (*I'm not dead yet*), a citrate transmembrane transporter and *velo* (*Veloren*), a SUMO protease (data not shown).

5.2 Analysis of Chinmo and Myc interaction

5.2.1 Chinmo and Myc function in partial redundant pathways

In 2003, A. Sulzer characterized a complementation group consisting of three different alleles, which had been found earlier in an ey-FLP-screen. This so called “pinhead”-screen had been performed (Sulzer, 2003) to identify genes, which are involved in growth control. The complementation group included the *CG31666* gene and was named *chnöpfli* because of the small heads resulting from the mutations. Later on, Zhu *et al.* (2006) identified *CG31666* in a screen for genes, required for temporal identity of mushroom body neurons in *Drosophila* and named it *chinmo* (*Chronologically inappropriate morphogenesis*). The small heads observed for the different *chinmo* alleles were not caused by differences in ommatidial size (Sulzer, 2003). Instead, the number of ommatidia was significantly lower than in wildtype animals (Figure 4-12 A). The number was even more reduced in homozygous mutant eyes. Surprisingly, $chinmo^{110}$ showed the strongest effect in the heterozygous background, while it showed the weakest in the homozygous background. The effect in heterozygous animals stands in contrast to what has been observed by A. Sulzer, who reported that $chinmo^{110}$ is the weakest allele. Both, $chinmo^{108}$ and $chinmo^{134}$ have a mutation leading to a stop, which produces a truncation after the BTB domain and do not contain the zinc fingers. In contrast, $chinmo^{110}$ only carries a mutation in the first zinc finger, maintaining the most functions of the wildtype protein. It is possible that $chinmo^{110}$ is unstable (5.2.2). Another possibility for the observation that $chinmo^{110}$ shows a stronger effect in heterozygous animals than the more severe mutations, $chinmo^{108}$ and $chinmo^{134}$, might be that $chinmo^{110}$ acts as a dominant negative allele.

The homozygous mutant eyes displayed a stronger phenotype for all alleles, consisting of fewer ommatidia. However, the heads and eyes were still quite normally shaped. Since also mutations affecting the insulin signaling pathway, show a reduction of eye size, A. Sulzer tested if Chinmo acts through this pathway. Interaction studies with different components of the pathway, like PKB, PTEN and TSC1 indicated that Chinmo does not function in the insulin receptor pathway.

Chinmo was not only found in the screen for growth defective mutants (Sulzer, 2003) but also in a screen looking for novel components of the “Myc pathway” (Schwinkendorf, 2008). The screen was based on the dominant genetic interaction between the hypomorphic Myc allele dm^{P0} and Myc’s transcriptional cofactor Pontin/ Tip49 (Bellosta *et al.,* 2005). The eyes of all 3 *chinmo* alleles are clearly distorted in an $ey{>}dm^{P0}$ background (Schwinkendorf, 2008), which is due to a reduction in cell number (Figure 4-12 B), while the control animals are unaffected. Again, $chinmo^{110}$ showed the strongest effect. In Myc-null mutant eyes, the number of ommatidia was even more reduced, independent of the presence or absence of Chinmo. This shows that while Chinmo only affects cell number, Myc affects both, cell number and size. This effect is similar to mutations in the insulin receptor pathway, where mutations in *chico* and the *insulin receptor* gene also affect cell number and size (Böhni *et al.,* 1999; Brogiolo *et*

al., 2001). Similar effects can be explained by the fact, that Myc acts downstream of InR (Parisi *et al.,* 2011). The effects on eye and head size are even exacerbated if both, Myc and Chinmo are completely eliminated. Animals that are homozygous mutant for *chinmo* or Myc in the eye-imaginal discs survive and show the formation of quite normally patterned eyes. The double mutants on the other hand, display almost no head structure anymore and are fully lethal (Schwinkendorf, 2008). Thus, Myc and Chinmo do not act in the same pathway in the control of eye development (Figure 5-2). Besides their function in eye development, Myc and Chinmo have been shown to genetically interact in other processes, too. Overexpression of different Chinmo transgenes with different Gal4-drivers always resulted in the death of the animals. This is probably due to apoptosis which is induced upon overexpression of Chinmo (Schwinkendorf, 2008). Reduction of Myc activity, however, enhances the survival rate of these flies. On the other hand, Myc is dependent upon Chinmo to promote cell growth. Taken together, these data demonstrate that Myc and Chinmo fulfill partially redundant functions in growth and development (Figure 5-2).

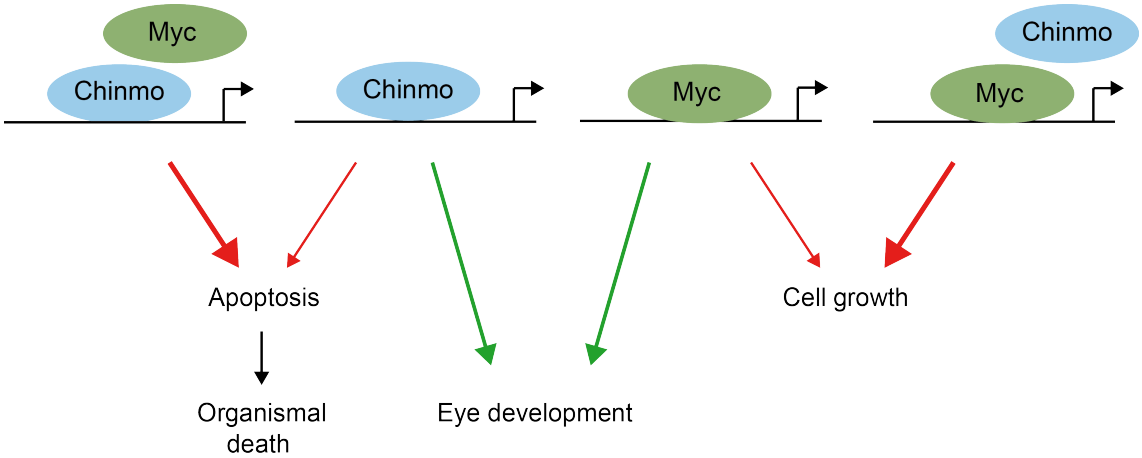

Figure 5-2: Model of genetic interactions between Myc and Chinmo

In the absence of Myc, Chinmo's ability to induce apoptosis is diminished, while Myc's ability to induce cell growth is partially dependent on Chinmo. In the process of eye development, Myc and Chinmo have an equally important function. Red arrows show overexpression of the depicted protein, whereas green arrows stand for endogenous expression.

5.2.2 Chinmo and Myc interact physically

The genetic data described above (5.2.1) suggest a close functional interaction between Myc and Chinmo. Therefore, the molecular basis of this interaction was investigated. Overexpression experiments by D. Schwinkendorf showed that Chinmo has no stabilizing effect upon Myc and no regulatory effect either (Schwinkendorf, 2008). Vice versa, the RNAseq data obtained from M. Stauch revealed that Myc does not transcriptionally regulate Chinmo (M. Stauch, pers. com.). On the other hand, Chinmo was shown to activate the transcription of a Myc-dependent luciferase reporter (*CG5033*) and to be important for the regulation of Myc target genes such as *fibrillarin* and *nnp1* (Schwinkendorf, 2008). These results led to the hypothesis that Chinmo might be a co-activator for Myc, necessary for its biological functions *in vivo*. A direct physical interac-

tion of Myc and Chinmo would support this hypothesis, and therefore Co-IPs with transiently transfected transgenes (AU1-Chinmo and HA-Myc) were performed. D. Schwinkendorf was able to show that HA-Myc is only immunoprecipitated in the presence of AU1-Chinmo. She also restricted the Chinmo binding site in Myc to the first 403 amino acids. To locate the Myc binding site within Chinmo, two mutants were established lacking either the zinc finger domain (Chinmo-ΔZf) or the BTB/POZ domain (Chinmo-ΔBTB) (Figure 4-13 A). Since ΔBTB was not detectable at all in Western blot experiments under different transfection conditions (Figure 4-13 B, it seems probable that the AU1-Chinmo-ΔBTB construct is unstable or not soluble and therefore no interaction was observed. For monitoring transfection efficiency more easily and eventually stabilize Chinmo-ΔBTB, all different Chinmo constructs were cloned behind GFP. And indeed, all GFP-Chinmo constructs were detectable in Western blot (Figure 4-13 C). A relative large fusion partner can change the N-terminal sequence of the protein and therefore lead to an increase in its yield and stability (Terpe, 2003). Another possibility why the GFP-Chinmo-ΔBTB was detected could be that addition of the large GFP-tag increased the solubility of the construct (Esposito and Chatterjee, 2006; Young *et al.,* 2012). However, all GFP-Chinmo constructs were able to co-precipitate Myc (Figure 4-13 D). The crude rabbit α-GST-Chinmo antibody also precipitates HA-Myc in the absence of any GFP-Chinmo construct, raising the possibility that HA-Myc was precipitated with the help of endogenous Chinmo.

Luciferase assays showed that not only GFP-Chinmo-ΔZf but also GFP-Chinmo-ΔBTB was able to transactivate the Myc dependent luciferase reporter (Figure 4-13 E), displaying that the fusion proteins retain their function. In comparison to luciferase experiments performed by D. Schwinkendorf, overexpression of any of the constructs was not sufficient to activate the reporter to the same extent as overexpression of Myc. Also co-expression of Chinmo and Myc did not lead to an increase in reporter activation in comparison to overexpression of Myc alone. It is possible that differences in the experimental setup (e.g. different time points, amount of used plasmids/ reagents) led to these differences. However, both setups were able to show that Chinmo is able to transactivate the Myc dependent luciferase reporter CG5033.

Considering the strong effect *chinmo*^{110} shows *in vivo,* it is surprising that the interaction between Myc and Chinmo is not impaired by the ΔZf-construct nor is Chinmo's ability to activate the Myc dependent luciferase reporter. Only one zinc finger is affected in the *chinmo*^{110} allele, leading to reduced eye size while loss of both zinc finger-domains has no effect in a Myc dependent reporter assay. One explanation for the strong genetic effect could be that the amino acid alteration from histidine (CAT) to tyrosine (TAT) at the first histidine of the first zinc finger somehow destabilizes the whole protein. Western blot analysis of protein lysates, obtained from *chinmo*^{110} homozygous heads, could reveal if Chinmo is stably expressed.

The direct physical interaction of Chinmo and Myc, which was obtained under overexpressed conditions, was also observed for an endogenous Co-IP performed with the rabbit α-Chinmo antibody (Figure 4-14 A). The co-precipitated Myc signal in the en-

dogenous Co-IP was rather weak but still indicates a physical interaction of the two proteins. The endogenous Co-IP was repeated once with exactly the same conditions, but failed. It remains open whether a higher amount of cells or changes in salt concentrations used for the IP could enhance the co-precipitation. It is also possible that the binding of Myc and Chinmo increases with enhanced expression levels, explaining the strong interaction upon overexpression versus the weak endogenous interaction. Another option could be that the complex is poorly soluble, which is overcome by addition of a tag (Terpe, 2003; Esposito and Chatterjee, 2006). Furthermore, the interaction of Myc and Chinmo might be indirect via other, still unknown factors.

5.2.3 **Chinmo directly activates Myc target genes**

To investigate whether Myc and Chinmo share common target genes, ChIP experiments were performed, using hoi-polloi and Nop5 as Myc positive targets and Pka-C1 as negative control (Figure 4-14 B). As expected, the ChIP performed with the mouse α-Myc antibody showed a higher enrichment over IgG for hoip and Nop5 than for Pka-C1. The very weak binding might be due to experimental problems, for example an old batch of antibody. In addition, the enrichment over IgG was often quite low, probably due to an unspecific background binding of the mouse-IgG (see also Table 4-4, mouse α-Myc). In contrast to Myc's poor binding behavior towards its target genes, Chinmo showed a strong enrichment over IgG for hoip and Nop5 and a weaker one for Pka-C1 (Figure 4-14 B). Since nothing is known about Chinmo's target genes it is possible that Pka-C1 is bound by Chinmo, too. The binding of Chinmo at hoip and Nop5 could either arise from a stable interaction of Chinmo and the respective gene, a high affinity of the antibody, or unspecific reactivity of the same. The specificity of the rabbit α-Chinmo antibody was never tested in ChIP before, because it is non-commercial and was produced by our own (immunoGlobe®; 4.2.2). To exclude unspecific binding of the antibody, ChIP was performed after Chinmo knockdown. The binding of all three genes was reduced after Chinmo depletion, but only by 30%-40% (Figure 4-14 C). It is possible that some binding persisted due to an incomplete knockdown of Chinmo (Figure 4-14 C'). Elongation of the incubation time with dsRNA, however, did not increase the knockdown efficiency. No differences in knockdown efficiency had been observed between 72 h and 120 h (compare Figure 4-13 D', Figure 4-14 C'). Besides the incomplete knockdown of Chinmo, it is very likely that the antibody features massive unspecific binding as it has been shown in several Western blots (Figure 4-13 D'; Figure 4-14 C'). Therefore the antibody should be purified further to reduce or even completely eliminate this background reactivity. Accordingly, Chinmo was cloned into a pMal-c5x vector (data not shown), which produces a maltose binding fusion protein upon induction in E.coli, and allows purification of the antibody via Amylose resins (Maina *et al.,* 1988; Park *et al.,* 1998). The purification still has to be performed. Nonetheless, the reduced binding after Chinmo depletion shows that at least some binding of Chinmo towards the shown genes was specific. To get a comprehensive list of Chinmo bound genes, ChIPseq should be performed. Considering the high background binding, the

antibody should be purified before and suitable controls should be included, for example knockdown control and non-immune IgGs. Chinmo not only binds to Myc target genes but has been shown to activate at least some of them, like *fibrillarin, nnp-1* and *CG12295* (Schwinkendorf, 2008). All of these genes are transcribed by RNA Pol II, contain an E-box and were shown to be Myc targets (Hulf *et al.,* 2005; Herter *et al.,* 2015). It is still open if Chinmo needs the presence of Myc for this activation. To investigate whether the activation of *nnp-1, fib* and *CG12295* is brought about by a physical recruitment of Chinmo, ChIP should be performed with these genes.

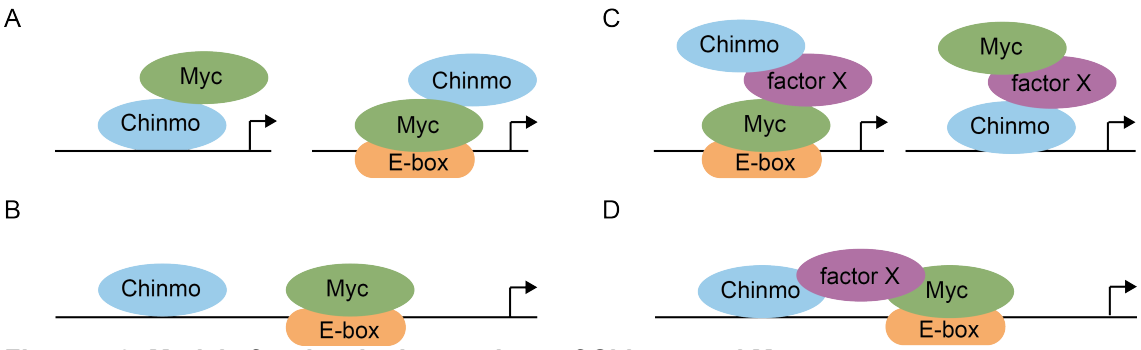

Figure 5-3: Model of molecular interactions of Chinmo and Myc

A. Myc and Chinmo bind each other directly at their target genes.
B. Chinmo and Myc individually bind to the same promoter region.
C. The interaction of Chinmo and Myc is achieved via a third, unknown protein (factor X).
D. Myc and Chinmo form a complex at the promoter region of their target genes, involving other and presently unknown proteins

The interaction of Chinmo and Myc is still not clear. Several possibilities of how they interact might be possible. One option would be that Myc and Chinmo directly interact with each other to activate common target genes (Figure 5-3 A). The existing data (exogenous and endogenous Co-IP) argue for this direct binding, yet it is possible that the interaction is mediated via third, still unknown factor (Figure 5-3 C). Independent of their binding, Myc and Chinmo could be recruited individually to the promoter region of the target gene for the correct expression (Figure 5-3 B). To investigate whether Chinmo and Myc are indeed concurrently bound to the same DNA sequences, Re-ChIP experiments should be performed. A last option could be that Chinmo and Myc interact in a complex including other, unknown proteins (Figure 5-3 D). Taken together, the molecular data obtained indicate for partially redundant functions of Chinmo and Myc in growth and development, but are still not sufficient to explain their exact way of interaction.

5.2.4 Myc is important for Chinmo's role in tumor induction

Already one century ago, C. Bridges and M. Stark suggested that *Drosophila* can develop tumors, based on their discovery of melanotic tumor-like granules in mutant larvae (Stark, 1917). Since then, several screens were performed to identify cancer related genes in flies, of which many have a mammalian homolog (Potter *et al.,* 2000). Studying the fly homologs of mammalian cancer genes has promoted the understand-

ing of the genetic pathways in which they act, and their role in developmental processes. Using the two yeast derived UAS/Gal4- and FLP/FRT-systems, R. Pagliarini and T. Xu (2003) tested several candidates in *Drosophila* eye discs, to search for tumors showing a metastatic behavior. They found that cooperation between the overexpressed oncogene Ras^{V12} and loss of genes affecting cell polarity, led to invasion, migration and secondary tumor formation (Pagliarini and Xu, 2003). While loss of *scribble* (*scrib*), *lethal giant larvae* (*lgl*) and *discs large* (*dlg*) caused metastatic behavior when combined with Ras^{V12} expression, loss of *large tumor suppressor* (*lats*) only resulted in tumor formation. Mutations of the tumor suppressor *lats* were shown before to cause massive overproliferation phenotypes (Xu *et al.,* 1995). In 2003, a study was published using the MARCM (mosaic analysis with repressible cell marker) system. In this study the authors showed that *scribble* mutant clones alone do not overgrow due to increased cell death, while co-activation of oncogenic Ras or Notch leads to neoplastic tumors (Brumby and Richardson, 2003). These authors stated that the tumor progression is dependent on the JNK pathway (Jun N-terminal kinase) and performed a comparative microarray to study the JNK-dependent transcriptional changes of Ras- and Notch-driven *scrib* tumors (Doggett *et al.,* 2010; Turkel *et al.,* 2013). The BTB/Zf domain containing protein family was highly enriched in their analysis, including Abrupt, Chinmo, Fruitless and Broad. Based on their results, we investigated whether ectopic activation of Ras and Chinmo leads to tumor formation. Indeed, overexpression of Chinmo and Ras led to the formation of massive tumors, while their individual overexpression had no effect (Figure 4-15 A, B). Activation of Chinmo alone even reduced the size of fluorescent tissue, what can be due to the apoptotic effect of Chinmo overexpression (Schwinkendorf, 2008). Activation of Ras alone led to a very weak increase in size of fluorescent tissue, which was not influenced by co-activation of Myc or loss of Chinmo. Co-activation of Chinmo and Myc also led to a slight increase, but considering the small number of tested animals (2) this effect has to be confirmed in further experiments. Some fluorescent tissue was observed outside the imaginal discs in "Ras^{V12} + Chinmo" animals (data not shown), which might have been metastasis. However it is quite likely that this was due to a misexpression of the eye-Gal4 driver, since the same observations were made with flies overexpressing only Ras. Consistent with data from R. Pagliarini and T. Xu (2003), this misexpression occurred mostly in the gonads. Since Myc plays such an important role in tumor formation in vertebrates and we have shown that Myc and Chinmo interact genetically and molecularly with each other, we wanted to know whether the "Ras^{V12} + Chinmo" tumors are dependent upon Myc. The tumorous tissue was significantly smaller for Myc hypomorphic as well as null mutant eye discs, revealing that Myc is important for this tumor induction (Figure 4-15 C). Interestingly the effect on the partial loss of Myc was bigger than for the complete loss. This difference might be negligible, considering the small sample size and the bigger fluctuations in the dm^4 animals. Therefore the experiment should be repeated with more individuals.

Regarding Myc's important role in the formation of "Ras^{V12} + Chinmo" tumors, a future goal should be to investigate whether Myc is generally required for all types of tumors

or if Myc's requirement is specific for the "Ras^{V12} + Chinmo" tumors. Therefore, Ras- and Notch-driven *scrib* tumors should be examined as well as additional genes known to be involved in tumorigenesis, for example genes involved in the JNK pathway.

References

1. Adhikary S, Eilers M: **Transcriptional regulation and transformation by Myc proteins.** *Nature Reviews Molecular Cell Bioogyl* 2005, **6**: 635-645.

2. Amati B, Dalton S, Brooks MW, Littlewood TD, Evan GI, Land H: **Transcriptional activation by the human c-Myc oncoprotein in yeast requires interaction with Max**. *Nature* 1992, **359**: 423-426.

3. Arabi A, Wu S, Ridderstrale K. Bierhoff H, Shiue C, Fatyol K, Fahlèn S, Hydbring P, Söderberg O, Grummt I, *et al.*: **c-Myc associates with ribosomal DNA and activates RNA polymerase I transcription**. *Nature Cell Biology* 2005, **7**: 303-310.

4. Atchley WR, Fitch WM: **Myc and Max: Molecular evolution of a family of proto-oncogene products and their dimerization partner**. *PNAS* 1995, **92**: 10217-10221.

5. Ayer DE, Kretzner L, Eisenman RN: **Mad: a heterodimeric partner for Max that antagonizes Myc transcriptional activity.** *Cell* 1993, **72**: 211-222.

6. Bachellerie JP, Michot B, Nicoloso M, Balakin A, Ni J, Fournier MJ: **Antisense snoRNAs: a family of nucleolar RNAs with long complementarities to RNA.** *Trends in Biochemical Science* 1995, **20**: 261-264.

7. Bachellerie JP, Cavaillé J, Hüttenhofer A: **The expanding snoRNA world.** *Biochimie* 2002, **84**: 775-790.

8. Bardwell VJ, Treisman R**: The POZ domain: A conserved protein-protein interaction motif.** *Genes & Development* 1994, **8**: 1664-1677.

9. Bellosta P, Hulf T, Balla Diop S, Usseglio F, Pradel J, Aragnol D, Gallant P: **Myc interacts genetically with Tip48/Reptin and Tip49/Pontin to control growth and proliferation during *Drosophila* development.** *PNAS* 2005, **102**: 11799-11804.

10. Benassayag C, Montero L, Colombie N, Gallant P, Cribbs D, Morello D: **Human c-Myc isoforms differentially regulate cell growth and apoptosis in *Drosophila* melanogaster.** *Molecular and Cellular Biology* 2005, **25**: 9897-9909.

11. Betschinger J, Mechtler K, Knoblich JA: **Asymmetric Segregation of the Tumor Suppressor Brat Regulates Self-Renewal in *Drosophila* Neural Stem Cells.** *Cell* 2006, **124**: 1241-1253.

12. Blackwell TK, Huang J, Ma A, Kretzner L, Alt FW, Eisenman RN, Weintraub H: **Binding of myc proteins to canonical and noncanonical DNA sequences.** *Molecular and Cellular Biology* 1993, **13**: 5216-5224.

13. Blackwell TK, Kretzner L, Blackwood EM, Eisenman RN, Weintraub H: **Sequence-specific DNA binding by the c-Myc protein.** *Science* 1990, **250**: 1149-1151.

14. Blackwood EM, Eisenman RN: **Max: a helix-loop-helix zipper protein that forms a sequence-specific DNA-binding complex with Myc.** *Science* 1991, **251**: 1211-1217.

15. Böhni R, Riesgo-Escova J, Oldham S, Brogiolo W, Stocker H, Andruss BF, Beckingham K, Hafen E: **Autonomous Control of Cell and Organ Size by CHICO, a *Drosophila* Homolog of Vertebrate IRS1–4.** *Cell* 1999**, 97**: 865-875.

16. Bonke M, Turunen M, Sokolova M, Vähärautio A, Kivioja T, Taipale M, Björklund M, Taipale J: **Transcriptional networks controlling the cell cycle.** *Genes/ Genomes/ Genetics* 2013, **3**: 75-90.

17. Boon K, Huib NC, van Asperen R, Valentijn L, Hermus MC, van Sluis P, Roobeek I, Weis I, Voûte PA, Schwab M, Versteeg R: **N-myc enhances the expression of a large set of genes functioning in ribosome biogenesis and protein synthesis**. *EMBO J.* 2001, **20**: 1383-1393

18. Bortolin ML, Ganot P, Kiss T: **Elements essential for accumulation and function of small nucleolar RNAs directing site-specific pseudouridylation of ribosomal RNAs.** *EMBO J.* 1999, **18**: 457-469.

19. Bouchard C, Marquardt J, Bras A, Medema RH, Eilers M: **Myc-induced proliferation and transformation require Akt-mediated phosphorylation of FoxO proteins.** *EMBO J.* 2004, **23**: 2830-2840.

20. Bradford MM: **A rapid and sensitive method for the quantitation of microgram quantities of protein utilizing the principle of protein-dye binding.** *Analytical Biochemistry* 1976, **72**: 248-254.

21. Bridges CB: *Drosophila* melanogaster**: Legend for symbols, mutants, valuations.** *Drosophila Information Service* 1935, **3**: 5-19.

22. Brogiolo W, Stocker H, Ikeya T, Rintelen F, Fernandez R, Hafen E: **An evolutionarily conserved function of the *Drosophila* insulin receptor and insulin-like peptides in growth control.** *Current Biology* 2001, **11**: 213-221.

23. Brumby AM, Richardson HE: ***scribble* mutants cooperate with oncogenic Ras or Notch to cause neoplastic overgrowth in *Drosophila.*** *EMBO J*. 2003, **22**: 5769-5779.

24. Cavaillé J, Buiting K, Kiefmann M, Lalande M, Brannan CI, Horsthemke B, Bachellerie JP, Brosius J, Hüttenhofer A: **Identification of brain-specific and imprinted small nucleolar RNA genes exhibiting an unusual genomic organization.** *PNAS* 2000, **97**: 14311-14316

25. Chang LS, Lin SY, Lieu AS, Wu TL: **Differential expression of human 5S snoRNA genes.** *Biochemical and Biophysical Research Communications* 2002, **299**: 196-200.

26. Chen X, Xu H, Yuan P, Fang F, Huss M, Vega VB, Wong E, Orlov YL, Zhang W, Jiang J, *et al.*: **Integration of external signaling pathways with the core transcriptional network in embryonic Stem cells.** *Cell* 2008, **133**: 1106-1117.

27. Clouet d'Orval B, Bortolin ML, Gaspin C, Bachellerie JP: **Box C/D RNA guides for the ribose methylation of archaeal tRNAs. The tRNATrp intron guides the formation of two ribose-methylated nucleosides in the mature tRNATrp.** *Nucleic Acids Research* 2001, **29**: 4518-4529.

28. Coller HA, Grandori C, Tamayo P, Colbert T, Lander ES, Eisenman RN, Golub TR: **Expression analysis with oligonucleotide microarrays reveals that MYC regulates genes involved in growth, cell cycle, signaling, and adhesion.** *PNAS* 2000, **97**: 3260-3265.

29. Cowling VH, Chandriani S, Whitfield ML, Cole MD: **A conserved Myc protein domain, MBIV, regulates DNA binding, apoptosis, transformation, and G2 arrest.** *Molecular and Cellular Biology* 2006, **26**: 4226-4239.

30. Dang CV, Lee WM: **Identification of the human c-myc protein nuclear translocation signal.** *Molecular and Celularl Biology* 1988, **8**: 4048-4054.

31. Dang CV, O'Donnell KA, Zeller KI, Nguyen T, Osthus RC, Li F: **The c-Myc target gene network.** *Seminars in cancer biology* 2006*,* **16:** 253-264.

32. de la Cova C, Abril M, Bellosta P, Gallant P, Johnston LA: ***Drosophila* myc regulates organ size by inducing cell competition.** *Cell* 2004, **117**: 107-116.

33. de Virgilio C, Loewith R: **The TOR signaling network from yeast to man**. *IJBCB* 2006, **38**: 1476-1481.

34. Dieci G, Preti M, Montanini B: **Eukaryotic snoRNAs: a paradigm for gene expression flexibility.** *Genomics* 2009, **94**: 83-8.

35. Doe C Q: **Chinmo and neuroblast temporal identity**. *Cell* 2006, **127**: 254-256.

36. Doggett K, Turkel N, Richardson H, Brumby A: **The role of BTB zinc-finger containing proteins in regulating *Drosophila* neoplastic tumours.** *51st Annual Drosophila Research Conference* 2010, Talk 96

37. Dong XY, Rodriguez C, Guo P, Sun X, Talbot JT, Zhou W, Petros J, Li Q, Vessella RL, Kibel AS, *et al*: **SnoRNA U50 is a candidate tumor-suppressor gene at 6q14.3 with a mutation associated with clinically significant prostate cancer.** *Human Molecular Genetics* 2008, **17**: 1031-1042.

38. Dong XY, Guo P, Boyd J, Sun X, Li Q, Zhou W, Dong JT**: Implication of snoRNA U50 in human breast cancer.** *Journal of Genetics and Genomics* 2009, **36**: 447-454.

39. Dong ZW, Shao P, Diao LT, Zhou H, Yu CH, Qu LH: RTL-P: **a sensitive approach for detecting sites of 2'-O-methylation in RNA molecules.** *Nucleic Acids Research* 2012, **40**: e157.

40. Eberhardy SR, Farnham PJ: **c-Myc mediates activation of the cad promoter via a post-RNA polymerase II recruitment mechanism.** *The Journal of biological chemistry* 2001, **276**: 48562-48571.

41. Edgar BA: **How flies get their size: genetics meets physiology.** *Nature Reviews Genetics* 2006, **7**: 907-916.

42. Ender C, Krek A, Friedlander MR, Beitzinger M, Weinmann L, Chen W, Pfeffer S, Rajewsky N, Meister G: **A human snoRNA with microRNA-like functions.** *Molecular Cell* 2008, **32**: 519-528.

43. Esposito D, Chatterjee DK: **Enhancement of soluble protein expression through the use of fusion tags.** *Current Opinion in Biotechnology* 2006, **17**: 353-358.

44. Evan GI, Wyllie AH, Gilbert CS, Littlewood TD, Land H, Brooks M, Waters CM, Penn LZ, Hancock DC: **Induction of apoptosis in fibroblasts by c-myc protein.** *Cell* 1992, **69**: 119-128.

45. Flaherty MS, Salis P, Evans CJ, Ekas LA, Marouf A, Zavadil J, Banerjee U, Bach EA: **Chinmo is a functional effector of the JAK/STAT pathway that regulates eye development, tumor formation, and stem cell self-renewal in *Drosophila*.** *Developmental Cell* 2010, **18**: 556- 568.

46. Freytag SO, Dang CV, Lee WM: **Definition of the activities and properties of c-myc required to inhibit cell differentiation.** *Cell growth & differentiation* 1990, **1**: 39-343.

47. Friedrich JK, Panov KI, Cabert P, Russel J, Zomerdijk JCMB: **TBP-TAF complex SL1 directs RNA polymerase I pre-initiation complex formation and stabilizes upstream binding factor at the rDNA promoter.** *The Journal of biological chemistry* 2005, **280**: 29551-29558.

48. Fu L, Pelicano H, Liu J, Huang P, Chi Lee C: **The circadian gene Period2 plays an important role in tumor suppression and DNA damage response in vivo.** *Cell* 2002, **111**: 41-50.

49. Furrer M, Balbi M, Albarca-Aguilera M, Gallant M, Herr W, Gallant P: ***Drosophila* Myc interacts with host cell factor (dHCF) to activate transcription and control growth.** *The Journal of biological chemistry* 2010, **285**: 39623-39636.

50. Gallant P, Shiio Y, Cheng PF, Parkhurst SM, Eisenman RN: **Myc and Max Homologs in *Drosophila*.** *Science* 1996, **274**: 1523-1527.

51. Gallant P: **Myc/ Max/ Mad in invertebrates: The evolution of the Max Network.** *Current Topics in Microbiology and Immunology* 2006, **302**: 235-253.

52. Gallant P: ***Drosophila* Myc.** *Advances in Cancer Research* 2009, **103**: 111-44.

53. Ganot P, Bortolin ML, Kiss T: **Site-specific pseudouridine formation in preribosomal RNA is guided by small nucleolar RNAs.** *Cell* 1997a, **89**: 799-809.

54. Ganot P, Caizergues-Ferrer M, Kiss T: **The family of box ACA small nucleolar RNAs is defined by an evolutionarily conserved secondary structure and ubiquitous sequence elements essential for RNA accumulation.** *Genes & Development* 1997b, **11**: 941–956.

55. Gartel AL, Ye X, Goufman E, Shianov P, Hay N, Najmabadi F, Tyner AL: **Myc represses the p21(WAF1/CIP1) promoter and interacts with Sp1/Sp3.** *PNAS* 2001, **98**: 4510-4515.

56. Gee HE, Buffa FM, Camps C, Ramachandran A, Leek R, Taylor M, Patil M, Sheldon H, Betts G, Homer J, *et al*.: **The small-nucleolar RNAs commonly used for microRNA normalisation correlate with tumour pathology and prognosis.** *British Journal of cancer* 2011, **104**: 1168-1177.

57. Gomez-Roman N, Grandori C, Eisenman RN, White RJ: **Direct activation of RNA polymerase III transcription by c-Myc.** *Nature* 2003, **421:** 290-294.

58. Grandori C, Gomez-Roman N, Felton-Edkins ZA, Ngouenet C, Galloway DA, Eisenman RN, White RJ: **c-Myc binds to human ribosomal DNA and stimulates transcription of rRNA genes by RNA polymerase I.** *Nature Cell Biology* 2005, **7**: 311-318.

59. Gregio APB, Cano VPS, Avaca JS, Valentini SR, Zanelli CF: **eIF5A has a function in the elongation step of translation in yeast.** *Biochemical and Biophysical Research Communications* 2009, **380**: 785-790.

60. Grewal SS, Li L, Orian A, Eisenman RN, Edgar BA: **Myc-dependent regulation of ribosomal RNA synthesis during *Drosophila* development.** *Nature Cell Biology* 2005, **7**: 295-302.

61. Grewal SS, Li L, Evans JR, Edgar BA: ***Drosophila* TIF-IA is required for ribosome synthesis and cell growth and is regulated by the TOR pathway**. *Journal of Cell Biology* 2007, **179**: 1105-1113.

62. Guccione E, Martinato F, Finocchiaro G, Luzi L, Tizzoni L, Dall' Olio V, Zardo G, Nervi C, Bernard L, Amati B: **Myc-binding-site recognition in the human genome is determined by chromatin context.** *Nature Cell Biology* 2006, **8**: 764-770.

63. Henras A, Henry Y, Bousquet-Antonelli C, Noaillac-Depeyre J, Gelugne JP, Caizergues-Ferrer M: **Nhp2p and Nop10p are essential for the function of H/ACA snoRNPs.** *EMBO J.* 1998, **17**: 7078-7090.

64. Herbst A, Hemann MT, Tworkowski KA, Salghetti SE, Lowe SW, Tansey WP: **A conserved element in Myc that negatively regulates its proapoptotic activity**. *EMBO Rep* 2005, **6**: 177-183.

65. Herold S, Wanzel M, Beuger V, Frohme C, Beul D, Hillukkala T, Syvaoja J, Saluz HP, Haenel F, Eilers M: **Negative regulation of the mammalian UV response by Myc through association with Miz-1.** *Molecular Cell* 2002, **10:** 509-521

66. Herter EK, Stauch M, Gallant M, Wolf E, Raabe T, Gallant P: **snoRNAs are a novel class of biologically relevant Myc targets.** *BMC Biology* 2015, **13**: 1-17

67. Hirose F, Yamaguchi M, Handa H, Inomata Y, Matsukage A: **Novel 8-base pair sequence (*Drosophila* DNA replication-related element) and specific binding factor involved in the expression of *Drosophila* genes for DNA polymerase alpha and proliferating cell nuclear antigen.** *The Journal of biological chemistry* 1993, **268**: 2092-2099.

68. Hirose F, Ohshima N, Shiraki M, Inoue YH, Taguchi O, Nishi Y, Matsukage A, Yamaguchi M: **Ectopic expression of DREF induces DNA synthesis, apoptosis, and unusual morphogenesis in the *Drosophila* eye imaginal disc: Possible interaction with Polycomb and trithorax group proteins.** *Molecular Cell Biology* 2001, **21**: 7231-7242.

69. Huang ZP, Zhou H, He HL, Chen CL, Liang D, Qu LH: **Genome-wide analyses of two families of snoRNA genes from *Drosophila melanogaster*, demonstrating the extensive utilization of introns for coding of snoRNAs.** *RNA* 2005, **11**: 1303-1316.

70. Hughes ME, Grant GR, Paquin C, Qian J, Nitabach MN: **Deep sequencing the circadian and diurnal transcriptome of *Drosophila* brain.** *Genome Research* 2012, **22**: 1266-1281.

71. Hüttenhofer A, Kiefmann M, Meier-Ewert S, O'Brien J, Lehrach H, Bachellerie JP, Brosius J: **RNomics: an experimental approach that identifies 201 candidates for novel, small, non-messenger RNAs in mouse.** *EMBO J.* 2001, **20**: 2943-2953.

72. Hulf T, Bellosta P, Furrer M, Steiger D, Svensson D, Barbour A, Gallant P: **Whole-genome analysis reveals a strong positional bias of conserved dMyc-dependent E-boxes.** *Molecular Cell Biology* 2005, **25**: 3401-3410.

73. Hurlin PJ, Queva C, Eisenman RN: **Mnt: a novel Max-interacting protein and Myc antagonist.** *Current Topics in Microbiology & Immunology* 1997, **224**: 115-121.

74. Hurlin PJ, Queva C, Koskinen PJ, Steingrimsson E, Ayer DE, Copeland NG, Jenkins NA, Eisenman RN: **Mad3 and Mad4: novel Max-interacting transcriptional repressors that suppress c-myc dependent transformation and are expressed during neural and epidermal differentiation.** *EMBO J.* 1995, **14**: 5646-5659.

75. Hurlin PJ, Steingrimsson E, Copeland NG, Jenkins NA, Eisenman RN: **Mga, a dual-specificity transcription factor that interacts with Max and contains a T-domain DNA-binding motif.** *EMBO J*. 1999, **18**: 7019-7028.

76. Ingvarsson S, Asker C, Axelson H, Klein G, Sumegi J: **Structure and expression of B-myc, a new member of the myc gene family.** *Molecular Cell Biology* 1988, **8**: 3168-3174.

77. Iritani B, Eisenman R: **c-Myc enhances protein synthesis and cell size during B lymphocyte development.** *PNAS* 1999, **96**: 13180-13185.

78. Isaac C, Yang Y, Meier UT: **Nopp140 functions as a molecular link between the nucleolous and the coiled bodies.** *The Journal of Cell Biology* 1998, **142**: 319-329.

79. Jacinto E, Hall MN: **TOR signaling in bugs, brain and brawn.** *Nature Reviwes Molecular Cell Biology* 2003, **4**: 117-126.

80. Johnston LA, Prober DA, Edgar BA, Eisenman RN, Gallant P: ***Drosophila* myc regulates cellular growth during development.** *Cell* 1999, **98**: 779-7904

81. Jouffe C, Cretenet G, Symul L, Martin E , Atger F, Naef F, Gachon F: **The Circadian Clock Coordinates Ribosome Biogenesis.** *PLoS Biology* 2013, **11**: e1001455.

82. Jünger MA, Rintelen F, Stocker H, Wasserman JD, Végh M, Radimerski T, Greenberg ME, Hafen E: **The *Drosophila* Forkhead transcription factor FOXO mediates the reduction in cell number associated with reduced insulin signaling.** *Journal of Biology* 2001, **2**: 20.

83. King TH, Decateur WA, Bertrand E, Maxwell ES, Fournier M: **A Well-Connected and Conserved Nucleoplasmic Helicase Is Required for Production of Box C/D and H/ACA snoRNAs and Localization of snoRNP Proteins.** *Molecular and Cellular Biology* 2001, **21**: 7731-7746.

84. Kiss-László Z, Henry Y, Kiss T: **Sequence and structural elements of methylation guide snoRNAs essential for site-specific ribose methylation of pre-RNA**. *EMBO J.* 1998, **17**: 797-807.

85. Kiss T: **Small nucleolar RNA-guided post-transcriptional modification of cellular RNAs**. *EMBO J.* 2001, **20**: 3617-3622.

86. Kockel L, Kerr KS, Melnick M, Brückner K, Hebrok M, Perrimon N: **Dynamic switch of negative feedback regulation in *Drosophila* Akt-TOR signaling.** *PLoS Genetics* 2010, **6**: e1000990.

87. Kohl NE, Kanda N, Schreck RR, Bruns G, Latt SA, Gilbert F, Alt FW: **Transposition and amplification of oncogene-related sequences in human neuroblastomas.** *Cell* 1983, **35**: 359-367.

88. Laemmli UK: **Cleavage of structural proteins during the assembly of the head of bacteriophage T4**. *Nature* 1970, **227**: 680-685.

89. Lafontaine DL, Tollervey D: **Nop58p is a common component of the box C + D snoRNPs that is required for snoRNA stability**. *RNA* 1999, **5**: 455-467.

90. Lee T, Lee A, Luo L: **Development of the *Drosophila* mushroom bodies: sequential generation of three distinct types of neurons from a neuroblast**. *Development* 1999, **126**: 4065-4076.

91. Lee KK, Workman JL: **Histone acetyltransferase complexes: one size doesn't fit all.** *Nature Reviews Molecular Cell Biology* 2007, **8**: 284-295.

92. Lee BK, Bhinge AA, Battenhouse A, McDaniell RM, Liu Z, Song L, Ni Y, Birney E, Lieb JD, Furey TS, Crawford GE, Iyer VR**: Cell-type specific and combinatorial usage of diverse transcription factors revealed by genome-wide binding studies in multiple human cells.** *Genome research* 2012, **22**: 9-24.

93. Lempiäinen H, Shore D: **Growth control and ribosome biogenesis.** *Current Opinion in Cell Biology* 2009, **21**: 855-63.

94. Li Z, van Calcar S, Qu C, Cavenee WK, Zhang MQ, Ren B: **A global transcriptional regulatory role for c-Myc in Burkitt's lymphoma cells.** *PNAS* 2003**, 100**: 8164-8169.

95. Li T, Zhou X, Wang X, Zhu D, Zhang Y: **Identification and characterization of human snoRNA core promoters.** *Genomics* 2010, **96**: 50–56.

96. Liao J, Yu L, Mei Y, Guarnera M, Shen J, Li R, Liu Z, Jiang F: **Small nucleolar RNA signatures as biomarkers for non-small-cell lung cancer.** *Molecular Cancer* 2010, **9**: 198-208.

97. Lin CY, Loven J, Rahl PB, Paranal RM, Burge CB, Bradner JE, Lee TI, Young RA: **Transcriptional amplification in tumor cells with elevated c-Myc.** *Cell* 2012, **151**: 56–67.

98. Loewith R: **TORC1 signaling in budding yeast.** The Enzymes: Structure, Function and Regulation of TOR complexes from Yeasts to mammals, Part1 2010, **Chapter 9**: 147-175.

99. Loo LW, Secombe J, Little JT, Carlos LS, Yost C, Cheng PF, Flynn EM, Edgar BA, Eisenman RN: **The transcriptional repressor dMnt is a regulator of growth in *Drosophila melanogaster*.** *Molecular Cell Biology* 2005, **25**: 7078-7091.

100. Lüscher B, Vervoorts J: **Regulation of gene transcription by the oncoprotein MYC.** *Gene* 2012, **494**: 145-160.

101. Ma Q, Wawersik M, Matunis EL: **The Jak-STAT target Chinmo prevents sex transformation of adult stem cells in the *Drosophila* testis niche.** *Developmental Cell* 2014, **31**: 474-486.

102. Machanick P, Bailey TL: **MEME-ChIP: motif analysis of large DNA datasets.** *Bioinformatics* 2011, **27**: 1696–1697. http://meme.nbcr.net/meme/.

103. Maden BE: **Mapping 2'-O-methyl groups in ribosomal RNA.** *Methods* 2001, **25**: 374-382.

104. Maina CV, Riggs PD, Grandea AG, Slatko BE, Moran LS, Tagliamonte JA, McReynolds LA, di Guan C: **An *Escherichia coli* vector to express and purify foreign proteins by fusion to and separation from maltose-binding protein.** *Gene* 1988, **74**: 365-373.

105. Mannoor K, Liao J, Jiang F: **Small nucleolar RNAs in cancer.** *Biochimica et Biophysica Acta* 2012, **1826**: 121-128.

106. Martens-Uzunova ES, Jalava SE, Dits NF, van Leenders GJLH, Moller S, Trapman J, Bangma CH, T Litman T, Visakorpi T, Jenster G: **Diagnostic and prognostic signatures from the small non-coding RNA transcriptome in prostate cancer.** *Oncogene* 2012, **31**: 978-991.

107. Martens-Uzunova ES, Olvedy M, Jenster G: **Beyond microRNA-Novel RNAs derived from small non-coding RNA and their implication in cancer**. *Cancer letters* 2013, **340**: 201-211.

108. Martín FA, Herrera SC, Morata G: **Cell competition, growth and size control in the *Drosophila* wing imaginal disc.** *Development* 2009, **136**: 3747-3756.

109. Marygold SJ, Roote J, Reuter G, Lambertsson A, Ashburner M, Millburn GH, Harrison PM, Yu Z, Kenmochi N, Kaufman TC, *et al*.: **The ribosomal protein genes and *Minute* loci of *Drosophila melanogaster.*** *Genome Biology* 2007, **8**: R216.

110. McMahon SB, Wood MA, Cole MD: **The essential cofactor TRRAP recruits the histone acetyltransferase hGCN5 to c-Myc.** *Molecular and cellular biology* 2000, **20**: 556-562.

111. Mei YP, Liao JP, Shen J, Yu L, Liu BL, Liu L, Li RY, Ji L, Dorsey SG, Jiang ZR, et al: **Small nucleolar RNA 42 acts as an oncogene in lung tumorigenesis.** *Oncogene* 2012, **31:** 2794-2804.

112. Menegazzi P: **Discussion in person.** Institute of Neurobiology and Genetics 2014.

113. Meyer N, Penn LZ: **Reflecting on 25 years with MYC.** *Nature Reviews Cancer* 2008, **8**: 976-990.

114. Mikhaylova LM, Boutanaev AM, Nurminsky DI: **Transcriptional regulation by Modulo integrates meiosis and spermatid differentiation in male germ line**. *PNAS* 2006, **103**: 11975-11980.

115. Morata G, Ripoll P: Minutes: **Mutants of *Drosophila* autonomously affecting cell division rate.** *Developmental Biology* 1975, **42**: 211-221.

116. Motorin Y, Muller S, Behm-Ansmant I, Branlant C: **Identification of modified residues in RNAs by reverse transcription-based methods.** *Methods in Enzymology* 2007, **425**: 21-53.

117. Müller J, Samans B, van Riggelen J, Fagà G, Peh KNR, Wei CL, Müller H, Amati B, Felsher D, Eilers M: **TGFβ-dependent gene expression shows that senescence correlates with abortive differentiation along several lineages in Myc-induced lymphomas.** *Cell Cycle* 2010, **9**: 4622-4626.

118. Mullis K, Faloona F, Scharf S, Saiki R, Horn G, Erlich H: **Specific enzymatic amplification of DNA in vitro: the polymerase chain reaction.** *CSH Symposia on Quantitative Biology* 1986, **24**: 17-27.

119. Nau MM, Brooks BJ, Battey J, Sausville E, Gazdar AF, Kirsch IR, McBride OW, Bertness V, Hollis GF, Minna JD: **L-myc, a new myc-related gene amplified and expressed in human small cell lung cancer.** *Nature* 1985, **318**: 69-73.

120. Neumüller RA, Richter C, Fischer A, Novatchkova M, Neumüller KG, Knoblich JA: **Genome-wide analysis of self-renewal in *Drosophila* neural stem cells by transgenic RNAi.** *Cell Stem Cell* 2011; **8**: 580-593.

121. Neumüller RA, Gross T, Samsonova AA, Vinayagam A, Buckner M, Founk K, Hu Y, Sharifpoor S, Rosebrock AP, Andrews B, Winston F, Perrimon N: **Conserved Regulators of Nucleolar Size Revealed by Global Phenotypic Analyses.** *Science Signaling* 2013, **6**: ra70.

122. Newsome TP, Asling B, Dickson BJ: **Analsyis of *Drosophila* photoreceptor axon guidance in eye-specific mosaics.** *Development* 2000, **127**: 851-860.

123. Nie Z, Hu G, Wei G, Cui K, Yamane A, Resch W, Wang R, Green DR, Tessarollo L, Casellas R *et al.*: **c-Myc is a universal amplifier of expressed genes in lymphocytes and embryonic stem cells.** *Cell* 2012, **151**: 68-79.

124. Nilsen T: **RNA sequencing by primer extension.** *CSH Protocols* 2013, **12**: 1182-1185.

125. Oldham S, Montagne J, Radimerski T, Thomas G, Hafen E: **Genetic and biochemical characterization of dTOR, the *Drosophila* homolog of the target of rapamycin.** *Genes & Development* 2000, **14**: 2689-2694.

126. Orian A, van Steensel B, Delrow J, Bussemaker HJ, Li L, Sawado T, Williams E, Loo LW, Cowley SM, Yost C, *et al.*: **Genomic binding by the *Drosophila* Myc, Max, Mad/Mnt transcription factor network**. *Genes & Development* 2003, **17**: 1101-1114.

127. Parisi F, Riccardo S, Daniel M, Saqcena M, Kundu N, Pession A, Grifoni D, Stocker H, Tabak E, Bellosta P: ***Drosophila* insulin and target of rapamycin (TOR) pathways regulate GSK-3b activity to control Myc stability and determine Myc expression in vivo.** *BMC Biology* 2011, **9**: 65.

128. Park JH, Choi EA, Cho EW, Hahm KS, Kim KL: **Maltose binding protein (MBP) fusion proteins with low or no affinity to amylose resins can be single-step purified using a novel anti-MBP monoclonal antibody.** *Molecular Cell* 1998, 8: 709-716.

129. Pagliarini RA, Xu T: **A genetic screen in *Drosophila* for metastatic behavior.** *Science* 2003, **302**: 1227-1231.

130. Panov K, Friedrich J, Russel J, Zomerdijk JCMB: **UBF activates RNA polymerase I transcription by stimulating promoter escape.** *EMBO J.* 2006, **25**: 3310-3322.

131. Perrin L, Benassayag C, Morello D, Pradel J, Montagne J: **Modulo is a target of Myc selectively required for growth of proliferative cells in *Drosophila*.** *Mechanisms of Development* 2003, **120**: 645-655.

132. Peukert K, Staller P, Schneider A, Carmichael G, Hanel F, Eilers M: **An alternative pathway for gene regulation by Myc.** *The EMBO journal* 1997, **16:** 5672-5686.

133. Pierce SB, Yost C, Britton JS, Loo LW, Flynn EM, Edgar BA, Eisenman RN**: dMyc is required for larval growth and endoreplication in *Drosophila*.** *Development* 2004, **131**: 2317-2327.

134. Poortinga G, Hannan KM, Snelling H, Walkley CR, Jenkins A, Sharkey K , Wall M, Brandenburger Y, Palatsides M, B Pearson RB, *et al.*: **MaD1 and c-MYC regulate UBF and rDNA transcription during granulocyte differentiation.** *EMBO J.* 2004, **23**: 3325-3335.

135. Potter CJ, Turenchalk GS, Xu T: ***Drosophila* in cancer research: an expanding role**. *TRENDS in Genetics* 2000, **16**: 33-39.

136. Prendergast GC, Lawe D, Ziff EB: **Association of Myn, the murine homolog of Max, with c-Myc stimulates methylation-sensitive DNA binding and ras cotransformation.** *Cell* 1991, **65**: 395-407.

137. Puig O, Tjian R: **Nutrient availability and growth. Regulation of insulin signaling by dFOXO/FOXO1.** *Cell Cycle* 2006, **5**: 503-505.

138. Raha D, Wang Z, Moqtaderi Z, Wu L, Zhong G, Gerstein M, Struhl K, Snyder M: **Close association of RNA polymerase II and many transcription factors with Pol III genes.** *PNAS* 2010, **107**: 3639-3644.

139. Rahl PB, Lin CY, Seila AC, Flynn RA, McCuine S, Burge CB, Sharp PA, Young RA: **c-Myc regulates transcriptional pause release.** *Cell* 2010, **141:** 432-445.

140. Razin SV, Borunova VV, Maksimenko OG, Kantidze OL: **Cys_2His_2 zinc finger protein family: Classification, functions, and major members.** *Biochemistry (Moscow)* 2012, **77**: 217-226.

141. Reichow SL, Hamma T, Ferre-D'Amare AR, Varani G: **The structure and function of small nucleolar ribonucleoproteins.** *Nucleic Acids Research* 2007, **35**: 1452-1464.

142. Roeder RG, Rutter WJ: **Specific nucleolar and nucleoplasmic RNA Polymerases.** *PNAS* 1970, **65**: 675-682.

143. Sabo A, Kress TR, Pelizzola M, de Pretis S, Gorski MM, Tesi A, Morelli MJ, Bora P, Doni M, Verrecchia A *et al.*: **Selective transcriptional regulation by Myc in cellular growth control and lymphomagenesis.** *Nature* 2014, **511**: 488-92.

144. Saini P, Eyler DE, Green R, Dever TE: **Hypusine-containing protein eIF5A promotes translation elongation.** *Nature* 2009, **459**: 118-121.

145. Salih DAM, Brunet A: **FoxO transcription factors in the maintenance of cellular homeostasis during aging.** *Current Opinion in Cell Biology* 2008, **20**: 126-136.

146. Schmidt EV: **The role of c-myc in regulation of translation initiation**. *Oncogene* 2004, **23**: 3217-3221.

147. Schramm A, Koster J, Marschall T, Martin M, Schwermer M, Fielitz K, Buchel G, Barann M, Esser D, Rosenstiel P, *et al.*: **Next-generation RNA sequencing reveals differential expression of MYCN target genes and suggests the mTOR pathway as a promising therapy target in MYCN-amplified neuroblastoma.** *International journal of cancer* 2013, **132**: 7-11.

148. Schreiber-Agus N, Stein D, Chen K, Goltz JS, Stevens L, DePinho RA: ***Drosophila* Myc is oncogenic in mammalian cells and plays a role in the diminutive phenotype.** *PNAS* 1997, 94: 1235-1240.

149. Schuhmacher M, Kohlhuber F, Holzel M, Kaiser C, Burtscher H, Jarsch M, Bornkamm GW, Laux G, Polack A, Weidle UH, Eick D: **The transcriptional program of a human B cell line in response to Myc.** *Nucleic acids research* 2001, **29:** 397-406.

150. Schwinkendorf D: **Mutational Identification of *cis*- and *trans*-acting Determinants of dMyc Protein Function.** Zürich, Universität Zürich, *Ph.D. thesis*, 2008.

151. Sears R, Nuckolls F, Haura E, Taya Y, Tamai K, Nevins JR: **Multiple Ras-dependent phosphorylation pathways regulate Myc protein stability.** *Genes & development 2000,* **14:** 2501-2514.

152. Seitz V, Butzhammer P, Hirsch B, Hecht J, Gutgemann I, Ehlers A, Lenze D, Oker E, Sommerfeld A, von der Wall *E et al.*: **Deep sequencing of MYC DNA-binding sites in Burkitt lymphoma.** *PloS one* 2011, **6:** e26837.

153. Seoane J, Le HV, Massague J: Myc suppression of the p21(Cip1) **Cdk inhibitor influences the outcome of the p53 response to DNA damage.** *Nature* 2002, **419:** 729-734.

154. Sheiness D, Fanshier L, Bishop JM: **Identification of nucleotide sequences which may encode the oncogenic capacity of avian retrovirus MC29.** *Journal of Virology* 1978, **28**: 600-610.

155. Solomon D L, Amati B, Land H: **Distinct DNA binding preferences for the c-Myc/Max and Max/Max dimers.** *Nucleic Acids Research* 1993, **21**: 5372-5376.

156. Staller P, Peukert K, Kiermaier A, Seoane J, Lukas J, Karsunky H, Moroy T, Bartek J, Massague J, Hanel F, Eilers M: **Repression of p15INK4b expression by Myc through association with Miz-1.** *Nature cell biology* 2001, **3:** 392-399.

157. Stark MB: **An hereditary tumor in the fruit fly, *Drosophila.*** *Cancer Research* 1918, **3**: 279-300.

158. Stauch M, Gallant M: **Discussion in person.**

159. Steiger D, Furrer M, Schwinkendorf D, Gallant P: **Max-independent functions of Myc in *Drosophila*.** *Nature Genetics* 2008, **40**: 1084-1091.

160. Stone J, de Lange T, Ramsay G, Jakobovits E, Bishop JM, Varmus H, Lee W: **Definition of regions in human c-myc that are involved in transformation and nuclear localization.** *Molecular and Cellular Biology* 1987, **7**: 1697-1709.

161. Stogios PJ, Downs GS, Jauhal JJS, Nandra SK, Privé GG: Sequence and structural analysis of BTB domain proteins. *Genome Biology* 2005, 6: R82.

162. Sugiyama A, Kume A, Nemoto K, Lee SY, Asami Y, Nemoto F, Nishimura S, Kuchino Y: **Isolation and characterization of s-myc, a member of the rat myc gene family.** *PNAS* 1989, **86**: 9144-9148.

163. Sulzer A: **A Screen for Mutations in Genes Involved in Growth Control in *Drosophila melanogaster***. Zürich, Universität Zürich, *Diploma thesis*, 2003.

164. Taft RJ, Glazov EA, Lassmann T, Hayashizaki Y, Carninci P, Mattick JS: **Small RNAs derived from snoRNAs.** *RNA* 2009, **15**: 1233-40.

165. Tansey WP: **Mammalian MYC proteins and cancer.** *New Journal of Science* 2014, Article ID 757534, 27 pages.

166. Teleman AA, Hietakangas V, Sayadian AC, Cohen SM: **Nutritional control of protein biosynthetic capacity by insulin via Myc in *Drosophila*.** *Cell Metabolism* 2008, **7**: 21-32.

167. Terpe K: **Ovierview of tag protein fusions: from molecular and biochemical fundamentals to commercial systems.** *Applied Microbiology Biotechnology* 2003, **60**: 523-533.

168. Terry NA, Tulina N, Matunis E, DiNardo S: **Novel regulators revealed by profiling *Drosophila* testis stem cells within their niche.** *Developmental Biology* 2006, **294**: 246-257.

169. Trumpp A, Refaeli Y, Oskarsson T, Gasser S, Murphy M, Martin GR, Bishop JM: **c-Myc regulates mammalian body size by controlling cell number but not cell size.** *Nature* 2001, **414**: 768-773.

170. Tollervey D, Kiss T: **Function and synthesis of small nucleolar RNAs.** *Current Opinion in Cell Biology* 1997, **9**: 337-342.

171. Tschochner H, Hurt E: **Pre-ribosomes on the road from the nucleolus to the cytoplasm.** *TRENDS in Cell Biology* 2003, **13**: 255-263.

172. Turkel N, Sahota VK, Bolden JE, Goulding KR, Doggett K, Willoughby LF, Blanco E, Martin-Blanco E, Corominas M, Ellul J, *et al.*: **The BTB-zinc Finger transcription factur Abrupt acts as an epithelial oncogene in *Drosophila melanogaster* through maintaining a progenitor-like cell state.** *PLOS genetics* 2013, **9**: e1003627.

173. Tycowski KT, Shu MD, Steitz JA: **A mammalian gene with introns instead of exons generating stable RNA products.** *Nature* 1996, **379**: 464-466.

174. Tycowski KT, Steitz JA: **Non-coding snoRNA host genes in *Drosophila*: expression strategies for modification guide snoRNAs.** *European Journal of Cell Biology* 2001, **80**: 119-125.

175. van Nues RW, Granneman S, Kudla G, Sloan KE, Chicken M, Tollervey D, Watkins NJ: **Box C/D snoRNP catalysed methylation is aided by additional pre-rRNA base-pairing.** *EMBO J.* 2011, **30**: 2420-2430

176. van Riggelen J, Yetil A, Felsher DW: **MYC as a regulator of ribosome biogenesis and protein synthesis.** *Nature Reviews Cancer* 2010, **10**: 301-309.

177. van Steensel B: **Mapping of genetic and epigenetic regulatory networks using microarrays.** *Nature genetics* 2005, **37**: 18-24.

178. Valleron W, Laprevotte E, Gautier EF, Quelen C, Demur C, Delabesse E, Agirre X, Prosper F, Kiss T, Brousset P: **Specific small nucleolar RNA expression profiles in acute leukemia.** *Leukemia* 2012, **26**: 2052-2060.

179. Vennstrom B, Sheiness D, Zabielski J, Bishop JM: **Isolation and characterization of c-myc, a cellular homolog of the oncogene (v-myc) of avian myelocytomatosis virus strain 29.** *Journal of Virology* 1982, **42**: 773-779.

180. Vita M, Henriksson M: **The Myc oncoprotein as a therapeutic target for human cancer.** *Seminars in Caner Biology* 2006, **16**: 318-330.

181. Walz S, Lorenzin F, Morton J, Wiese KE, von Eyss B, Herold S, Rycak L, Dumay-Odelot H, Karim S, Bartkuhn M, *et al.*: **Activation and repression by oncogenic MYC shape tumour-specific gene expression profiles.** *Nature* 2014, **511**: 483-7.

182. Wanzel M, Herold S, Eilers M: (2003). **Transcriptional repression by Myc.** *Trends in Cell Biology* 2003, **13**: 146-150.

183. Warner J: **The economics of ribosome biosynthesis in yeast.** *Trends in Biochemical Sciences* 1999, **24**: 437-440.

184. Watkins NJ, Gottschalk A, Neubauer G, Kastner B, Fabrizio P, Mann M, Luhrmann R: **Cbf5p, a potential pseudouridine synthase, and Nhp2p, a putative RNA- binding protein, are present together with Gar1p in all H BOX/ACA-motif snoRNPs and constitute a common bipartite structure.** *RNA* 1998, **4**: 1549-1568.

185. Weinmann R, Roeder RG: **Role of DNA-dependent RNA Polymerase III in the transcription of the tRNAs and 5S RNA genes.** *PNAS* 1974, **71**: 1790- 1794.

186. Williams GT, Farzaneh F: **Are snoRNAs and snoRNA host genes new players in cancer?** *Nature Reviews Cancer* 2012, **12**: 84-88.

187. Wolf E, Lorenzin F: **Discussion in person about unpublished data.** 2015

188. Wood MA, McMahon SB, Cole MD: **An ATPase/helicase complex is an essential cofactor for oncogenic transformation by c-Myc.** *Molecular cell* 2000, **5**: 321-330.

189. Xu T, Wang W, Zhang S, Stewart RA, Yu W**: Indentifying tumor suppressors in genetic mosaics: the *Drosophila lats* gene encodes a putative protein kinase.** *Development* 1995, **121**: 1053-1063.

190. Yang J, Sung E, Donlin-Asp PG, Corces VG: **A subset of *Drosophila* Myc sites remain associated with mitotic chromosomes colocalized with insulator proteins.** *Nature communications* 2013, **4**: 1464.

191. Yoshihama M, Nakao A, Kenmochi N: **snOPY: a small nucleolar RNA orthological gene database.** *BMC Research Notes* 2013, **6**: 426.

192. Young CL, Britton ZT, Robinson AS: **Recombinant protein expression and purification: A comprehensive review of affinity tags and microbial applications.** *Biotechnology Journal* 2012, **7**: 620-634.

193. Zhang H, Stallock JP, Ng JC, Reinhard C, Neufeld TP**: Regulation of cellular growth by the *Drosophila* target of rapamycin dTOR.** *Genes & Development* 2000. **14**: 2712-2724.

194. Zeller KI, Zhao XD, Lee CWH, Chiu KP, Yao F, Yustein JT, Ooi HS, Orlov YL, Shahab A, Yong HC *et al.*: **Global mapping of c-Myc binding sites and target gene networks in human B cells.** *PNAS* 2006, **103**: 17834-17839.

195. Zemann A, op de Bekke A, Kiefmann M, Brosius J, Schmitz J: **Evolution of small nucleolar RNAs in nematodes.** *Nucleic Acids Research* 2006, **34**: 2676-2685

196. Zervos AS, Gyuris J, Brent R: **Mxi1, a protein that specifically interacts with Max to bind Myc-Max recognition sites.** *Cell* 1993, **72**: 223-232.

197. Zhu S, Lin S, Kao CF, Awasaki T, Chiang AS, Lee T: **Gradients of the *Drosophila* Chinmo BTB-Zinc Finger protein govern neuronal temporal identity.** *Cell* 2006, **127**: 409-422.

6 Appendix

6.1 List of abbreviations

Selections of abbreviations that can be found in this thesis are explained below. Furthermore the abbreviations of the IUPAC (International union of pure und applied Chemistry) and of the SI-System (Système international d'unités) were used.

6.1.1 **Prefixes**

Table 6-1: abbreviations for prefixes and multiplication factors

abbreviation	prefix	factor
p	Pico-	10^{-12}
n	Nano-	10^{-9}
µ	Micro-	10^{-6}
m	Milli-	10^{-3}
c	Centi-	10^{-2}
k	Kilo-	10^{3}

6.1.2 **Units**

A	ampere
Da	dalton
g	gram
h	hour
J	joule
l	liter
m	meter
min	minute
M	mol/l
OD	optical density
s	second
U	unit
v/v	volume per volume

w/v	weight per volume
°C	degree Celsius

6.1.3 **Proteins, protein domains and other biomolecules**

A	adenine
aa	amino acid
bp	basepair(s)
bHLH	basic helix-loop-helix
BTB	broad-complex, tramtrack and bric à brac
C	cytosine
cDNA	complementary DNA
dATP	deoxyadenosine triphosphate
dCTP	deoxycytidine triphosphate
dGTP	deoxyguanosine triphosphate
dTTP	deoxythymidine triphosphate
DNA	deoxyribonucleic acid
ddNTPs	dideoxyribonucleoside triphosphates
dNTPs	deoxyribonucleoside triphosphates
dsRNA	double stranded RNA
FRT	flipase recombination target
G	guanine
GFP	green fluorescent protein
GST	glutathione-S-transferase
HRP	horseradish peroxidase
nt	nucleotide(s)
ORF	open reading frame
POZ	pox virus and zinc finger
RNA	ribonucleic acid
rNTPs	ribonucleotide triphosphates
LZ	leucine zipper
T	thymine
UAS	upstream activating sequence

UTR	untranslated region
Zf	zinc finger

6.1.4 Chemicals and solutions

APS	ammoniumpersulfate
ddH_2O	bidestilled water
DMSO	dimethylsulfoxide
EDTA	ethylendiamintetraacetate
FBS	fetal bovine serum
PBS	phosphate-buffered saline
SDS	sodium dodecyl sulfate
TBE	Tris-borate-EDTA-buffer
TBS	Tris-buffered saline
TBS-T	Tris-buffered saline with tween-20
TE	Tris-EDTA-buffer
TEMED	N,N,N',N'-tetramethylethylendiamine
Tris	Tris-(hydroxymethyl)-aminomethan

6.1.5 Other abbreviations

E. coli	Escherichia coli
e.g.	for example
hs	heat shock
IP	immunoprecipitation
PAGE	polyacrylamide-gelelectrophoresis
PCR	polymerase chain reaction
pers. com.	personal communication
qPCR	quantitative PCR
qRT-PCR	quantitative Reverse Transcriptase PCR
rpm	rotations per minute
RT	room temperature
SC	Santa Cruz
o./n.	overnight; 16-20 h
wt	wildtype

6.2 Acknowledgements

First and foremost, I want to thank my supervisor, Prof. Dr. Peter Gallant, for the guidance, encouragement and advice he constantly provided and for his open ear whenever I had any problems to solve.

I would especially like to thank my committee members Prof. Dr. Thomas Raabe and Prof. Dr. Charlotte Förster for their support in my progress over the years.

I would like to thank all present and former members of the Gallant lab for assistance, discussions and a wonderful working atmosphere: Jennifer Gerlach, Oriel Carreno, Maria Gallant, André Kutschke, Maria Weide (née Stauch), Dirk Birkel, Reinhold Krug, Senthil Kumar Devan and Yana Feodorova.

Furthermore I want to thank all members of the Eilers, Murphy and Popov group who stood by me with technical help and countless discussions. I am especially grateful to Dr. Elmar Wolf for his steady support throughout the years and to him, Francesca, Jennifer and Oriel for correcting my thesis.

In addition I want to thank Thomas Ziegenhals for his support in the Isotope lab and all the perfect gels.

A special thanks to Anne, Francesca, Francesca, Jiajia, Maria, Sarah and Jenny for the wonderful time we spent inside and outside the lab. I will never forget our smaller and bigger journeys.

Finally, I want to thank Alexander and my whole family for their continued support and encouragement, and for enduring all the ups and downs of my research. You have been an indispensable source of spiritual support.

6.3 Curriculum vitae

6.4 Affidavit

I hereby confirm that my thesis entitled “Characterization of direct Myc target genes in *Drosophila melanogaster*” and “Investigating the interaction of Chinmo and Myc” is the result of my own work. I did not receive any help or support from commercial consultants. All sources and/or materials applied are listed and specified in the thesis.

Furthermore, I confirm that this thesis has not yet been submitted as part of another examination process neither in identical nor in similar form.

Gerbrunn, 10. August 2015 _____

Place, Date Signature